SPECTROSCOPY AND SPECTROPHOTOMETRY OF CATACLYSMIC VARIABLE STARS

thesis by

Richard Alan Wade

In Partial Fulfillment of the Requirements

for the Degree of

Doctor of Philosophy

California Institute of Technology

Pasadena, California

1981

(Submitted October 23, 1980)

To my parents

ACKNOWLEDGMENTS

My advisor, J. B. Oke, taught me to do research nearly from my earliest days at Caltech. He was extraordinarily generous with his observing time and his advice, and he refused to let me take myself too seriously.

I am indebted to Horace W. Babcock and Maarten Schmidt, Directors of the former Hale Observatories, for permission to use the telescopes and auxilary equipment of the Observatories in my research. I thank the superintendent, day crews, and cooks at Mt. Wilson and Palomar, and especially the night assistants with whom I worked: Gene Hancock, Howard Lanning, Larry Webster, and Mike Deak; and, Gary Tuton, Juan Carrasco, Ranney Adams, Roger Higson, Chip Williams, Spencer Shidner, Tom Murphy, and in particular Skip Staples, who was sometimes more enthusiastic than I was on those long, cold, winter nights of 1978-79. I want also to thank Larry Blakeé and all of his assistants, who kept the equipment in working order, and who still make house calls. I thank Barbara Zimmerman, Stefan Mochnacki, and Bill Sebok for their help with computers and computing problems. Steve Shectman, Gary Yanik and Ken Clardy designed and built the Varo-Reticon system, without which Chapter 3 could not have been written. Thanks also to Steve Kent and the not-AEL Corporation for their efforts on behalf of the P60 SIT spectrograph.

I also with to thank:

- The other members of my committee, Jesse Greenstein, Roger Blandford, and Peter Young; and all of the other faculty-type pundits from whom I learned many things, especially Wal Sargent, Jim Gunn (who gave good advice, but not often enough), Maarten Schmidt, and Bob Kraft (while he was here).

- The staff at Santa Barbara Street for instruction, disputation, and good talk on mountaintops and off.

- My collaborators on various observing and thinking projects, Kirk Borne, John Hoessel, Jay Elias, Paula Szkody, Keith Horne; and also Bev Oke and Jesse Greenstein, and Janet Mattei and the rest of the AAVSO.

- My classmates, Kirk, Roger, and Howard; my officemate, Doug Rabin, and the other inmates of Room 10 through the years, who answered the phone for me while I answered it for them; the other students, past and present, with whom I talked about Life and Science, especially John Hoessel, Richard Green, Don Schneider, Graham Berriman, France Córdova, and Alex Filippenko.

- Ray Ballard and Lilo Hauck, who really ran the place.

- The librarians and secretaries of Robinson Lab and Santa Barbara Street, especially Helen Knudsen.

- Basil Katem and Charles Kowal, who showed me how to run the engines; and Bill St. John and Bill Qualls for their chauffeuring services.

- Todd Boroson, who sympathized.

Thanks to all the other observers-of and thinkers-about cataclysmic variables, especially Rob and Ed, and Bohdan Paczynski, for their encouragement. Thanks to my apartment-mate, and co-holder of season tickets, Jim Schilling, for most of the quasi-philosophical discussion and a fair fraction of the laughs I had at Caltech. Thanks to Graphic Arts, and minimal thanks to the Computing Center.

It gives me great pleasure to thank Stirling L. Huntley (and the Institute) for financial support during my summers and later years as a student here. The National Science Foundation supported me in part during my first three years, and I thank Uncle Sam also.

Last, I give a very special thank you to Helen Holloway, who went the extra mile with me in my mad scramble to finish by a self-imposed deadline.

ABSTRACT

Distances and luminosities of individual cataclysmic variable stars (as opposed to statistical properties of the group as a whole) can best be acquired by studying the secondary stars of these short-period binary systems. Since the secondary stars are of late spectral type, observations in the near infrared are especially useful.

Spectrophotometry of the dwarf nova U Geminorum has been carried out from 0.3μ to 1μ using the Hale 5m telescope. The energy distribution can be interpreted as the sum of fluxes from an M4.5 or M5 star and a source giving a flat continuum. The M companion, referred to as U Gem B, is less dense than a main-sequence star of the same color index. The absolute spectrophotometry allows a distance modulus of 4.4 ± 0.8 mag to be derived for U Geminorum. The absolute visual magnitude of the quiescent system is about $M_V = 10.3$.

The Na I infrared doublet in the spectrum of U Geminorum has been observed at high resolution around the orbit. The velocity semi-amplitude of U Gem B is 283 ± 15 km s^{-1}, and spectroscopic conjunction occurs before mid-eclipse of the bright spot. These results, combined with previous analysis of the emission-line velocity variations, have been used to deduce $M_1 = 1.01 \pm 0.25$ and $M_2 = 0.36 \pm 0.10$ (solar units) for the masses of the component stars. U Gem B is too cool and probably too large, compared to a zero-age main-sequence star of the same mass.

A spectrophotometric survey of about 30 cataclysmic variable stars has been carried out from 0.3μ to 1μ. Old novae, nova-like variables, and erupting dwarf novae are characterized by spectral energy distributions which are flat (f_ν = constant) or rising toward shorter wavelengths. These objects have Balmer jumps in absorption or else no Balmer jump at all. No trace of a red stellar spectrum is evident in these stars, except for the nova-like system RW Tri. Quiescent dwarf novae show emission Balmer jumps and emission lines of the Balmer series and He I. Some quiescent dwarf novae show no trace of the spectrum of the secondary star, while others show the secondary star with various degrees of observability.

These spectral energy distributions are analyzed to determine the spectral types of the secondary stars and the fraction of light contributed by the primary stars and their accretion disks. The analysis makes use of flux-ratio diagrams to eliminate those spectral decompositions which result in physically implausible energy distributions for the accretion disks. The Balmer jump is especially useful in eliminating unphysical distributions. Refined estimates of spectral type and fractional light contribution are made in favorable cases, using an interactive computer program. It is argued that the secondary stars in cataclysmic variable systems should be expected to deviate from the normal main-sequence relations among mass, radius, spectral type, and

luminosity. The results of the analysis support previous workers' estimates of the absolute visual magnitudes of cataclysmic variable stars; the spectral types assigned to the secondary stars of individual systems on the basis of this work are generally later than those assigned by previous workers.

TABLE OF CONTENTS

Chapter 1.	Introductory Remarks	1
	I. Observations of Cataclysmic Variable Stars	2
	II. Models of Cataclysmic Variable Stars	4
	III. Distances and Luminosities of Cataclysmic Variables	7
	IV. Outline of Thesis	9
	References	12
Chapter 2.	A Spectrophotometric Parallax for U Geminorum	14
	I. Introduction	15
	II. Observations	15
	III. The Spectral Type of U Geminorum B	15
	IV. The Evolutionary State of U Gem B	18
	V. The Distance to U Geminorum	18
	VI. Discussion	19
	References	19
Chapter 3.	Radial Velocity Observations of the Secondary Star in U Geminorum	20
	I. Introduction	21
	II. Observations	22
	III. Analysis	26
	IV. Discussion	33
	V. Conclusion	41
	References	43
	Figures	45

Chapter 4. A Spectrophotometric Survey of Cataclysmic Variable Stars 50

I. Introduction 51

II. Observations 52

III. Discussion 59

Appendix: Smoothing Multichannel Data 62

References 64

Figures 66

Chapter 5. Analysis of Cataclysmic Variable Star Energy Distributions: Spectral Types for the Secondary Stars and Absolute Visual Magnitudes for the Accretion Disks 72

I. Analysis of Composite Spectra 73

II. Standards for Comparison 75

III. The Flux-Ratio Diagram 80

IV. The Balmer Jump 90

V. Results 92

VI. The Secondary Stars in Cataclysmic Variable Systems 100

VII. Discussion of Individual Stars 104

VIII. Conclusion 107

Appendix: The Flux-Ratio Diagram 114

References 117

Figures 120

CHAPTER 1

INTRODUCTORY REMARKS

I. OBSERVATIONS OF CATACLYSMIC VARIABLE STARS

Dwarf novae, or "U Geminorum stars", are variable stars whose light curves are characterized by periods of steady light at faint levels ("quiescence") interrupted by briefer intervals at light levels 2 to 4 magnitudes brighter ("outbursts"). Outbursts recur on a semi-regular schedule with mean recurrence intervals varying from one object to the next but in the range from a week to several months. Outbursts last from less than a day to about ten days, again depending on the individual dwarf nova. Some dwarf novae, subclassified Z Camelopardalis stars, also exhibit "standstills" at an intermediate light level, lasting from a few weeks to several years. Other dwarf novae, those in the SU Ursae Majoris subclass, show "superoutbursts", unusually long and bright eruptions interspersed on a more or less predictable pattern among the regular outbursts. Some dwarf novae show long and short outbursts of about the same magnitude which succeed each other on a semi-regular basis. Further details of the visual light curves of dwarf novae can be found in the reports of the American Association of Variable Star Observers and the Variable Star Section of the British Astronomical Association.

Spectroscopically, quiescent dwarf novae show a blue continuum upon which are superposed broad or "hazy" emission lines of hydrogen, neutral helium, and singly ionized calcium. These emission lines are doubled in some dwarf novae.

He II λ4686 is occasionally seen. Recently emission at λ5169 from Fe II has been reported in the spectrum of U Geminorum (Sobel and Ulrich 1977). The Balmer discontinuity is in emission. Sometimes a heavily veiled absorption line spectrum from a late type star can be discerned under the blue continuum. In outburst, dwarf nova spectra resemble to first order early A stars, with broad hydrogen absorption lines and a Balmer discontinuity in absorption. Close inspection sometimes reveals emission cores in the Balmer lines and the presence of high excitation lines such as λ4686. These emission cores in the hydrogen lines gain strength as the star fades to minimum light. Forbidden lines have never been reported in the spectrum of a dwarf nova.

Novalike variables (of the "UX Ursae Majoris" type, not the "Z And" or "FU Ori" types) spectroscopically resemble old nova remnants or dwarf novae in permanent outburst. Absorption lines from a cool star have up to now not been reported in UX UMa stars or in classical nova remnants, which along with the dwarf novae and the recurrent novae make up the four kinds of "cataclysmic variable" stars.

In the 1940's, 50's, and early 60's, work by Joy (1954, 1956), Walker (1954, 1963), Kraft (1962, 1964), and others showed that most and probably all cataclysmic variable stars are binary systems with short orbital periods ($P \lesssim 1$ day; excluded from this discussion are the recurrent novae such as T CrB, which has a much longer orbit, P = 227 days; WZ

Sge, which has been called a recurrent nova, probably belongs in the dwarf nova class: its orbital period is 82 minutes). The use of high speed photometry during the 1950's and 60's by Walker, Warner and Nather, Robinson, and others showed the presence of short timescale ($\tau \lesssim 10^2$ sec) flickering and in some cases coherent oscillations in cataclysmic variables. Careful scrutiny of these data resulted in a "standard model" for all short-period cataclysmic variable stars (Warner and Nather 1971; Smak 1971). A fuller discussion of these data and the model can be found in the review articles by Warner (1976) and Robinson (1976).

II. MODELS OF CATACLYSMIC VARIABLE STARS

In the standard model, the primary star is a white dwarf and the secondary star is supposed to be a cool main sequence star which fills its Roche lobe. Matter leaves the secondary star from the inner Lagrangian point and, due to its excess specific angular momentum, forms an accretion disk around the white dwarf primary. At the point where the stream of gas from the secondary star intersects the disk, a bright spot is formed, which can contribute a large fraction of the visual light from the system. The bright spot is the seat of the incoherent flickering activity, but the coherent oscillations arise near the white dwarf. The emission lines seen in dwarf novae at minimum light arise in the accretion

disk where large Keplerian orbital velocities account for the breadth and occasional doubling of the lines. Eventual accretion of the material is possible because viscous processes in the disk transport excess angular momentum to the outer edge of the disk and allow matter to be transported inside to the star.

In the case of steady-state accretion via an optically thick viscous disk it can be shown that the effective temperature of the surface of the disk varies with radius according to

$$T_{eff}(x) = T_* \, x^{-3/4} \, (1-x^{-1/2})^{1/4}, \; 1 < x \leq x_{outer}$$

where $x = r/r(\text{inner})$, r(inner) being the inner radius of the disk. T_* is a function of the mass of the accreting star, the inner radius of the disk, and the mass accretion rate. For a white dwarf of mass 1 $M_\odot$ and radius 6×10^8 cm, and for $\dot{M} = 10^{16}$ gm $s^{-1} = 1.6 \times 10^{-10}$ $M_\odot$ yr^{-1}, T_* is 60,000 K.

If r(inner) were zero and x(max) were very large, and if each surface element of the disk radiated as a blackbody at the corresponding effective temperature T, the resultant spectrum from an optically thick disk would be of the form $f_\nu \propto \nu^{1/3}$ (Lynden-Bell 1969). In practice, the inner radius of the disk is finite, so that the maximum temperature in the disk is $T_{eff} = 0.488 \, T_*$. This produces a cutoff at the shortest wavelengths. Also the disk in short-period binary systems (but perhaps not in quasars!) is limited on the outside by tidal forces from the secondary star: the disk does

not exceed the size of the primary star's Roche lobe. This means that at long enough wavelengths, a thick disk must emit a Rayleigh-Jeans spectrum. Additionally, the disk surface radiates not as a blackbody but as a stellar atmosphere under slightly peculiar conditions, so that radiative transfer effects such as limb darkening and line formation processes will mold the emergent spectrum. These effects have recently been studied by several groups, including Tylenda (1977), Schwarzenberg-Czerny and Rozyczka (1977), Herter et al. (1979), Pacharintanakul and Katz (1980), and Mayo, Wickramasinghe, and Whelan (1979).

There is an additional effect which must be of importance in dwarf novae at minimum light, for none of the considerations just mentioned can produce a Balmer jump in emission or the emission lines which are actually observed. Williams (1980) has shown that for parameters believed to be typical in a dwarf nova, the outer parts of the accretion disk will be optically thin in the Paschen continuum, although the Balmer lines and lines of species such as Ca II and Na I remain thick. He further shows that, since the radiating efficiency of the outer disk drops rapidly with decreasing temperature, the outer disk will maintain its kinetic temperature near 7000 K. The consequences are that we must expect to see a continuum from a smaller (and therefore on the average hotter) inner disk which is optically thick,

together with emission from an optically thin gas at about 7000 K. The Balmer lines and emission discontinuity arise naturally from the recombination spectrum of the outer disk, without requiring an additional postulate of a "corona" above the disk.

In practical terms, all of this means that the "extra light" from a dwarf nova may be expected to contain contributions from stellar atmospheres hotter than 7000 K (which for the present discussion will be approximated by blackbodies at the corresponding effective temperature) and perhaps recombination spectra at temperatures close to or exceeding 7000 K (there may be situations in which the hotter parts of the disk are optically thin also). In principle, intermediate disk zones with optical depth about unity in the Paschen continuum may contribute a small fraction of the light to the residual spectrum, but the properties of these zones should fall between the extremes.

III. DISTANCES AND LUMINOSITIES OF CATACLYSMIC VARIABLES

To understand the short-period cataclysmic variable stars more fully, we need to have information about their luminosities and distances. The bolometric luminosity is a key parameter in determining the structure of the accretion disks in cataclysmic variables, and must be known in order to properly test disk models. Without reliable distances, discussion of the space density, kinematics or lifetimes of

cataclysmic variables is ill-founded.

Most methods of determining the distances to astronomical objects are not useful in the study of cataclysmic variable stars. Only a few of these systems are close enough for reliable trigonometric parallaxes to be measured. An additional few stars may be in clusters or moving groups or have common proper motion companions, which allow their distances to be measured. Statistical parallax studies give results which are not applicable to individual stars. The present understanding of accretion disk spectra is not advanced enough to allow spectroscopic determinations of their luminosities to be made, although there is very rapid progress in the context of the steady-state viscous disk model (Herter et al. 1979; Mayo, Wickramasinghe, and Whelan 1980). There remain distance measurements based on the secondary stars.

If a reliable spectral type for the secondary star in a cataclysmic variable system can be determined, then the method of spectroscopic parallaxes can be used to obtain the distance to the object. Since every short-period binary has a secondary star which is in principle observable regardless of the distance to the system or the relation of the system to its stellar neighbors, spectroscopic analysis of the secondary star is a universally applicable method for determining distances and luminosities.

Of course, the secondary stars can be used to deduce much more than just the distance to the binary system. For instance, the motion of the secondary star in its orbit allows us to measure or set limits on the mass of the primary star. Recent infrared photometry (G. Berriman 1980, private communication) has shown that orbital inclinations can also be derived from observations of the ellipsoidal variations of the secondary stars. The same observations have confirmed that in U Geminorum, the secondary star fills its Roche lobe. Finally, an understanding of the secondary stars is essential to an understanding of the evolutionary state of cataclysmic variable stars.

IV. OUTLINE OF THESIS

This thesis presents the results of my investigation of the secondary stars in cataclysmic variable systems, especially the dwarf novae, and among this latter group U Geminorum in particular. The emphasis has been on using the secondary stars to determine the absolute magnitude of the disk component of the limit from cataclysmic variables. Some attention has also been directed to understanding the physical state of the secondary stars themselves, since incorrect assumptions at this step would result in errors in the derived luminosities and distances of the objects.

Chapter 2, reprinted from The Astronomical Journal (Wade 1979), presents a discussion of the spectral energy

distribution of U Gem. The secondary star dominates the spectrum longward of λ7000, and this allows the spectral type of the secondary star to be determined. From this the distance and luminosity of U Gem can be estimated. The secondary star deviates from the main sequence spectrum – density relation, and it is shown how this effect, if not allowed for, alters the derived distance modulus for the star.

Chapter 3 (submitted to The Astrophysical Journal) presents a follow-up spectroscopic study of the U Gem system, to measure the orbital radial velocity variations of the secondary star. The results confirm the detection of the secondary star (Chapter 2) and establish the essential correctness of Smak's (1976) discussion of the orbital parameters for U Gem.

Chapter 4 (in collaboration with J. B. Oke) presents a spectrophotometric survey of a sample of dwarf novae and other cataclysmic variable stars. The survey was made with the multichannel spectrophotometer (MCSP) at the Hale 5m telescope. The overall spectral characteristics of the various classes of cataclysmic variables are briefly discussed.

Chapter 5 analyzes the MCSP data using refinements of the method which was applied to U Gem in Chapter 2. Decomposition of the spectral energy distributions is done under non-restrictive assumptions about the structure of accretion

disks. A powerful technique, based on the properties of flux-ratio diagrams, is used to derive limits on the absolute visual magnitudes of the disks. Refinement of these limits is possible in favorable cases. Possible sources of error in the determination of the absolute magnitudes are discussed.

REFERENCES

Herter, T., LaCasse, M. G., Wesemael, F., and Winget, D. E. 1979, Ap. J. Suppl., 39, 513.

Joy, A. H. 1954, Ap. J., 120, 377.

——. 1956, Ap. J., 124, 317.

Kraft, R. P. 1962, Ap. J., 135, 408.

———. 1964, Ap. J., 139, 457.

Lynden-Bell, D. 1969, Nature, 223, 690.

Mayo, S. K., Wickramasinghe, D. T., and Whelan, J. A. J. 1979, Changing Trends in Variable Star Research (IAU Coll. 46), F. M. Bateson et al. eds. (Hamilton, N. Z.: University of Waikato), 52.

Pacharintanakul, P., and Katz, J. I. 1980, Ap. J., 238, 985.

Robinson, E. L. 1976, Ann. Rev. Astr. Ap., 14, 119.

Schwarzenberg-Czerny, A., and Rozyczka, M. 1977, Acta Astr., 27, 429.

Smak, J. 1971, Acta Astr., 21, 15.

——. 1976, Acta Astr., 26, 277.

Sobel, H., and Ulrich, R. K. 1977, Bull. AAS, 9, 310.

Tylenda, R. 1977, Acta Astr., 27, 235.

Wade, R. A. 1979, A. J., 84, 562.

Walker, M. F. 1954, Pub. A.S.P., 66, 230.

———. 1963, Ap. J., 138, 313.

Warner, B. 1976, Structure and Evolution of Close Binary Systems, P. Eggleton et al. eds. (Dordrecht: Reidel), 85.

Warner, B., and Nather, R. E. 1971, M.N.R.A.S., 152, 219.

Williams, R. E. 1980, Ap. J., 235, 939.

CHAPTER 2

A SPECTROPHOTOMETRIC PARALLAX FOR U GEMINORUM

Reprinted from:
THE ASTRONOMICAL JOURNAL -15- VOLUME 84, NUMBER 4 APRIL 1979

A SPECTROPHOTOMETRIC PARALLAX FOR U GEMINORUM

RICHARD A. WADE
Hale Observatories,[a] California Institute of Technology, Pasadena, California 91125
Received 16 November 1978; revised 18 January 1979

ABSTRACT

Spectrophotometry of U Geminorum from λ3200 to λ10 900 shows an upturn in flux for wavelengths longward of λ6000. The energy distribution can be interpreted as the sum of fluxes from an M4.5 or M5 star and a source giving a flat continuum. The presence of an M star is confirmed by a higher-resolution spectrum in the red and near infrared and by the work of Stauffer, Spinrad, and Thorstensen. The M companion is less dense than a main-sequence star of the same color index. The absolute photometry allows a distance modulus of 4.4±0.4 mag to be derived for U Geminorum. The absolute visual magnitude of the quiescent system at orbital phase 0.08 is $M_V = 10.3 \pm 0.8$.

I. INTRODUCTION

In recent years, a "standard model" for U Geminorum stars and other cataclysmic variables has been developed (see, e.g., Robinson 1976, Warner 1976). In this model, a cataclysmic variable star consists of a close binary system where mass is being transferred from a cool star which fills its Roche lobe through the inner Lagrangian point into an accretion disk or ring around a white dwarf. The cool star, conventionally referred to as the secondary, is usually taken to be a main-sequence star. A bright spot, located where the gas stream from the secondary encounters the disk, often contributes a substantial fraction of the light in the visible region of the spectrum.

U Geminorum itself has contributed much to our knowledge of this structure, since the bright spot in the system produces a broad "shoulder" in the light curve and undergoes eclipses as well. As is the case for most other cataclysmic variables whose orbital periods are shorter than 6 h, however, the secondary star in U Geminorum (hereafter referred to as U Gem B) has not been directly observed until now. It is the purpose of this paper to describe spectrophotometric observations of U Gem B and to discuss how they may be used to estimate the distance to the U Geminorum system. Recent observations at Lick Observatory by Stauffer, Spinrad, and Thorstensen (1978) confirm the discovery of U Gem B and the approximate spectral type assigned to it.

II. OBSERVATIONS

Observations of U Geminorum were obtained by J. B. Oke on 21 March 1976 UT, using the multichannel spectrophotometer (MCSP) at the Cassegrain focus of the Hale 5-m reflector. The detector has been described by Oke (1969). The data consist of monochromatic fluxes in bandpasses of 80 Å (shortward of λ5760) and 160 Å (longward of λ5760). The fluxes, reduced to zero airmass and corrected to an absolute system using the fundamental calibration of Oke and Schild (1970), are presented in Table I. Observations were made through circular apertures of 10 arcsec diameter. Each entry in Table I represents an integration of 500 s, with simultaneous sky subtraction. The orbital phase at midintegration was 0.08 according to the quadratic ephemeris of Arnold, Berg, and Duthie (1976). The most recent prior outburst of U Geminorum began about 28 February 1976 (Bortle 1976).

Observations of red dwarf stars using the MCSP were kindly made available by J. L. Greenstein for comparison with the U Geminorum data.

Flux calibrated spectra at higher resolution of U Gem and some M dwarf stars were acquired by the author on 3 December 1977 UT, using a new digital SIT spectrograph attached to the Palomar 1.5-m reflector. The SIT spectrograph will be described by Kent (1979). The wavelength coverage is from λ6200 to λ7800 at a dispersion of 3.3 Å pixel^{-1}, and a resolution element is about 3 pixels. The integration time for the U Geminorum spectrum was 3200 s, and the exposure was centered on orbital phase 0.58 (Arnold, Berg, and Duthie 1976). The most recent prior outburst of U Gem began on 19 October 1977 (Bortle 1977).

III. THE SPECTRAL TYPE OF U GEMINORUM B

The advantage of the exceptionally large wavelength coverage given by the MCSP is evident in Fig. 1, which shows a previously undetected upturn in flux for wavelengths longward of λ6000. At each wavelength in the composite spectrum of U Geminorum, the observed flux is presumed to arise from a cool star, a white dwarf, an accretion disk or ring around the white dwarf, and a bright spot in the accretion disk. Because the spectral energy distributions and the relative contributions of the latter three components to the total light are poorly

[a]Operated jointly by the Carnegie Institution of Washington and the California Institute of Technology.

 0004-6256/79/040562-05$00.90

TABLE I. Spectral energy distribution of U Geminorum.

λ(Å)	*AB*	λ(Å)	*AB*	λ(Å)	*AB*
3180	14.41	4780	14.82	7360	13.71
3260	14.46	4860	14.40	7520	13.51
3340	14.46	4940	14.71	7840	13.73
3420	14.46	5020	14.67	8000	13.54
3500	14.44	5100	14.66	8160	13.26
3580	14.43	5180	14.59	8320	13.22
3660	14.38	5260	14.58	8480	13.22
3740	14.46	5340	14.57	8640	13.16
3820	14.51	5420	14.55	8800	13.09
3900	14.63	5500	14.68	8960	13.04
3980	14.68	5760	14.69	9280	12.85
4060	14.67	5920	14.69	9440	12.84
4140	14.76	6080	14.53	9600	12.78
4220	14.85	6240	14.57	9760	12.82
4300	14.60	6400	14.41	9920	12.82
4380	14.71	6560	13.95	10080	12.70
4460	14.72	6720	14.38	10240	12.62
4540	14.73	6880	14.28	10400	12.59
4620	14.75	7040	14.12	10720	12.62
4700	14.79	7200	14.20	10880	12.24

$AB = -2.5 \log f_\nu - 48.60$, where f_ν is in erg cm^{-2} s^{-1} Hz^{-1}. Random errors in the measured fluxes are generally smaller than 4%, as judged from photon counting statistics and overlapping measurements. Small systematic errors from flickering in U Gem may also be present. Fluxes for certain bandpasses have been deleted because of instabilities in the detector or other problems. The standard deviations in magnitudes for λ10720 and λ10880 are 0.164 and 0.356, respectively, from counting statistics alone.

known, it would be unwise to attempt to subtract their fluxes from the observed flux in order to expose the spectrum of the red star. The reverse procedure, namely subtracting the observed spectrum of a late-type star (assumed to match the spectrum of the red star in U Geminorum) to reveal the contribution of the hot components alone, is better defined and has been adopted here. The shape of this residual flux spectrum can then be used to determine whether the late-type star which was used is a "match" for U Gem B, according to the following set of physically plausible constraints:

(1) The residual flux must be positive,
(2) the residual flux must vary smoothly (monotonically) as a function of wavelength, and
(3) the residual flux must not show a sharp upturn in flux at the longest wavelength.

It is assumed that any volume of gas or dust which might surround the U Gem system does not affect the optical spectrum of U Gem. This assumption is based on the following considerations. If the entire measured flux in Hβ, 1.8×10^{-13} erg cm^{-2} s^{-1} above the continuum, arises from a surrounding cloud of pure hydrogen gas (which it must not, since Hβ reflects the motion of the gas near the accretion disk), then the emission measure of the gas is $n_e^2 r_*^3 d_{100}^{-2} = 1.2 \times 10^{21}$ cm^{-6}, where r_* is the radius of a spherical cloud in units of the solar radius and d_{100} is the distance to U Gem in units of 100 pc. The corresponding continuum emission from bremsstrahlung and free-bound emission (Osterbrock 1974) is fainter than $AB = 17.5$ mag for all observed wavelengths and for $T \leq 2 \times 10^4$ K. Similarly, an upper limit of $\sim 10^{20}$ cm^{-2} for the neutral hydrogen column density to U Gem has been derived from the HEAO-1 soft x-ray observations of U Gem during its October 1977 outburst (Córdova 1978). This allows an upper limit of 0.02 mag to be placed on the color excess, $E(B-V)$, due to interstellar reddening (Ryter, Cesarsky, and Audouze 1975). While a dust shell surrounding U Gem in which the dust is greatly enhanced relative to the neutral gas cannot be ruled out so simply, it will be assumed that the optical spectrum of U Gem is reddening free.

The first and third constraints provide upper and lower limits to the brightness of the red star. In the analysis as

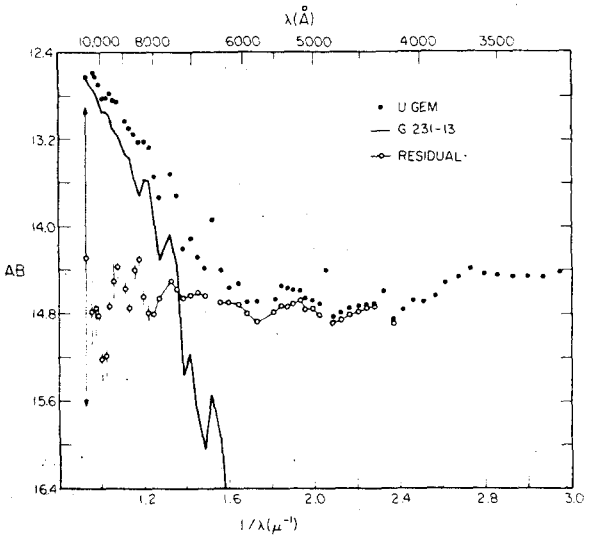

FIG. 1. Comparison of U Geminorum and the late-type star G 231-13. The fluxes for G 231-13 were scaled down by 2.15 mag before the subtraction was carried out; this is the optimum scaling for G 231-13. The residual points corresponding to Hα, Hβ, and Hγ have not been plotted. The error flags are representative of photon counting statistics only and extend to $\pm 2\sigma$.

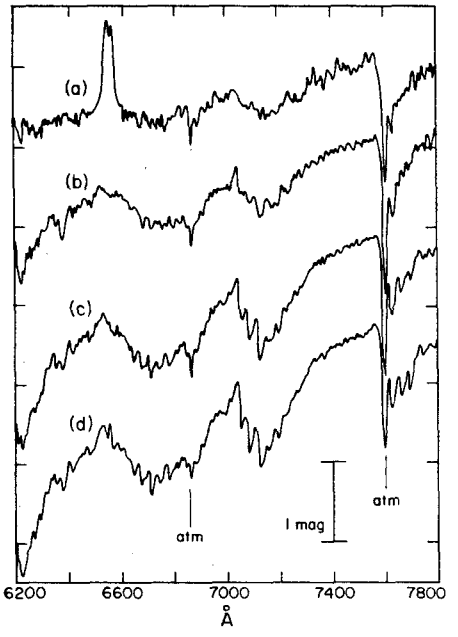

FIG. 2. Digital spectra of U Geminorum and some M dwarfs: (a) U Geminorum, (b) G 5-43, (c) G 32-7, and (d) G 87-26. The wavelength scale is only approximate. The vertical scale is indicated by the line at the lower right; arbitrary vertical shifts have been applied to the individual spectra to prevent overlapping. The instrumental response of the detector and differential atmospheric extinction have been removed by observation of standard stars and use of mean extinction tables for Palomar Observatory. The spectra have been smoothed numerically, using a three-point triangular weighing function. It is clear that the spectral features of U Gem B have been diluted substantially by the continuum flux from the hot source(s).

actually carried through, the apparent magnitude of the comparison star is scaled by a free parameter (*DM*, measured in magnitudes) before the flux subtraction is carried out. For each comparison star, *DM* can be optimized to provide a best fit.

The second condition acts to constrain the spectral type (i.e., continuum slope) of the red star. For example, suppose the comparison star used were of a later type than the red star actually present in the U Gem system; the residual flux would then show a hump at intermediate wavelengths (λ6000–λ8000) and be depressed at the extreme longward end (λ8000–λ10000). Or, if the comparison star were of earlier type than U Gem B, the residuals would exhibit a dip at intermediate wavelengths and a rise at the longest wavelengths. The spectral type of the comparison star is the second free parameter, expressed in this paper by Ake's (1978) color index [2.14] − [1.20], which is the measured difference between the star's monochromatic magnitudes at 2.14 and 1.20 μm^{-1}. This index is designed specifically for use with MCSP data as an indicator of continuum slope for late type stars, and it correlates well with Boeshaar's (1976) spectral types.

To test the sensitivity of this method, an artificial spectrum similar to that of U Gem was created by adding a flat (f_ν = const) continuum to the observed MCSP spectrum of G 34-15 (Giclas 1971). This star has color index [2.14] − [1.20] = 3.6 mag. Each of nine other late-type stars, ranging in color index from 3.15 to 4.60 mag, was then used as a comparison star, the scaling parameter *DM* being adjusted in each case to provide the best match to the artificial spectrum. The results indicate that, for this low-noise test case, it is possible to determine the true color index of the red star in such a composite spectrum to within 0.3 or 0.4 mag, and also that the apparent magnitude of the red star can be fixed to within 0.05 or 0.10 mag.

For U Geminorum, nine comparison stars, ranging in [2.14] − [1.20] from 3.45 to 4.60 mag, were used. The four stars of color bluer than 3.6 mag were all clearly bluer than U Gem B, and the two stars redder than 4.4 mag were clearly redder than U Gem B. The three intermediate stars gave residual fluxes which most nearly matched the conditions set down earlier for an acceptable fit. These stars are G 185-18 (color = 3.84 mag), G 3-33 (3.96 mag), and G 231-13 (4.28 mag), all of which are of spectral class M4.5 or M5 in Boeshaar's (1976) classification scheme. Figure 1 shows the best fit to the spectrum of U Gem that was obtained, using G 231-13, where the required scaling is *DM* = 2.15 mag. The best fits obtained using the other two stars are not significantly different from that of Fig. 1.

On the basis of these comparisons, U Gem B has a color index within 0.4 mag of [2.14] − [1.20] = 4.0 mag, and an apparent magnitude at 1.10 μm^{-1} of $m_{[1.10]}$ = 13.15 ± 0.10. The probability that U Gem B lies outside these intervals is subjectively estimated to be less than 20%, if the assumptions used in the determination are valid.

The SIT spectra can be treated in similar fashion. The fluxes f_ν from five dwarf M stars were scaled so that the difference in flux between λ7450 and λ6380 matched the observed difference in U Gem. The spectra were then compared to U Gem over the whole wavelength range from λ6200 to λ7800. Assuming a flat residual flux, the rescaled spectrum of a star of the same spectral type as U Gem B will match the observed spectrum of U Gem with a simple displacement of the zero point in the flux. Two stars, G 29-68 (color index = 2.45 mag) and G 5-43 (color ≃ 3.0 mag), are too blue to pass this test. The other three stars, G 32-7 (color = 3.54 mag), G 3-33 (3.96 mag), and G 87-26 (3.96 mag), provide fits which are adequate within the errors of observation. These spectra are shown in Fig. 2. The zero point shifts indicate that the match to G 32-7 occurs if the assumed flat residual flux is equal to the flux from the red star at λ7000, while for the latter two stars, the residual flux and the flux from U Gem B would be equal to λ7300. It would be stretching a point to say that observations of a fluctuating source made at different orbital phases and 20 months apart are strictly comparable, but it is interesting to note that the MCSP result shown in Fig. 1 indicates that the residual flux and the M star contribute equally at λ7300. In fact, to shift the point of equal fluxes from

λ7300 to λ7000 would require a change of 0.6 mag in the level of the residual flux, which is more than can be accounted for by orbital phase effects alone. In summary, the agreement between the MCSP data and the SIT data is excellent.

IV. THE EVOLUTIONARY STATE OF U GEM B

It is important to ascertain whether U Gem B lies on the main sequence, both in order to assign a distance and in order to understand better the nature of the U Gem system. In previous studies of this kind (e.g., Robinson 1974), it has been customary to plot the locus of the lower main sequence on a mass–radius diagram, along with the star in question, to see whether the star falls on the main sequence line. In the present case of U Gem B, however, neither the mass nor the radius is known very accurately. [Smak (1976) gives errors of 30% for his determination of the mass of U Gem B from spectroscopic and photometric data.] It is nevertheless possible to solve the problem by plotting the locus of the main sequence and the point for U Gem B on a mean density–color index diagram; this has the advantage that, for U Gem B, both quantities are directly observable.

For close binary systems where the secondary star fills its Roche lobe, the volume of the secondary star is a function of the mass ratio and the orbital separation alone. For stars where the mass ratio $m_2/m_1 < 0.5$, it happens that an analytic fit to this function can be constructed so that, when it is combined with Kepler's third law, all unknown quantities are eliminated, except for the period and the mean density of the secondary star. [This is just the well-known dimensional relation $T \propto (G\bar{\rho})^{-1/2}$, with the geometrical factors taken into account; the equations are given by Warner (1976).] For U Gem B Smak's work shows that the mass ratio is sufficiently small, so the orbital period yields directly the mean density $\bar{\rho}_{UGB} = 6.3\ \mathrm{g\,cm^{-3}}$. The color index $3.6 <$ [2.14] − [1.20] < 4.4 mag (80% confidence) has been derived in Sec. III.

For the locus of the main sequence in the mean density–color index diagram, mean densities have been derived from the masses and radii of M dwarf stars taken from Table II of Lacy (1977a). Lacy has used a surface brightness–color index relation to determine radii for those visual binary stars, whose distances and masses are known. Observations with the MCSP were used to obtain [2.14] − [1.20] for these stars. (Since both components of these double stars were observed through a single large aperture, it was necessary to decompose the combined light into the individual contributions from each of the two stars, using visual magnitude differences taken from Gliese (1969) and the relation given in sec. V between [1.10] and [2.14] − [1.20].)

The resulting diagram is shown in Fig. 3. It is clear that U Gem B does not lie on the main-sequence line. [Lacy (1977a) points out that *theoretical* models of lower main-sequence stars have radii which are smaller, and hence densities which are higher, than his measured values; thus, using theoretical models would place U Gem B even further from the main sequence.] Whether the color index (i.e., temperature) alone or the mean density (i.e., mass and/or radius) alone is responsible for the non-main-sequence nature of U Gem B, or whether motion in both coordinates of the diagram has occurred, awaits better determinations of the mass and radius.

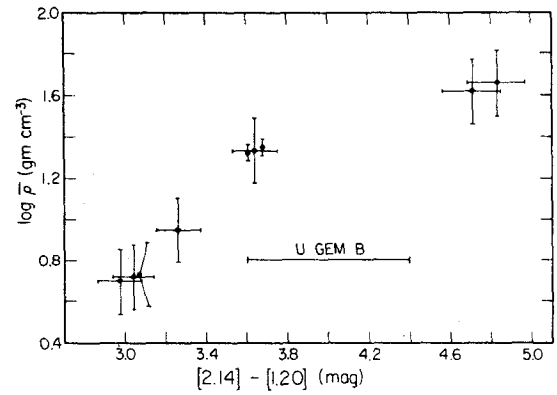

FIG. 3. The color index–log $\bar{\rho}$ plane for the lower main sequence. The mean density for U Gem B is determined from observations, and its color index must be on the indicated line segment. The main sequence is represented by Gl 65 AB (color indices = 4.71, 4.83 mag), CM Dra AB [3.61 and 3.68, see Lacy (1977b) for masses and radii], Gl 860 AB (3.26, 3.64), Gl 661 AB (2.97, 3.05), and Gl 644 (color index of mean component = 3.04). The error bars extend 1σ to each side.

The referee has pointed out that the peculiar environment of U Gem B may alter its atmosphere so that the color and mean density are not consistent with main-sequence membership, without requiring the deep interior structure of the star to be evolved. It remains true that a distance estimate using the observed color to fix the absolute magnitude of the star, as if it were on the main sequence, will be in error. A way around this difficulty is discussed in the next section.

V. THE DISTANCE TO U GEMINORUM

It is possible to obtain an estimate of the distance to U Gem, even though U Gem B is not a main-sequence star, because knowledge of the spectral type (or color index) fixes the effective temperature of U Gem B. An assumed mass and the deduced density give the radius, and the change in radius from a main-sequence star of the same color can be determined approximately from Lacy's (1977a) results. Finally, a correction $\Delta M = -5(\log R_{UGB} - \log R_{MS})$ can be applied to the absolute magnitude of a main-sequence star of the appropriate temperature.

Ake (1978) has used a sample of 52 late-type dwarfs of known parallax and with tangential velocities smaller than 100 km s^{-1} to derive a relation between the absolute monochromatic magnitude at 1.10 μm^{-1} and the color index [2.14] − [1.20]. (This index is denoted by X in the equations which follow.) His quadratic expression is

$$M_{[1.10]} = 3.075 + 2.182X - 0.0878X^2 \pm 0.49\,\text{mag}. \quad (1)$$

If U Gem B fills its Roche lobe, its radius is

$$\log R_{\text{UGB}} = -0.37 + \tfrac{1}{3}\log[M/0.35]. \quad (2)$$

A linear fit by eye to Lacy's (1977a) main-sequence data in a log(radius)–X diagram gives

$$\log R_{\text{MS}} = -0.7 - 0.16(X - 4.0) \pm 0.07 \quad (3)$$

for $X > 3.6$ mag. This last relation is the weakest of the three, because only a handful of stars is common to Lacy's list and the set of MCSP observations.

Combining Eqs. (1)–(3) gives

$$M_{[1.10]} = 8.75 + 0.68(X - 4.0) - \tfrac{5}{3}\log[M/0.35] \pm 0.60\,\text{mag}. \quad (4)$$

The adopted values of $X = 4.0 \pm 0.4$ mag, $m_{[1.10]} = 13.15 \pm 0.10$, and $\log(M/0.35) = 0.0 \pm 0.3$ (Smak 1976 gives $M = 0.35M_{\odot}$, and a factor of 2 either way is ample margin for error) therefore imply a distance modulus for U Geminorum of

$$m - M = 4.40 \pm 0.83\,\text{mag}, \quad (5)$$

corresponding to a distance of 76 (+36,−24) pc or a parallax of 0.013 (+0.006,−0.004) arcsec. The tangential velocity (Kraft and Luyten 1965) is 16 (+7,−5) km s^{-1}.

In this discussion, no account has been taken of interstellar reddening and extinction. These effects should be small. The results described in this paper differ from the preliminary values reported at the meeting of the AAS in Austin, Texas (Wade 1977), where it was assumed that U Gem B is a normal main-sequence star.

VI. DISCUSSION

Two trigonometric parallaxes have been reported for U Geminorum. Van Maanen (1938) gave 0.010 ± 0.012 arcsec. Vasilevskis *et al.* (1975) report a relative parallax of 0.004 ± 0.005 arcsec, which they suggest represents an absolute parallax of about 0.006 ± 0.005 arcsec. These results are consistent with the spectrophotometric result derived here.

The distance modulus of Eq. (5) fixes the absolute visual magnitude for the combined light from U Gem at $M_V = 10.3 \pm 0.8$ mag. The light from the hot components alone is $M_V = 10.4 \pm 0.9$ mag. These numbers refer to orbital phase 0.08, where the hot spot contributes only a small portion of the light. The derived M_V is substantially fainter than the mean magnitude for quiescent dwarf novae of $M_V \sim 7.5$ mag found by Kraft and Luyten (1965), who used a statistical parallax approach. It will be interesting to see whether spectrophotometric parallaxes for other dwarf novae are also systematically faint, or whether U Geminorum is an exceptional case.

It is my pleasure to thank Dr. J. B. Oke and Dr. J. L. Greenstein for their generosity in making available the MCSP observations on which this paper is based, and for wide-ranging and useful discussions. Thanks are due also to John Stauffer, who kindly made the results of the Lick observations known to me ahead of publication. Helpful criticism and encouragement came from K. D. Borne, B. Paczynski, and the participants in the Third Annual Workshop on Cataclysmic Variable Stars. D. Meier, J. B. Oke, and J. Pringle read an early version of this paper and made useful comments. Support for this research came in part from a National Science Foundation Graduate Fellowship.

REFERENCES

Ake, T. B. (1978). Private communication.
Arnold, S., Berg, R. A., and Duthie, J. (1976). Astrophys. J. **206**, 790.
Boeshaar, P. (1976). Ph.D. thesis, Ohio State U.
Bortle, J. E. (1976). AAVSO Circ. No. 65, 1.
Bortle, J. E. (1977). AAVSO Circ. No. 85, 1.
Córdova, F. (1978). Private communication.
Giclas, H. L. (1971). *Lowell Proper Motion Survey, Northern Hemisphere; the G Numbered Stars* (Lowell Obs., Flagstaff, AZ).
Gliese, W. (1969). *Catalogue of Nearby Stars* (Braun, Karlsruhe).
Kent, S. L. (1979). In preparation.
Kraft, R. P., and Luyten, W. J. (1965). Astrophys. J. **142**, 1041.
Lacy, C. H. (1977a). Astrophys. J. Suppl. **34**, 479.
Lacy, C. H. (1977b). Astrophys. J. **218**, 444.
Oke, J. B. (1969). Publ. Astron. Soc. Pac. **81**, 11.
Oke, J. B., and Schild, R. E. (1970). Astrophys. J. **161**, 1015.
Osterbrock, D. E. (1974). *Astrophysics of Gaseous Nebulae* (Freeman, San Francisco), Chap. 4.
Robinson, E. L. (1974). Astrophys. J. **193**, 191.
Robinson, E. L. (1976). Annu. Rev. Astron. Astrophys. **14**, 119.
Ryter, C., Cesarsky, C., and Audouze, J. (1975). Astrophys. J. **198**, 103.
Smak, J. (1976). Acta Astron. **26**, 277.
Stauffer, J., Spinrad, H., and Thorstensen, J. (1978). Private communication.
van Maanen, A. (1938). Astrophys. J. **87**, 424.
Vasilevskis, S., Harlan, E. A., Klemola, A. R., and Wirtanen, C. A. (1975). Lick Obs. Publ. **22**, Pt. V.
Wade, R. A. (1977). Bull. Am. Astron. Soc. **9**, 557 (A).
Warner, B. (1976). In P. Eggleton *et al.*, *Structure and Evolution of Close Binary Systems* (Reidel, Dordrecht), p. 85.

CHAPTER 3

RADIAL VELOCITY OBSERVATIONS OF THE SECONDARY STAR IN U GEMINORUM

I. INTRODUCTION

Because it is one of the brighter dwarf novae, and especially because it is an eclipsing binary system, U Geminorum has proven crucial to our understanding of the structure of cataclysmic variable stars. Smak (1971) and Warner and Nather (1971) made use of photometry of U Geminorum obtained throughout the 1960s to argue that a "bright spot", located where the stream of material from the secondary star intersects the edge of the accretion disk around the primary star, can contribute a large fraction of the visual flux from a dwarf nova in quiescence. They showed that in U Geminorum at minimum light, it is the bright spot rather than the primary star which is eclipsed, and that the outbursts of the system originate near the primary star. Smak (1976) used this model to determine physical parameters for the U Gem system, a task which at the time could not have been done by the usual spectroscopic method, since the secondary star had not been detected, except as the eclipsing body.

Wade (1979) and Stauffer, Spinrad, and Thorstensen (1979) have recently reported the detection of the secondary star in the U Gem system. It is of approximate spectral type M5 in Boeshaar's (1976) system of classification. Wade pointed out that the density of the secondary star, which may be deduced solely from the orbital period of U Gem, is not consistent with the observed spectral type, so that the

secondary star cannot be a normal main sequence star.

Since the secondary star has now been observed, it is of interest to obtain a radial velocity curve for it. This new information will (1) act as a check on Smak's method of determining masses (and by extension on other orbital solutions for cataclysmic variable stars where similar assumptions have been made), and (2) further elucidate whether and how the secondary star (hereafter referred to as U Gem B) differs from main sequence stars. These conclusions should have implications for research on the evolution of cataclysmic variables and the origin of x-radiation from some of these systems (the motion of the secondary star reflects the mass of the white dwarf primary). Thus U Gem promises to continue its historical role as a key to our understanding of these interacting binary systems.

II. OBSERVATIONS

Figure 1 of the paper by Wade (1979) shows that U Gem B contributes less than 50% of the light from the system at all wavelengths shorter than 7300 Å, even at the most favorable orbital phase. The radial velocity observations were therefore carried out using the Na I infrared doublet ($\lambda\lambda$ 8183, 8194, multiplet 4). The feature is strong in M dwarfs, is at long enough wavelength that veiling is not as overwhelming difficulty, is at short enough wavelength that the response from an S-25 photocathode is still acceptable, is

in a spectral region free of night sky lines, and is a doublet, so that a cross-correlation of U Gem against a reference M dwarf spectrum will show a recognizable signature of three peaks, even with a very low signal-to-noise ratio. Unfortunately, the Na I infrared doublet is in a spectral region heavily populated by weak telluric absorption lines due to water vapor.

The observations were made with the Varo-RETICON detector designed by S. Shectman (see Shectman and Hiltner 1976 for a description of a similar machine; see Young and Schneider 1979 and Mochnacki and Schommer 1979 for details of the present device) at the coudé spectrograph of the Mt. Wilson 2.5-m reflector. The central reciprocal dispersion was 44 Å mm^{-1}, which corresponds to about 0.37 Å $pixel^{-1}$. The reciprocal dispersion decreases to about 0.2 Å $pixel^{-1}$ near the ends of the two 3744-pixel arrays.

The entrance slit projected onto the sky was 1.1 arcsec wide, and this width gave a resolution of about 8 pixels (FWHM) at the center of each array, as judged from the lines of the Ar-Fe comparison lamp. A Schott GG495 filter isolated the first order of the spectrum.

On each of the three nights of observations, listed in Table 1, a series of 150 second integrations of the spectrum of U Geminorum was acquired in the first array. The second array was used to measure the contribution from the night sky, which amounted to about 40% of the stellar signal

TABLE 1

JOURNAL OF OBSERVATIONS[1]

UT Date	Begin	End	Phase Interval	N	M Star
1978 Nov 3	9:22 (.177)	12:52 (.001)	0.824	45	BD +43°44 B
1978 Nov 4	9:23 (.838)	12:31 (.568)	0.730	68	G 87-26
1979 Mar 5	4:55 (.775)	7:50 (.451)	0.676	55	G 87-26

[1]Begin and end times are listed in UT; the corresponding phases according to the quadratic ephemeris of Arnold, Berg, and Duthie (1976) are indicated in parentheses. N is the number of 150-second integrations acquired. The final column indicates the M star which was used as a model for the cross-correlation template (see Section 3). The most recent outburst of U Geminorum immediately prior to the November 1978 observations began on 1978 October 14 (Bortle 1978); the most recent outburst prior to the March 1979 observations began on 1979 January 30 (Bortle 1979).

during the November 1978 observations, and about 5% of the stellar signal during the March 1979 observations. The night-sky spectrum is essentially smooth in the region near the infrared Na I doublet. Table 1 also indicates the number of integrations which was acquired each night, and the range of orbital phase covered by each night of observation. Throughout this paper, orbital phases of U Geminorum are based on the photometric ephemeris of Arnold, Berg, and Duthie (1976):

$$HJD = 2437638.82685 + 0.17690602\ E + (5.4 \times 10^{-12})\ E^2$$

for the time of mid-eclipse of the bright spot.

Immediately before or after the observations of U Gem on each night, spectra were acquired of a late M dwarf star (listed in Table 1) and of one or more non-variable K stars whose velocities have been measured by Griffin (1971).

The Varo-RETICON detector counts photon events with high discrimination against thermal cathode emission, and is thus linear and essentially noise-free. The accumulated signal after 150 seconds integration on U Geminorum in the near infrared region of the spectrum was typically two or three photons detected per pixel.

Before the analysis described below was carried out, the data were corrected for sensitivity variations by dividing each spectrum pixel-for-pixel by a spectrum of a tungsten lamp. A mean night-sky spectrum was subtracted from each observation of U Gem, since the individual sky spectra

were considered to be too noisy for this purpose. Each spectrum was smoothed by a five-point running average filter, with weights in the proportion 1:3:3:3:1.

III. ANALYSIS

Because the photon-counting rate from U Gem is so low, it is generally not possible to measure (or even detect) the spectrum of U Gem B from a single 150 second integration. A preliminary summing of the spectra taken near phase 0.25 and the spectra taken near phase 0.75 gave immediate confirmation that the Na I absorption lines were present in the spectrum of U Gem, and moving with the phasing appropriate to their origin in the secondary star.

The detailed cross-correlation analysis of the U Gem spectra to extract a radial velocity curve for U Gem B was carried out, as follows.

1) The observations of a normal M dwarf were used to create a template/mask of the Na I lines. The effect of the telluric H_2O absorption lines was approximately removed by dividing the M-star spectrum by the spectrum of an O-star, obtained at similar airmass. The spectrum was modelled simply as a pair of triangular absorption dips with zero residual intensity, which were smoothed with the same running average filter that was applied to the U Gem spectra. The width and separation of the two dips were measured from the observed M-dwarf spectrum. Smoothed triangles provided a

sufficient approximation to the actual line profiles, in view of the uncertainty in correcting for water vapor absorption. Only the two Na I lines were modelled, because only they were of sufficient strength to be detected against the noise of the U Gem spectra.

This template represents a compromise between a digital analog of Griffin's (1967) photoelectric technique, which models absorption lines with infinite contrast (see also Lacy 1977), and a full cross-correlation technique which simply uses an observed spectrum with high-signal-to-noise ratio as a template (see e.g. Tonry and Davis 1979, or Stover et al. 1980). The latter possibility is difficult to use in a spectral region which is crowded with telluric features, since it requires that the template spectrum be free from telluric absorption. The attempt to model the profile of the strong lines is, on the other hand, an improvement over Griffin's method, since it provides a closer representation of the spectrum, and hence a clearer signal in the cross-correlation function.

2) The template described above was used to produce a cross-correlation function from each observed spectrum of U Gem. In practice, small groups of U Gem spectra were added together to produce fewer "observations", but each with better signal-to-noise properties; this did not result in any significant velocity smearing, since none of these grouped observations spans more than about 4% of the orbital

period. Since only a very small region of the spectrum was involved in the cross-correlation, it was unnecessary to re-bin the data logarithmically before carrying out this procedure. Examples of these cross-correlation functions are shown in Figure 1.

3) Each cross-correlation function was searched for local maxima. These maxima, typically three or four per observation, were plotted versus orbital phase as in Figure 2. The stronger peaks of the cross-correlation function move in velocity in a roughly sinusoidal fashion with one cycle per orbital period. The signature of a double absorption line in a cross-correlation function consists of three equally spaced peaks, the middle of which is twice as strong as the two extreme peaks (if the doublet ratio is unity). It is in fact possible to trace three parallel sets of peaks in the diagram — the main peak and the "sidelobes", which are generally made up of less significant maxima in the cross-correlation functions. The few remaining peaks in the diagram are to be expected from photon statistics.

Diagrams such as Figure 2 were used to decide which maxima in the cross-correlation functions represent the radial velocity of U Gem B. In those cases where two peaks seem to be equally plausible, or where no peak seems to be a likely candidate, the observation was rejected. For each peak thus identified as the principal cross-correlation maximum, the five highest points around that peak were fitted

by least-squares to a parabola, and the analytic maximum of the parabola (when converted from pixels to velocity units) was taken to represent the radial velocity shift of U Gem B relative to the template.

Steps 1-4 were carried out separately for each night of observations. Least-squares fits of the function

$$V = \gamma + K_2 \sin (2\pi[\phi_{ph} - \phi_o]) \qquad (1)$$

to the data pairs (ϕ_{ph},V) indicated satisfactory agreement in the fitted parameters K_2 and ϕ_o from night to night. At this stage in the analysis γ was still an arbitrary parameter, reflecting an arbitrary offset introduced in the construction of the template.

If complete orbital phase coverage is not available, the parameters γ and K_2 will in general be strongly correlated (e.g. if one has only data from one zero crossing to the next, a shift in γ will tend to produce an equal shift in the value of K_2, without significantly increasing the residuals to the fit). Since none of the nights of observations of U Gem covers a full orbit, it was necessary to combine nights in order to produce complete phase coverage and reduce the correlation between the fitted parameters. This required knowledge of the absolute offset of the template for each night.

The template offset is the sum of two terms. First, a small offset was determined for each night by producing a cross-correlation function of each template against the

M-dwarf spectrum which was used to create the template. The peak of the cross-correlation function always lay (as was expected) within one pixel of zero displacement (corresponding to a velocity difference of less than 10 km s^{-1}).

Second, the (topocentric) radial velocity of the corresponding M-dwarf star on the night in question must be determined. For BD +43°44B, this was easily found by reference to the catalogue of Abt and Biggs (1972), but for G 87-26 (= Gl 268 = Ross 986 = Wilson 4708), the literature showed discrepant heliocentric velocities, presumably indicating that the star has a variable radial velocity. For 1978 November 4, it was possible to determine the topocentric velocity of G 87-26 by comparing its spectrum with that of the well-observed star HD 13057 (Griffin 1971). A visual cross-correlation procedure, using large-scale plots of the spectra, was sufficient to establish the velocity to an accuracy of about 5 km s^{-1}. For 1979 March 5, it was unfortunately not possible to determine the velocity of the star, because the available velocity standards were of too early a spectral type to allow a meaningful cross-correlation to be carried out. In the absence of a list of effective wavelengths for late-type stars appropriate to the Varo-RETICON detector in this spectral region, it was unwise to rely on the wavelength calibration afforded by the Ar-Fe lamp to determine a velocity for G 87-26. Therefore, the observations of 1978 March 5 could not be combined successfully

with the observations from 1978 November 3 and 4.

The two nights from 1978 November nevertheless do provide complete phase coverage as well as substantial overlap, so that the loss of the third night is not critical. The velocities from these nights are presented in Table 2. A final non-linear least-squares fit to the function given in equation (1) using the combined data of these nights gives

$$\gamma = 84.3 \pm 9.6 \text{ km s}^{-1} \text{ (heliocentric)}$$

$$K_2 = 283.9 \pm 15.0 \text{ km s}^{-1}$$

$$\phi_o = -0.026 \pm 0.0070$$

Standard errors are quoted, and the correlations between the estimates of the various parameters are satisfactorily low. The November data and the curve representing the solution are plotted in Figure 3. The residuals (O-C) to the fit are shown in Figure 4.

Inspection of Figures 3 and 4 suggests that an elliptical orbit might represent the velocity data better (the velocity extremum near phase 0.25 appears to be somewhat sharper than that near 0.75, for example). Therefore, a five-parameter least-squares fit of an elliptical orbit to the data was carried out. The values of interest are:

$$\gamma = 84.9 \pm 9.9 \text{ km s}^{-1} \text{ (heliocentric)}$$

$$K_2 = 282.7 \pm 14.9 \text{ km s}^{-1}$$

$$e = 0.086 \pm 0.049$$

The r.m.s. deviation of the data from the fit to equation

TABLE 2

VELOCITIES OF U GEMINORUM B[1]

HJD 2443810+	Phase 34910+	V (km s^{-1})	HJD 2443810+	Phase 34910+	V (km s^{-1})
5.8939	7.186	357	6.8954	12.848	-118
5.9055	7.252	444	6.9015	12.881	-127
5.9286	7.383	221	6.9073	12.915	- 79
5.9349	7.418	211	6.9128	12.946	50
5.9414	7.455	98	6.9186	12.979	110
5.9492	7.499	- 82	6.9244	13.011	179
5.9578	7.548	- 39	6.9300	13.043	171
5.9651	7.589	- 87	6.9357	13.076	195
5.9724	7.630	-211	6.9413	13.107	239
5.9812	7.680	-176	6.9475	13.142	286
5.9895	7.727	-254	6.9593	13.209	311
5.9981	7.775	-163	6.9649	13.240	311
6.0057	7.818	- 99	6.9707	13.273	464
6.0113	7.850	- 96	6.9765	13.306	383
6.0172	7.883	- 47	6.9823	13.339	336
6.0256	7.931	96	6.9878	13.370	356
6.0345	7.981	111	6.9936	13.403	168
			6.9994	13.435	60
			7.0052	13.468	77
			7.0107	13.499	- 31
			7.0165	13.532	112
			7.0215	13.560	11

[1]The heliocentric cross-correlation radial velocities of U Gem B from the nights of 1978 November 3 and 4. The entries refer to the grouped observations mentioned in Section III, rather than to individual 150-second integrations. See Section IV for discussion of a possible zero-point error in determining these velocities.

(1) is 60.0 km s^{-1} with 36 degrees of freedom, while the r.m.s. deviation from the fit to an elliptical orbit is 59.6 km s^{-1} with 34 degrees of freedom. The difference is not significant, and the values of γ and K_2 are not changed. Also, the pattern of O-C residuals for the fit to an eccentric orbit is virtually the same as that of Figure 4, which is for the circular orbit: corresponding points lie above and below the axes in the two cases. The circular orbit fits the data as well as the elliptical one does.

IV. DISCUSSION

a) Errors

The least-squares value of ϕ_o indicates that spectroscopic conjunction occurs slightly but significantly before the time of mid-eclipse predicted by the ephemeris of Arnold, Berg, and Duthie (1976). This phase difference is in the same sense and of the same size as that found by Smak (1976) in his investigation of the emission line radial velocities of U Geminorum, and is to be expected, since the eclipse is supposed to be due primarily to the occultation of the bright spot, which moves ahead of the line joining the centers of the two stars. The present result serves to establish a fiducial epoch for spectroscopic conjunction, but it is not clear whether the photometric variations were occurring "on schedule" during 1978 November. (The time of U Gem's primary eclipse drifts relative to any simple ephemeris, depending

inter alia on the interval which has elapsed since the previous outburst. However, Arnold, Berg, and Duthie based their ephemeris on eclipse observations made well after eruptions of the U Gem system, so that the present data, which refer to a time about 17 days after the start of an outburst (Bortle 1978), may be expected to adhere to this schedule.) The scatter of Arnold, Berg, and Duthie's eclipse timings about their parabolic regression line is about 0.0003 day or about 0.002 of one orbit.

The γ velocity fitted to the data of this paper differs significantly from the emission line γ velocity (γ_{em} = +42 km s^{-1}, Kraft 1962; γ_{em} = +40 ± 6 km s^{-1}, Smak 1976). This discrepancy should not be taken too seriously until the present result has been confirmed by additional work. It is encouraging to note, however, that the residuals for the two nights of data are scattered more or less evenly about zero, even though different templates and different radial velocity standard stars were used for the two nights; this suggests that systematic errors arising from an improper calibration at this step should not amount to more than about 20 km s^{-1}.

The principal interest lies in the third fitted parameter, K_2. There is ample reason to expect some form of systematic error in the velocities, primarily because the cross-correlation function may be distorted by telluric absorption features. It would clearly be desirable to repeat the determination of the orbital elements of U Gem B in some

region of the spectrum where this would pose less of a problem. The residuals to the least-squares fit are nonetheless distributed normally, so the formal standard error of $\pm$ 15 km s^{-1} is probably a realistic assessment of the error in determining the apparent velocity semi-amplitude of U Gem B.

There are two phenomena which may cause the observed value of K_2 to differ from the true (dynamical) value of K_2. First, U Gem B is nonspherical ("distortion effect"). Second, hard radiation is incident upon one hemisphere of U Gem B from the neighborhood of the white dwarf primary star ("heating effect"). The result of both of these effects is to move the photocenter of the secondary star in the light of a particular absorption line away from the mass center of the star. Rotation of the star will then cause the observed velocity to be larger or smaller than the true velocity, according as the photocenter is further away from or closer to the center of mass of the binary system. (The second effect has been discussed briefly in connection with cataclysmic variables by Kiplinger (1979) and by Cowley, Crampton, and Hutchings (1980); see also Batten (1973) and references therein.) The equatorial velocity of U Gem B is probably about 130 km s^{-1} (assuming synchronous rotation; Warner 1976) and $i \approx 67°$. If the photocenter of the Na I doublet is displaced ε (radii) from the center of mass of the star, then the dynamical value of K_2 will differ by about 120ε.

km s^{-1} from the apparent value of K_2.

An estimate of the size of the distortion and heating effects can be made as follows. Wilson and Sofia (1976) have modelled the distortion effect for early-type stars in binary systems with extreme mass ratios. An extrapolation from their results, for the cases where the Roche-lobe filling star is 100, 10, or 3.3 times more massive than the companion, to the case of U Gem where the Roche-lobe filling star is about 1/3 as massive as its companion, indicates that the maximum deviation of the observed velocity curve from the true velocity curve of U Gem B should be less than about 10 percent. Moreover, the sign of the deviation changes four times per orbit, so that to first order its effect on the measured value of K_2 cancels out. The heating effect is also small. U Gem B intercepts only about 2 percent of the radiation from the neighborhood of the white dwarf primary (assuming that this radiation is isotropic). From Section IV (c), the luminosity of U Gem B is about 5×10^{31} erg s^{-1}. Combining the estimate $M_V \approx 10.4$ from Wade (1979) for the radiation from the white dwarf and the disk with a bandpass of about 10^{16} Hz gives a crude luminosity estimate of 3×10^{32} erg s^{-1}. The incident flux thus amounts to only about 0.1 of the luminosity of U Gem B. The displacement of the photocenter will probably be much less than 0.1 radii. It thus appears safe to assume that $K_2 = 284$ km s^{-1} does represent the true orbital motion of U Gem B.

b) m_1

In addition to K_2, i and K_1 are required in order to determine m_1 and m_2. The observed value of K_1 is 143 ± 10 km s^{-1} (Smak 1976). However, Smak measured K_1 from the peaks of the (doubled) emission lines. These peaks arise in the outer parts of the accretion disk (Smak 1969, Huang 1972), where non-Keplerian motions due to the presence of the secondary star cause the observed K_1 to differ from the true K_1, which is the motion of the central star (Paczynski 1977). The ratio K_1(observed)/K_1(dynamical) depends on both the mass ratio $q = m_2/m_1$ and on the size of the accretion disk. The size of the accretion disk and the orbital inclination must be derived from a detailed analysis of the eclipse phenomena, and for this purpose, it is necessary to know q (the trajectory for a test particle falling toward the primary star from the Ll point depends on the mass ratio). Thus the masses of the U Gem system must be found by an iterative process or by comparing observations with numerical models.[1]

---

[1] If K_1 is measured from the wings of the emission lines, rather than the peaks, q can be found immediately. This is because the wings represent high velocity material moving in near-circular orbits close to the surface of the white dwarf.

Smak (1976) has performed the necessary model-building, based on the emission velocities and the eclipses, without making use of K_2. It is therefore possible to compare the observed value of K_2 derived in this work with predictions of K_2 from Smak's analysis. Table 4 of Smak (1976) sets forth three solutions for the masses and orbital parameters of U Gem, which cover the range of uncertainty allowed by Smak's data. Table 3 of this paper recapitulates his values and adds predicted values of K_1 and K_2. An inclination of 67° is assumed, and the changes in K_1 and K_2, denoted by ΔK_1 and ΔK_2, when i is changed by ±8° are indicated.

It can be seen that the prediction of model A agrees with the observed value of K_2, while models B and C are ruled out. (Note that the true values of K_1 are much smaller than the observed value of 143 km s^{-1}.)

The mass function from the present determination of K_2 is

$$\frac{PK_2^{\,3}}{2\pi G} = \frac{m_1^{\,3} \sin^3 i}{(m_1 + m_2)^2} = 0.420 \pm 0.066\ M_\odot$$

so that

$$m_1 = \frac{(0.420 \pm 0.066)}{\sin^3 i}\ (1 + q)^2\ M_\odot$$

Taking $q = m_2/m_1 = 0.37 \pm 0.03$ from Smak's model A, and using $i = 67° \pm 8°$, it can be seen that

$$m_1 = 1.01 \pm 0.25\ M_\odot$$

TABLE 3

SMAK'S MODELS FOR U GEMINORUM[1]

Model	A	B	C
m_2/m_1	0.37	0.43	0.54
m_1 ($M_\odot$)	0.97	0.77	0.61
m_2 ($M_\odot$)	0.36	0.33	0.33
K_1, pred (km s^{-1})	104	108	120
K_2, pred (km s^{-1})	280	252	222
ΔK_1 (km s^{-1})	+5 -7	+5 -7	+6 -8
ΔK_2 (km s^{-1})	+14 -19	+12 -17	+11 -15

[1] K_1, pred and K_2, pred are based on an assumed inclination of 67 degrees. The changes in K_1 and K_2 if the inclination is changed by 8 degrees either way are indicated also.

c) m_2

The determination of K_2 does not help to decrease the size of the errors of m_2 directly, because K_2 mostly reflects the mass of the primary star. Once a directly measured value of K_1(dynamical) becomes available, q will be known directly, and it will be possible to rediscuss the determination of m_2. The impact of the present work on our knowledge of m_2 comes mostly in the form of increased confidence that Smak's unconventional solution of the U Gem system is basically correct (it has been shown how a knowledge of K_2 allows the correct value of m_1 to be chosen).

Smak's estimate of $0.36 \pm 0.10\ M_\odot$ is the most reliable value for the mass of U Gem B. The remainder of this section is a discussion of the star's physical state. The mass and the mean density combine to give the radius of U Gem B:

$$r_2 = 0.43 \pm 0.04\ R_\odot .$$

From the observed M4.5 spectral type, the effective temperature of U Gem B is 3000 ± 160 K (Veeder 1973; T. B. Ake 1979, private communication), so that

$$L_2 = 4\pi r_2^2 \sigma T^4 = (0.014 \pm 0.004)\ L_\odot .$$

These values can be compared to

$$M = 0.237\ M_\odot \qquad T = 3150\ K$$

$$R = 0.252\ R_\odot \qquad L = 0.0055\ L_\odot$$

for the dM4e star CM Draconis A (Lacy 1977). Thus U Gem B is overluminous compared to a main-sequence star of similar

spectral type (as was pointed out by Wade 1979). This is because the surface of the star is cool for its mass, while its radius is large:

$$\frac{r_2}{m_2} = \left(\frac{3}{4\pi\bar{\rho}m_2^2}\right)^{1/3} = (1.20 \pm 0.19)\ \frac{R_\odot}{M_\odot}$$

It is therefore inadvisable to assume that the masses or radii of the secondary stars in dwarf novae and other cataclysmic variables can be inferred from the observed spectral type, merely by assuming that they are just like main-sequence stars.

The lower main-sequence mass-luminosity relation (Veeder 1973),

$$\log (L/L_\odot) = (-0.72 \pm 0.12) + (2.2 \pm 0.2) \log (M/M_\odot)$$

can be used to predict the luminosity of U Gem B:

$$L_{2,\text{predicted}} = 0.020\ (+0.020, -0.010)\ L_\odot\ .$$

It is therefore not possible to tell whether U Gem B is over- or underluminous for its mass. Even if the mass of U Gem B were known perfectly, the uncertainty in the predicted luminosity would be reduced by a factor of 1.4 only.

V. CONCLUSION

This paper reports the determination of K_2, the radial velocity semi-amplitude of U Geminorum B, based on observations of the near-infrared Na I absorption doublet. Spectroscopic conjunction occurs 0.026 ± 0.007 periods before mid-eclipse of the bright spot. K_2 is determined well

enough to discriminate among Smak's (1976) solutions for the masses of the stars in the U Geminorum system. The white dwarf primary star is massive, $m_1 = 1.01 \pm 0.25\ M_\odot$. The best estimate for the mass of the secondary star continues to be Smak's value of $0.36 \pm 0.10\ M_\odot$. Based on this mass and a previous determination of its spectral type (Wade 1979), U Gem B is overluminous for its spectral type, too cool for its mass, and (tentatively) too large compared to an $0.36\ M_\odot$ zero-age main sequence star. It is not possible to say whether the luminosity of U Gem B is appropriate for its mass.

The result that U Gem B seems to be larger than a ZAMS star of the same mass casts some doubt on those studies of cataclysmic variables where the component masses have been determined under the assumption that the secondary star obeys some particular mass-radius relation. It would be useful for future studies of that kind to explicitly state how the derived masses would change if the assumed ratio $R = r_2/m_2$ were changed by some standard amount (say 0.1 in solar units), so that the potential systematic errors in the masses due to this assumption can more readily be borne in mind by the reader.

REFERENCES

Abt, H. A., and Biggs, E. S. 1972, Bibliography of Stellar Radial Velocities (Tucson: Kitt Peak National Observatory).

Arnold, S., Berg, R. A., and Duthie, J. G. 1976, Ap. J., 206, 790.

Batten, A. H. 1973, Binary and Multiple Systems of Stars (Oxford: Pergamon Press), Ch. 5.

Boeshaar, P. 1976, Ph.D. Thesis, Ohio State University.

Bortle, J. 1978, A.A.V.S.O. Circ., No. 97.

———. 1979, A.A.V.S.O. Circ., No. 100.

Cowley, A. P., Crampton, D., and Hutchings, J. B. 1980, preprint.

Griffin, R. F. 1967, Ap. J., 148, 465.

———. 1971, M.N.R.A.S., 155, 1.

Huang, S. 1972, Ap. J., 171, 549.

Kiplinger, A. L. 1979, Astron. J., 84, 655.

Kraft, R. P. 1962, Ap. J., 135, 408.

Lacy, C. H. 1977, Ap. J., 218, 444.

Mochnacki, S. W., and Schommer, R. A. 1979, Ap. J., 231, L77.

Paczynski, B. 1977, Ap. J., 216, 822.

Papaloizou, J. C. B., and Whelan, J. A. J. 1973, M.N.R.A.S., 164, 1.

Shectman, S. A., and Hiltner, W. A. 1976, P.A.S.P., 88, 960.

Smak, J. 1969, Acta Astr., 19, 155.

———. 1971, Acta Astr., 21, 15.

———. 1976, Acta Astr., 26, 277.

Stauffer, J., Spinrad, H., and Thorstensen, J. 1979, P.A.S.P., 91, 59.

Stover, R. J., Robinson, E. L., Nather, R. E., and Montemayor, T. J. 1980, preprint.

Tonry, J., and Davis, M. 1979, Astron. J., 84, 1511.

Veeder, G. J. 1973, Ph.D. Thesis, California Institute of Technology.

Wade, R. A. 1979, Astron. J., 84, 562.

Warner, B. 1976, Structure and Evolution of Close Binary Systems, P. Eggleton et al., eds. (Dordrecht: Reidel), 85.

Warner, B., and Nather, R. E. 1971, M.N.R.A.S., 152, 219.

Wilson, R. E., and Sofia, S. 1976, Ap. J., 203, 182.

Young, P. J., and Schneider, D. P. 1979, Ap. J., 230, 502.

FIGURE CAPTIONS

Fig. 1 A representative sample of the cross-correlation functions from 1978 November 4. From the top of the figure down are presented functions for the M dwarf G 87-26, and for U Geminorum at orbital phases 0.04, 0.88, and 0.31. The peaks which correspond to the radial velocity of U Gem B are indicated. Tick marks along the vertical axis indicate the approximate level of the cross-correlation functions at large displacements.

Fig. 2 A schematic illustration of the cross-correlation function versus time, for the data of 1978 November 4. Filled circles represent maxima which are higher than 65% of the total range in each cross-correlation function; open circles are peaks which lie between 0.25 and 0.65 of the total range. The solid line indicates a crude prediction (to the nearest pixel) of the location of the principle maximum, based on an assumed value of $K_2 = 280$ km s^{-1}. The broken lines represent predictions of where the secondary maxima (the "sidelobes" of the cross-correlation function) should lie. The agreement is satisfactory; in particular, the sidelobes closely follow the behavior of the main maximum, showing that the Na I doublet was actually detected.

Fig. 3 The heliocentric radial velocity of U Gem B versus photometric phase ϕ_{ph}. Filled circles represent the observations from 1978 November 3, and crosses represent the data of 1978 November 4. The curve represents the least-squares best fit to equation (1).

Fig. 4 The residuals, observed minus calculated values, to the least-squares curve of Figure 3. The symbols retain their meanings from Figure 3.

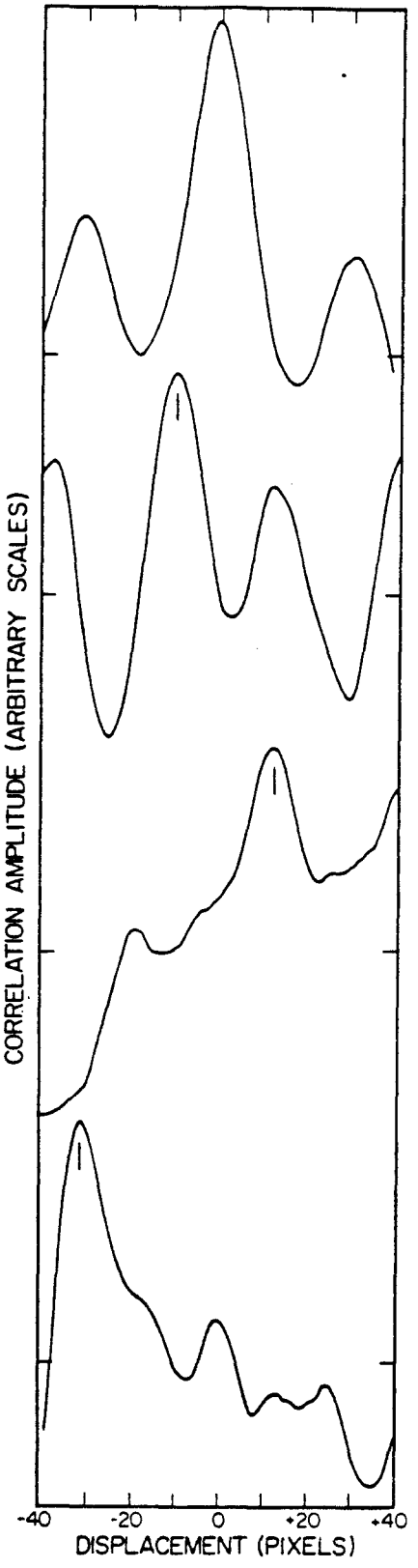
CORRELATION AMPLITUDE (ARBITRARY SCALES)
-40
-20
0
+20
+40
DISPLACEMENT (PIXELS)

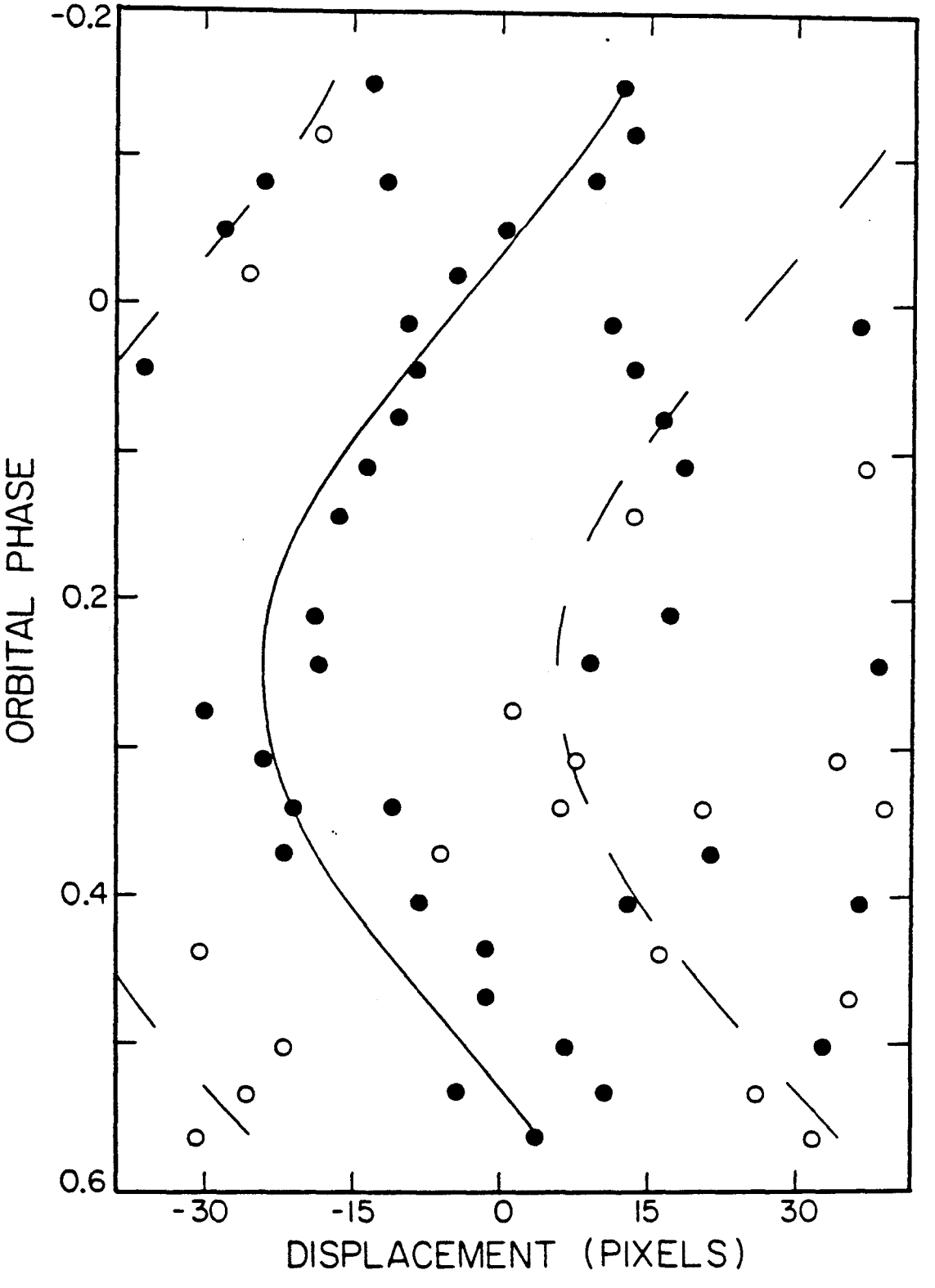
-0.2
0
0.2
0.4
0.6
ORBITAL PHASE
-30
-15
0
15
30
DISPLACEMENT (PIXELS)

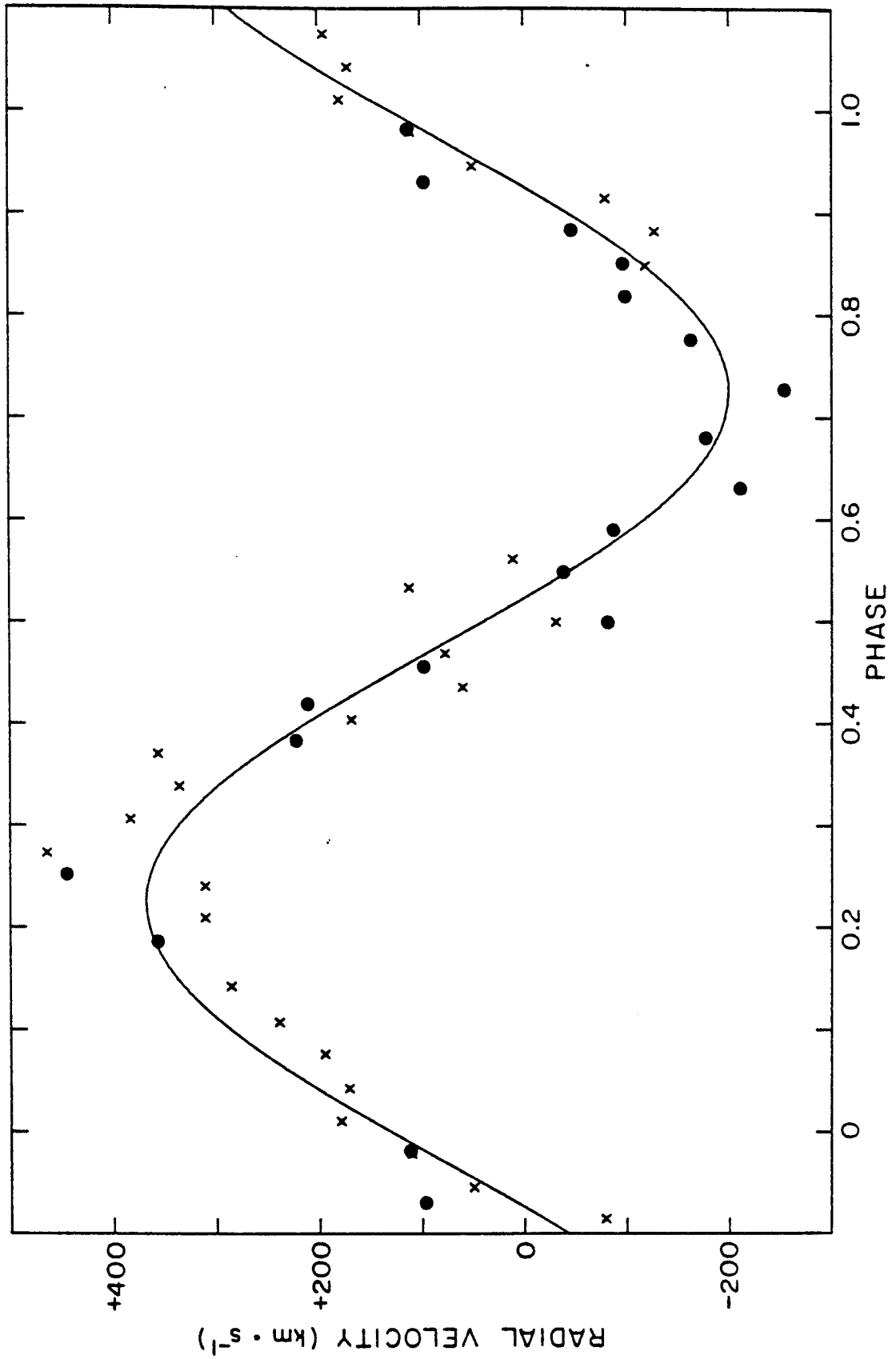
RADIAL VELOCITY (km · s⁻¹)
+400
+200
0
-200
0
0.2
0.4
0.6
0.8
1.0
PHASE

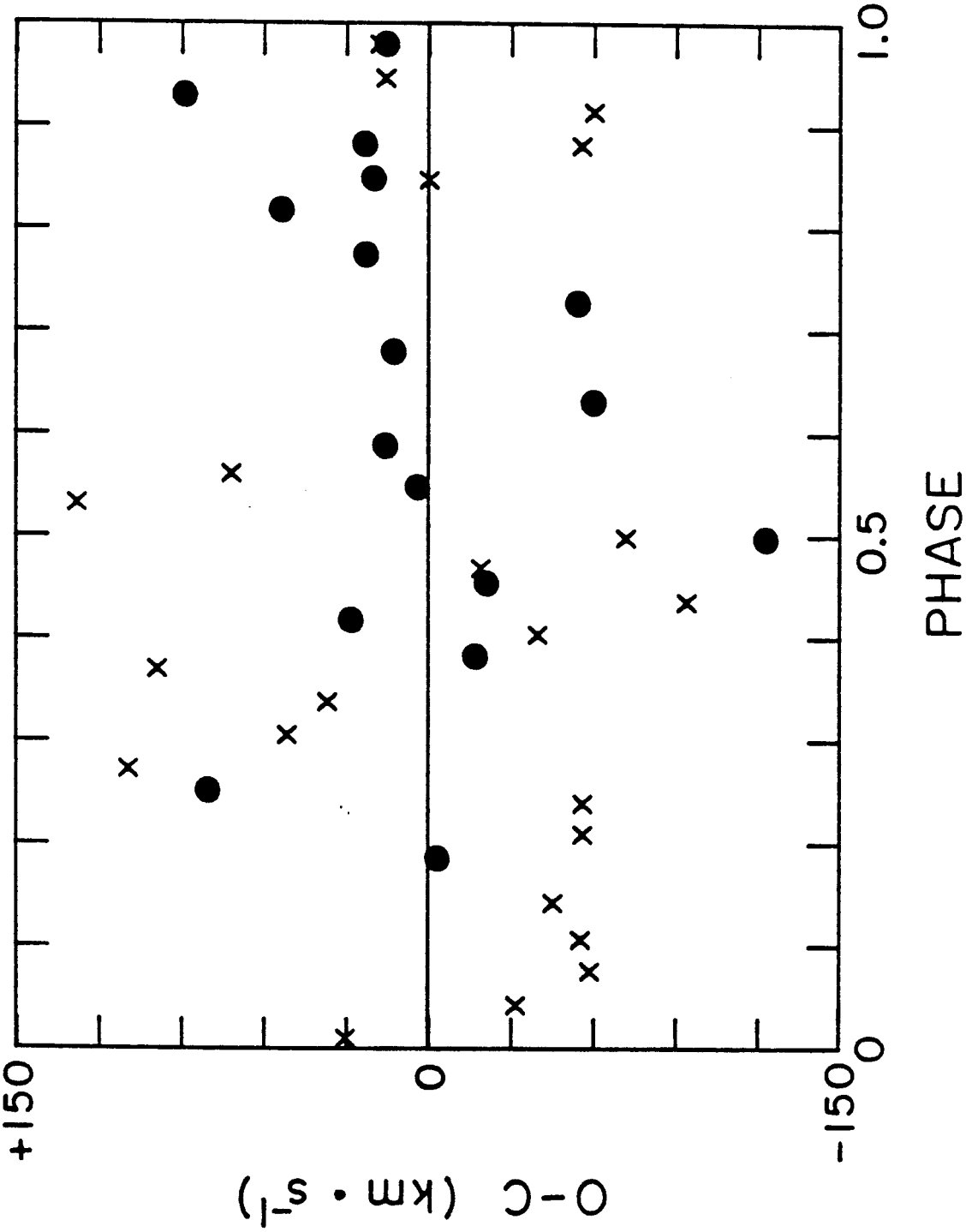
+150
0
-150
0
0.5
1.0
PHASE
O-C (km • s⁻¹)

CHAPTER 4

A SPECTROPHOTOMETRIC SURVEY OF CATACLYSMIC VARIABLE STARS

"Data! data! data!" [Holmes] cried impatiently. "I can't make bricks without clay."

- A. Conan Doyle
  The Adventure of the Copper Beeches

I. INTRODUCTION

Since in dwarf novae and other cataclysmic variable stars the secondary stars generally are red and the other components of light (the white dwarf, the accretion disk or ring, and the bright spot in the accretion disk) generally are blue ($f_\nu \simeq$ constant), it makes sense to study the secondary stars in the red part of the spectrum, where the blue components will provide less contamination. For example, in Chapter 1 it was shown that the secondary star in U Geminorum could be detected spectrophotometrically in the spectral region longward of $\lambda = 6000$ Å.

In view of these considerations, it was decided to observe a sample of dwarf novae and other cataclysmic variable stars using the multichannel spectrophotometer (MCSP) on the 5m Hale reflector. The exceptionally wide wavelength coverage of the instrument makes it ideal for detecting the presence of the secondary stars if it is possible to do so (see Chapter 1). For the same reason, the data gathered in this survey will be useful for (1) characterizing the spectral energy distribution of the accretion disk and other components of the "blue" light, (2) providing for the first time accurate emission line fluxes, which will be valuable for understanding physical conditions in the cataclysmic variables, and (3) in combination with infrared, ultraviolet, and x-ray data providing the largest possible wavelength coverage of cataclysmic variables. This wavelength coverage

is required in order to adequately test current and future models of accretion disks.

II. OBSERVATIONS

The MCSP has been described by Oke (1969). The data presented here were acquired in general by observing each star in each of two round focal-plane apertures, using the other aperture for simultaneous sky subtraction. For the bandpasses of 40 Å in the blue ($\lambda \leq$ 5760 Å) and 80 Å in the red, five settings of the grating angle are required to obtain complete spectral coverage from 0.32 micron to 1.1 micron. A few objects were observed with wider bandpasses (80 Å in the blue, 160 Å in the red) or with incomplete coverage in the red portion of the spectrum. For these objects, which are noted in Table 1, fewer changes of the grating angle were required.

Table 1 presents the Journal of Observations and some remarks on the quality of each spectrum. The MCSP observations were obtained by J. B. Oke. The spectrum of CN Ori was obtained by J. L. Greenstein. The goal was to obtain the spectral energy distribution of each object, so the aperture sizes (generally either 7 or 10 arcseconds in diameter) were chosen to assure that none of the light incident from the star was excluded at the focal plane. Reduction of the data from photon counts to absolute fluxes was done using standard sky-subtraction techniques, correcting for

TABLE 1

JOURNAL OF OBSERVATIONS

Object	JD 2440000+	Visual Mag.	Quality[1]	Remarks[2]
Old Novae				
V603 Aql	4173.67	11.6	B	sm
BT Mon	3542.81	15.4	B	
Nova-like Objects				
TT Ari	4173.91	11.4	B	sm, = BD +14°341
RW Tri	3485.69	14.2	B	sm, ph = 0.69
UX UMa	3213.92	12.7	A	ph = 0.77
Dwarf Novae in Outburst				
Z Cam	3486.88	12.3	B	3, ab, standstill
SY Cnc	3866.05	12.3	A	4
YZ Cnc	3867.01	11.5	A	super-outburst
EM Cyg	3336.97	12.2	A	
SS Cyg	3335.95	8.5	A	nbp
AB Dra	4173.69	13.9	A	
Dwarf Novae in Quiescence				
RX And	3485.67	14.4	B	sm
AE Aqr	4172.69	11.3	A	
SS Aur	3485.01	14.6	A	
Z Cam	4026.67	13.6	A	
YZ Cnc	4024.66	14.9	B	
WW Cet	3485.64	14.2	B	
EM Cyg	4024.97	13.6	A	
SS Cyg	3485.62	11.7	A	
U Gem	3213.79	14.5	A	wbp, ph = 0.67
AH Her	4023.97	13.9	A	
EX Hya	4294.91	13.7	C	5, ph = 0.5
T Leo	3543.06	15.8	B	
X Leo	3543.75	15.9	B	
AY Lyr	4025.83	17.8	C	
CN Ori	4191.00	....	A	6, wbp, ab
RU Peg	3337.98	12.6	A	
BX Pup	4294.74	16.6	C	5
WZ Sge	3337.96	15.4	A	
SU UMa	3485.03	14.8	B	sm
Other				
AM CVn	3867.02	14.1	A	= HZ 29

NOTES TO TABLE 1

[1]See text for description of the Quality index.

[2]The following general symbols are used: sm = smoothed spectrum, ph = orbital phase, nbp = narrow bandpasses were used (20 Å in the blue, 40 Å in the red), wbp = wide bandpasses were used (80 Å in the blue, 160 Å in the red), ab = old (AB69) spectral energy distributions for the standard stars were used.

[3]Z Cam: AAVSO records indicate the star was near magnitude 11.7; clouds were suspected but not seen at Palomar.

[4]SY Cnc: the star was probably about 0.5 mag below maximum light.

[5]EX Hya and BX Pup: these stars were observed at high airmass, and some of the ultraviolet light was not detected.

[6]CN Ori: heavy cirrus; AAVSO records indicate the star was near magnitude 14 at the time of observation.

atmospheric extinction using mean coefficients, and calibrating the instrumental response by nightly observations of secondary standard stars. These procedures have been described in greater detail by de Bruyn and Sargent (1978). Recently updated values for the extinction coefficients and absolute fluxes of the MCSP standard stars have been used (Oke 1980).

When necessary, the fluxes in certain wavelength bins have been corrected by hand to account for residual uncertainties in the absolute fluxes of the standards or for easily identifiable instrumental difficulties. The size of the corrections was determined by demanding that the instrumental response of the MCSP vary smoothly with wavelength or that overlapping observations (from adjacent photomultiplier tubes at different grating settings) agree. Particular attention was paid to the wavelength regions near the Balmer discontinuity and the hydrogen Balmer lines. In cases where corrections could not be made with certainty, the dubious points have been deleted from the spectrum. The overall point-to-point consistency of the spectra, after these corrections and excluding consideration of photon-counting statistics, is about 2 per cent.

One factor which affects the quality of some of the spectra is the intrinsic variability of cataclysmic variable stars. The flickering timescale for some objects is shorter than the 10^3 seconds typically needed to obtain a MCSP

spectrum, so that the flux incident from the star may be different for each setting of the grating angle. The result is that the final spectrum has a jagged appearance, with the flickering pattern imposed upon each phototube's section of the spectrum. In practice, this flickering is strong enough to be objectionable only in five of the scans (noted in Table 1), and heavy smoothing of the data has been used to recover the overall spectral energy distribution at the expense of wavelength resolution. The smoothing operation is discussed in detail in the Appendix.

In Table 1, the "Quality" index represents an estimate of the reliability of the spectra. "A" denotes the best data, for which random errors from photon statistics are less than 0.02 mag for wavelengths shorter than 8000 Å and for which no fluctuations during the scan were noted. "B" denotes data having statistical errors in the range 0.02 to 0.04 mag, or where thin clouds or flickering contributed to the scatter of the data. Also included in category "B" are scans which have been smoothed to eliminate the effect of clouds or flickering (see the Appendix) and two scans which are calibrated on the old system of standard star energy distributions. Category "C" contains scans whose random errors exceed 0.04 mag, or where poor atmospheric seeing (at high airmass) caused a portion of the ultraviolet light to be lost at the focal plane.

For the eclipsing variables in Table 1, the approximate orbital phases of the observations are indicated in the Remarks column. The sources for the ephemerides were: RW Tri, Africano et al. 1978, eq. (2); UX UMa, Nather and Robinson 1974; EX Hya, Vogt, Krzeminski, and Sterken 1980; U Gem, Arnold, Berg, and Duthie 1976.

Whenever possible, the AAVSO light curves (Mattei 1980, private communication) for the dwarf novae have been examined to establish whether the stars were in outburst or quiescence when they were observed. In general, the AAVSO magnitudes agree within about 0.2 mag with the AB magnitude at λ5480. Exceptions are Z Cam at standstill (AAVSO = 11.7 mag, AB[5480] = 12.3), where clouds were suspected at Palomar, and CN Ori (AAVSO $\simeq$ 14 mag, AB[5480] = 15.8), where "pretty heavy cirrus" was noted by Greenstein. For some dwarf novae, light curves from AAVSO are unavailable or incomplete, and for these stars the outburst phase was estimated from the known visual magnitudes at outburst and in quiescence. By this criterion, SY Cnc was probably slightly past maximum light during an outburst.

Figures 1 through 4 illustrate these spectra of cataclysmic variable stars. The logarithm of the monochromatic flux density f_ν (per unit frequency interval) has been plotted versus wavenumber $1/\lambda$ (in inverse microns). Tick marks on the ordinate axes are at intervals of 0.4 in log f_ν. The longer horizontal bars on either side of each spectrum

indicate a reference level, and the number printed above the left bar denotes the absolute AB magnitude of the reference level. AB is expressed in magnitudes and is related to f_ν by the expression

$$AB = -2.5 \log (f_\nu) - 48.60$$

where f_ν is in erg cm^{-2} s^{-1} Hz^{-1}. The reference level is chosen to approximate the V magnitude of the object (AB at λ5480 is approximately equal to Johnson V). A wavelength scale is included inside each figure, along the bottom edge; it is labelled in units of 1000 Å. Also indicated at the lower left in each figure are the positions of the A band at λ7600, due to telluric O_2 absorption, and the portion of the infrared spectral region which is severely affected by telluric water vapor and therefore photometrically unreliable.

Objects which are of similar type or which were in similar outburst states when they were observed have been grouped together in the figures. Figure 1 presents two classical post-novae, three UX UMa-type variables, and two dwarf novae in outburst. Also included in Figure 1 is a spectrum of AM CVn = HZ 29.

Figure 2 illustrates spectra of four dwarf novae which were observed both in quiescence and in outburst. The four outburst spectra are at the top of the figure. YZ Cnc was observed in a super-outburst in December 1978, and Z Cam was observed in standstill in December 1977 and again when it briefly dropped to near minimum light in June 1979.

Figures 3 and 4 illustrate spectra of dwarf novae and suspected dwarf novae near minimum light.

III. DISCUSSION

The spectra in Figures 1-4 may with a few exceptions be divided into three groups. The first group contains the old novae, the nova-like (UX UMa-type) systems, and the dwarf novae in outburst (including Z Cam in standstill and YZ Cnc in super-outburst). These spectra show Balmer discontinuities in absorption or no Balmer jump at all. The continua are blue (f_ν = constant or rising with increasing frequency). No trace of a red stellar spectrum is evident. The exceptions are BT Mon and RW Tri. BT Mon, an old nova, is faint and distant, and at galactic latitude -2°.6 must be moderately reddened. Applying a reddening correction E(B-V) = 0.31 mag brings the flux distribution to $f_\nu \simeq$ constant. This correction is consistent with the expected amount, E(B-V) $\simeq$ 0.2 mag from a distance of about 1 kpc (Payne-Gaposchkin 1957; Deutschman, Davis, and Schild 1976). RW Tri shows an upturn in the red which is not easily accounted for by interstellar reddening. Borne (1977) has discussed RW Tri and finds that the MCSP spectrum may be explained by the combined energy distribution of an M0 dwarf and a residual flux of the form f_ν = constant.

The second group of spectra is that of quiescent dwarf novae, such as EX Hya, SU UMa, and YZ Cnc, which show flat

continua with Balmer jumps in emission, as well as the usual emission lines of hydrogen and He I. In this second group of objects there is no trace of the secondary star's spectrum. EX Hya is an eclipsing system whose orbital period is 98 min. The periods of SU UMa and YZ Cnc are not known directly, but indirect arguments based on their membership in the SU UMa subclass (dwarf novae which undergo super-outbursts) suggests that their orbital periods are shorter than about 2 hours (Patterson 1979). In the standard model, the requirement that the secondary star fill its Roche lobe means that for short period systems the secondary stars will be small and probably faint. Thus it is not surprising that no evidence of the secondary stars is seen in the 0.3 to 1.1 micron region for these three systems. Infrared observations of EX Hya in an effort to observe ellipsoidal variations of the secondary star would prove enlightening.

The third group of spectra consists of dwarf novae which show evidence for the presence of a late-type stellar component. These included well studied stars such as AE Aqr, SS Cyg, and RU Peg, and previously unknown secondaries such as CN Ori and AH Her. Some cases are marginal; BX Pup, for example, seems to show an upturn in the red, but the quality of the spectrum is not high and the corresponding decomposition of the spectrum into red star and the residual light will not be very precise. AY Lyr is similarly tantalizing but also not suitable for a detailed discussion. (AY Lyr

also probably has an orbital period shorter than 2 hours (Patterson 1979), suggesting that the secondary star would not be seen in the MCSP spectral range).

T Leo shows especially strong emission in the Balmer lines and the Balmer jump. It is possible that this is related to the long mean interval between outbursts for this system. No secondary star is visible in T Leo.

A few stars do not fall neatly into one of the three groups discussed above. AM CVn = HZ 29 is a system with ultrarapid photometric variations (P = 18 min). Robinson and Faulkner (1975) have suggested that HZ 29 is a system similar to the other cataclysmic variables, except that both stellar components are degenerate stars with hydrogen envelopes. In such a case, one would of course not expect to see a late-type dwarf spectrum. WZ Sge seems to share characteristics of the dwarf novae and the recurrent novae. The period between successive outbursts is about 30 years like the recurrent novae, but the orbital period is 82 minutes, quite unlike the 227 day period of the recurrent nova T CrB. The quiescent spectrum of WZ Sge shows no trace of a red star. This is not surprising because the mass ratio m_2/m_1 must be very small (Robinson, Nather, and Patterson 1978; Fabian et al. 1978; Ritter and Schroeder 1979).

APPENDIX

SMOOTHING MULTICHANNEL DATA

With the MCSP and the relatively narrow bandpasses that were used, it is necessary to make several settings of the grating angle in order to observe the full spectrum from 0.32 to 1 micron with no gaps. If the light incident from the star changes during the course of these several observations, due to intrinsic variability or to obscuration by clouds, then the resultant spectrum must be smoothed by a running average.

The smoothing process will recover the original spectral energy distribution, provided that each point in the smoothed spectrum contains a fixed contribution from each grating setting (the weightings of different grating settings need not be equal in general). In this case the overall brightness level of the smoothed spectrum will be in error by some amount, but the error will be the same for each point in the new spectrum. Wavelength resolution is of course lost by the smoothing process.

The effective wavelengths of points in the new spectrum (interpolated by the same running average) will differ from the original wavelengths. To keep the even wavelength spacing of the data points in the blue part of the spectrum, we have deleted the points corresponding to one of the two

cycles which overlap in the blue. The resulting irregular wavelength spacing in the red is of little concern.

REFERENCES

Africano, J. L., Nather, R. E., Patterson, J., Robinson, E. L., and Warner, B. 1978, Pub. A. S. P., 90, 568.

Arnold, S., Berg, R. A., and Duthie, J. G. 1976, Ap. J., 206, 790.

Borne, K. D. 1977, Bull. AAS, 9, 556.

deBruyn, A. G., and Sargent, W. L. W. 1978, A. J., 83, 1257.

Deutschman, W. A., Davis, R. J., and Schild, R. E. 1976, Ap. J. Suppl., 30, 97.

Fabian, A. C., Lin, D. N. C., Papaloizou, J., Pringle, J. E., and Whelan, J. A. J. 1978, M.N.R.A.S., 184, 835.

Kukarkin, B. V. et al. 1969, General Catalogue of Variable Stars, (3rd edition: Moscow: Academy of Sciences in the USSR).

Nather, R. E., and Robinson, E. L. 1974, Ap. J., 190, 637.

Oke, J. B. 1969, Pub. A. S. P., 81, 11.

——. 1980, in preparation.

Patterson, J. 1979, A. J., 84, 804.

Payne-Gaposchkin, C. 1957, The Galactic Novae (Amsterdam: North-Holland).

Ritter, H., and Schroeder, R. 1979, Astr. Ap., 76, 168.

Robinson, E. L., and Faulkner, J. 1975, Ap. J. (Letters), 200, L23.

Robinson, E. L., Nather, R. E., and Patterson, J. 1978, Ap. J., 219, 168.

Vogt, N., Krzeminski, W., and Sterken, C. 1980, Astr. Ap., 85, 106.

Warner, B. 1979, Inf. Bull. Var. Stars, #1707.

Young, A., and Lanning, H. H. 1975, Pub. A. S. P., 87, 461.

FIGURE CAPTIONS

Fig. 1 - Spectral energy distributions of cataclysmic variable stars. The logarithm of the monochromatic flux density (per unit frequency interval) is plotted against $1/\lambda$. The scale inside the figure is wavelength in units of 1000 Å. The distance between tick marks on the vertical axis is 0.4 in log f_ν (1 magnitude). The spectra have been separated by arbitrary vertical shifts. The number at the left of each spectrum is the AB value at the level indicated by the long horizontal bars (see text for definition of AB). Error bars are plotted when the standard deviation due to photon-counting statistics exceeds 0.1 mag. Points for which the error bars would exceed 0.6 mag are omitted. Marks at the lower left of the figure indicate the atmospheric A-band and water vapor absorption regions. See Table 1 for further information about each spectrum.

Fig. 2 - Spectral energy distributions of cataclysmic variable stars. The top four spectra were obtained during outburst or standstill. The bottom four spectra are of the same objects near minimum light. The symbols are the same as in Figure 1.

Fig. 3 - Spectral energy distributions of quiescent dwarf novae. The symbols are the same as in Figure 1.

Fig. 4 - Spectral energy distributions of quiescent dwarf novae. The symbols are the same as in Figure 1.

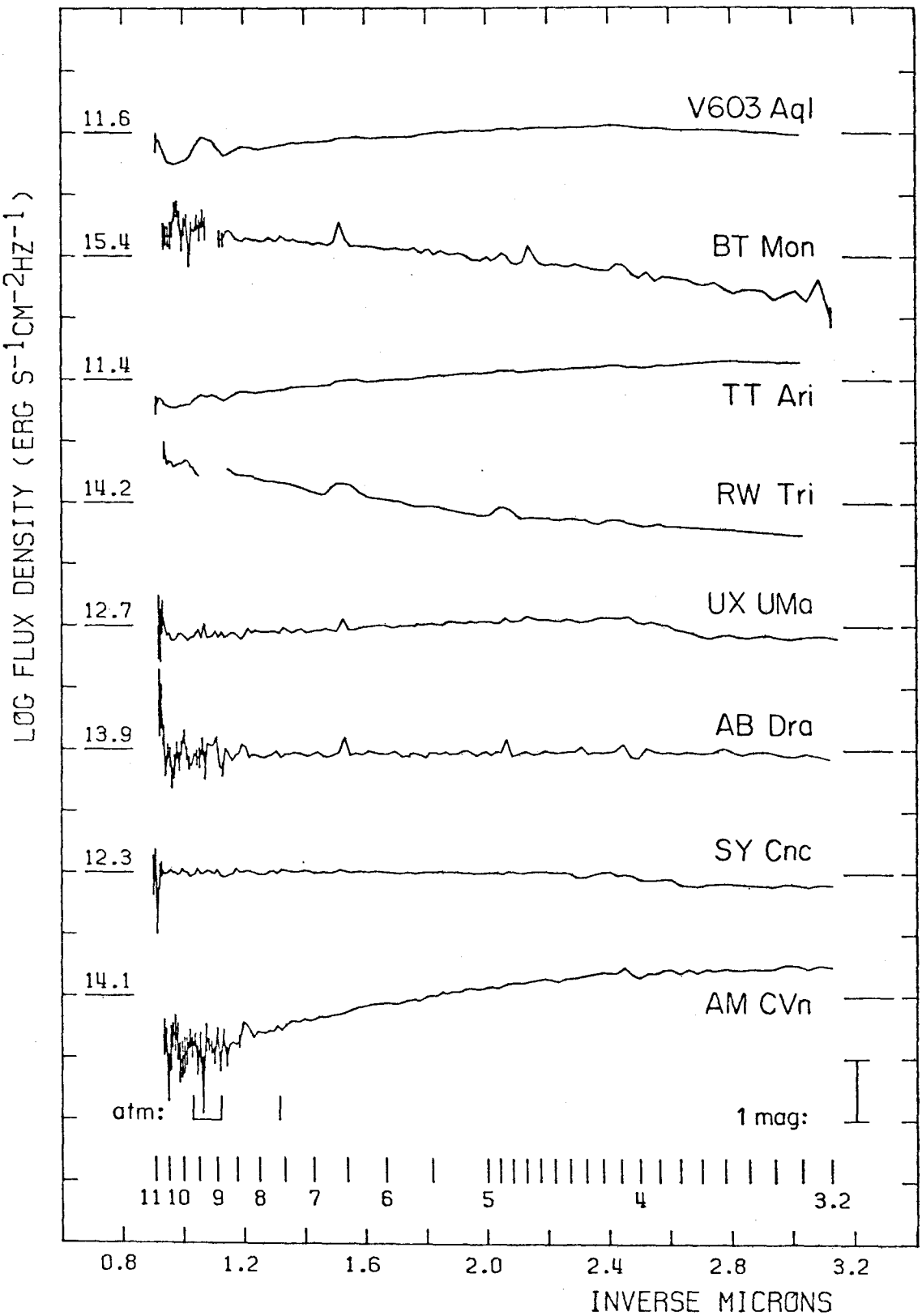
V603 Aql
11.6
BT Mon
15.4
TT Ari
11.4
RW Tri
14.2
UX UMa
12.7
AB Dra
13.9
SY Cnc
12.3
AM CVn
14.1
atm:
1 mag:
11 10 9 8 7 6 5 4 3.2
0.8 1.2 1.6 2.0 2.4 2.8 3.2
INVERSE MICRONS
LOG FLUX DENSITY (ERG S^{-1}CM^{-2}HZ^{-1})

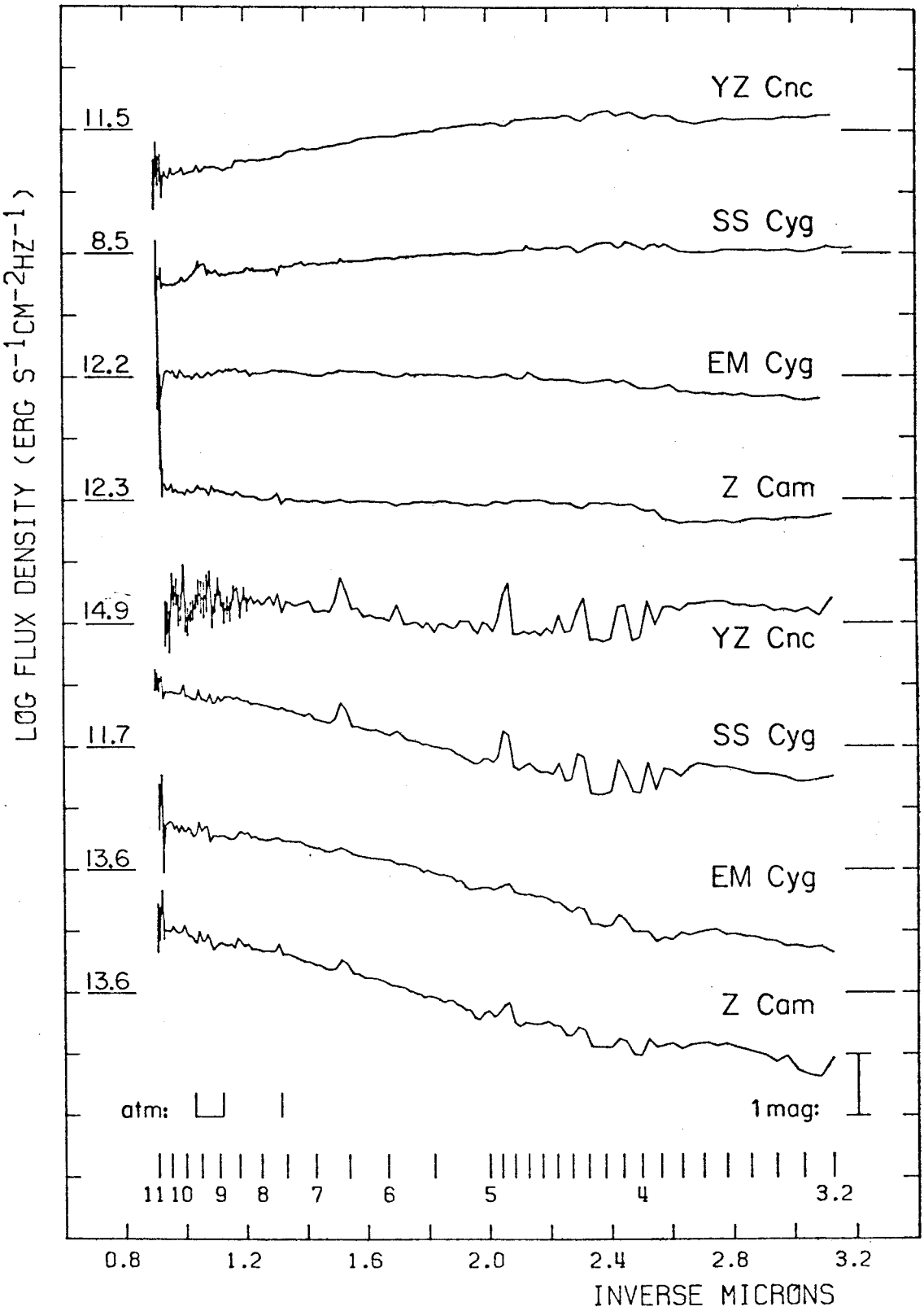
YZ Cnc
11.5
SS Cyg
8.5
EM Cyg
12.2
Z Cam
12.3
YZ Cnc
14.9
SS Cyg
11.7
EM Cyg
13.6
Z Cam
13.6
atm:
1 mag:
11 10 9 8 7 6 5 4 3.2
0.8 1.2 1.6 2.0 2.4 2.8 3.2
INVERSE MICRONS
LOG FLUX DENSITY (ERG S^{-1}CM^{-2}HZ^{-1})

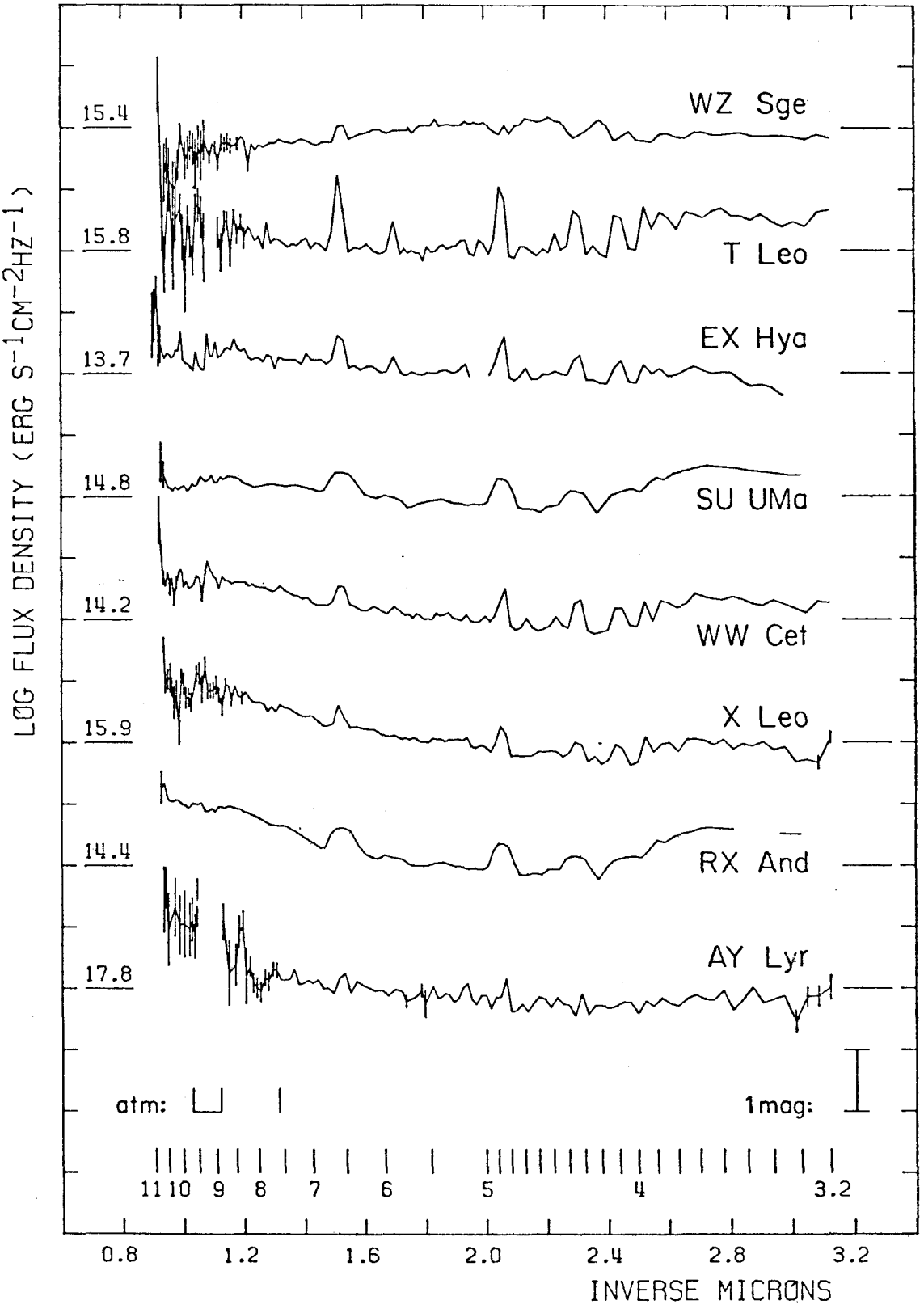
LØG FLUX DENSITY (ERG S^{-1}CM^{-2}HZ^{-1})
15.4
WZ Sge
15.8
T Leo
13.7
EX Hya
14.8
SU UMa
14.2
WW Cet
15.9
X Leo
14.4
RX And
17.8
AY Lyr
atm:
1mag:
11 10 9 8 7 6 5 4 3.2
0.8 1.2 1.6 2.0 2.4 2.8 3.2
INVERSE MICRØNS

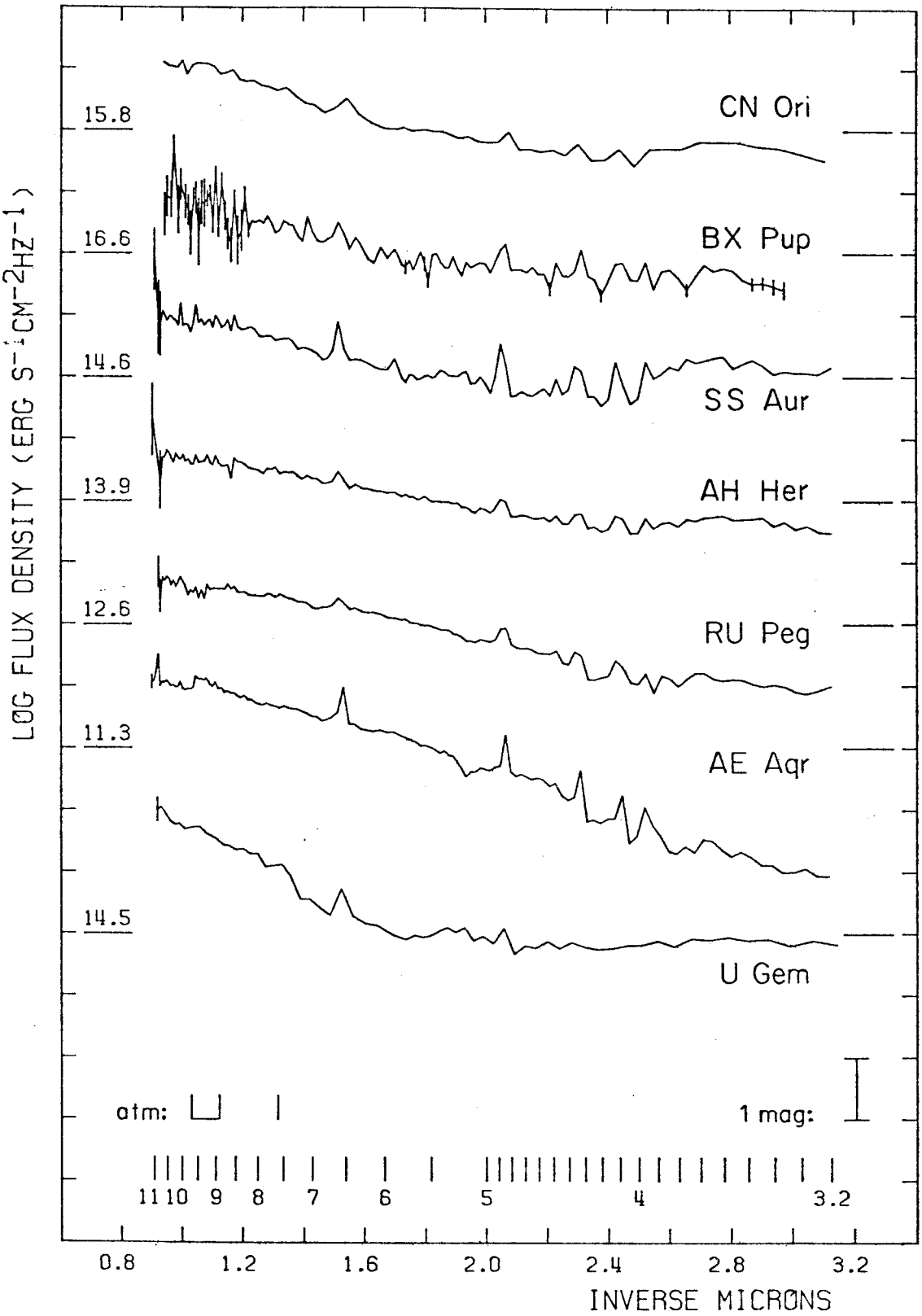
LOG FLUX DENSITY (ERG S⁻¹CM⁻²HZ⁻¹)
15.8
CN Ori
16.6
BX Pup
14.6
SS Aur
13.9
AH Her
12.6
RU Peg
11.3
AE Aqr
14.5
U Gem
atm:
1 mag:
11 10 9 8 7 6 5 4 3.2
0.8 1.2 1.6 2.0 2.4 2.8 3.2
INVERSE MICRONS

CHAPTER 5

ANALYSIS OF CATACLYSMIC VARIABLE STAR ENERGY DISTRIBUTIONS: SPECTRAL TYPES FOR THE SECONDARY STARS AND ABSOLUTE VISUAL MAGNITUDES FOR THE ACCRETION DISKS

I. ANALYSIS OF COMPOSITE SPECTRA

The goal of this chapter is to use the spectral energy distributions described in Chapter 4 to obtain the spectral classes of the secondary stars and the visual absolute magnitudes of the cataclysmic variable systems observed with the MCSP.

From inspection of the figures in Chapter 4, it is apparent that there are some systems, such as AE Aqr, which are dominated by the secondary star, and there are some systems, for example the dwarf novae in outburst, which are dominated by the disk. In the former case it is straightforward to determine the spectral type and magnitude of the secondary star, but the spectrum of the "extra light" (due to the primary star, bright spot if any, and accretion disk) is poorly determined. In the latter case, only an upper limit on the fraction of the light due to the secondary star (as a function of its assumed spectral type) may be determined. It is the intermediate cases, where neither secondary star nor disk dominates, or where the two components dominate in different wavelength intervals, which allow, in principle, the spectra and relative contributions of both components to be determined. Nonetheless, the extreme cases are of interest in establishing the range of luminosities spanned by accretion disks in close binary systems.

The method of spectral decomposition used here is to postulate a spectral type for the secondary star, subtract

varying amounts of this spectrum from the observed composite spectrum, and judge whether the residual energy distribution is physically plausible in terms of what we expect accretion disks to look like. (The residual spectrum includes contributions from the white dwarf primary star and from bright spots, gas streams, etc. The disk is expected to dominate the spectrum in the optical region, however.) From this process, one tries to derive upper and lower limits to the fraction of light (at some standard wavelength) which comes from the secondary star. These steps are repeated for a variety of spectral types, covering the range expected for the secondary star. In favorable cases the range of allowed spectral types, and the range of allowed fractional contributions at each spectral type, will be small enough that the distance and luminosity of the cataclysmic variable system in question can be determined. In less favorable cases, the allowed range of decomposition will not be so restricted, and only broad limits on the luminosity can be obtained. Chapter 2 illustrated the procedure in detail for the case of U Gem.

"Physically plausible" flux distributions for the residual light are those in which:

1) The residual flux is positive everywhere (else too much secondary star light has been subtracted).

2) The residual spectrum does not show spectral features which belong to a late-type star (else not enough secondary spectrum has been subtracted), nor does it show "inverse" late-type spectral features (else too much secondary spectrum has been removed). In other words, the residual spectrum is "smooth" from point to point, except of course for the usual emission lines and features such as the Balmer jump.

3) The overall continuum distribution of the residual light can be built up from known physical processes such as blackbody radiation (or more accurately, radiation from hot stellar atmospheres) and hydrogen recombination radiation.

II. STANDARDS FOR COMPARISON

Table 1 lists eight main sequence stars, which have been used to represent the main-sequence in the subsequent analysis. The three earliest-type stars are members of the Hyades, and for these stars the absolute magnitude AB[λ5500] was derived from the apparent magnitude using an assumed distance modulus of 3.2 mag. The van Bueren (1952) number is given in the remarks column. The remaining stars are from Gliese's (1969) catalog, and the absolute magnitudes AB[λ5500] are derived from trigonometric parallaxes.

TABLE 1

MAIN SEQUENCE STARS[1]

No.	Star	Sp[2]	AB[λ5500] (Absolute)	Flux Ratios[3] x	y	z	Remarks[4]
1	+21°612	K0 V	5.86	0.43	1.40	0.15	= vB 21
2	+15°650	K2 V	6.48	0.36	1.63	0.11	= vB 183
3	+15°616	dK5	7.19	0.22	2.33	0.06	= vB 173
4	Gl 673	K7 V	8.09	0.18	2.93	0.05	
5	Gl 49	M1.5	9.61	0.17	5.08	0.04	SB
6	Gl 15 A	M1.5	10.29	0.14	5.11	0.04	SB
7	Gl 109	M3.5	11.09	0.10	7.31	0.04	
8	Gl 15 B	M4	13.35	0.09	10.73	0.03	

NOTES TO TABLE 1

[1]Stars 1 through 3 are members of the Hyades cluster, for which a distance modulus of 3.20 mag has been assumed. The remaining stars are from Gliese (1969) and have trigonometric parallaxes of good precision.

[2]For the M dwarfs, the spectral classifications are on the system of Boeshaar (1976).

[3]The flux ratios, $x = f_\nu(\lambda 4200)/f_\nu(\lambda 5500)$, $y = f_\nu(\lambda 8000)/f_\nu(\lambda 5500)$, and $z = f_\nu(\lambda 3560)/f_\nu(\lambda 5500)$, have been corrected to the AB79 system.

[4]vB is the van Bueren (1952) number; SB = suspected spectroscopic binary.

The stars in Table 1 were observed by J. E. Gunn, using the narrowest bandpasses available on the MCSP deckers. The data were rebinned to match the 40 Å (blue) and 80 Å (red) passbands typically used by Oke for the observations of the cataclysmic variable stars. The observations of the main sequence stars were reduced using the old (AB69) spectral energy distributions of the standard stars. This makes a difference mostly in the region shortward of λ4000 and near the Balmer lines; since the Balmer jump and the Balmer lines in dwarf novae are in emission during quiescence, these wavelengths are not used directly in judging the plausibility of the residual fluxes.

The other difference between the old and new (AB79) calibration systems is that the slope of the Paschen continuum is slightly different in the two systems. To assess the significance of this effect, three MCSP spectra having widely different continuum slopes were reduced using both old and new calibrations; for each star the balance-factors and choice of standard stars were the same for both reductions. The result is that if the two spectra are matched up at λ7000, then the AB79 spectrum is ∿0.06 mag fainter at λ10000 and ∿0.10 mag fainter at λ4000. Thus the overall difference in slope is only about 0.04 mag from 0.4 to 1.0 micron, and the uncertainty in the size of the correction is somewhat less. The flux ratios x, y, and z, listed in Table 1, have been corrected to the AB79 system.

The stars in Table 1 have been used to establish a color-magnitude relation for the main sequence. The absolute magnitude at 5500 Å is related to the color $Y = 2.5$ [log $f_\nu(\lambda 8000)$ - log $f_\nu(\lambda 5500)$] by

$$AB[\lambda 5500] = 4.97 + 2.60\ Y, \quad Y \leq 2.0 \text{ mag}$$
$$AB[\lambda 5500] = -0.53 + 5.38\ Y, \quad Y \geq 2.0 \text{ mag} \qquad (1)$$

Stars 1 through 4 were used to define the first relation, while stars 7 and 8 were used to define the second relation. The two M1.5 stars were omitted because they are suspected spectroscopic binaries (Gl 49 = +61°195, Joy and Mitchell 1948; Gl 15 A = HD 1326 A, Abt 1970). The residuals to the color-magnitude relation given by equation (1) are generally about 0.1 mag, but it must be expected that equation (1) does not define the main sequence to better than 0.5 mag, both because few stars were used and because there is an intrinsic width of $\Delta M_V \simeq \pm 0.4$ mag on the main sequence (Upgren 1973).

A principal assumption of the decomposition technique is that the spectrum of the secondary star can be represented adequately by a main-sequence dwarf. Giant spectra are not useful, because for orbital periods shorter than 12 hours, the radius of the secondary star must be $\leq 1\ R_\odot$, so that the surface gravity is close to that of a main-sequence star. If the star is rotating rapidly, there will be a small reduction in the effective gravity and the spectral lines will

be broadened, but the kinds of spectral features, their equivalent widths, and the slope of the continuum will still be those of some late-type main-sequence star.

III. THE FLUX-RATIO DIAGRAM

The first condition listed in Section I for a physically plausible residual energy distribution is easy to satisfy. The eye does well in judging whether the second condition is satisfied, by inspecting plots of the residual spectrum. The eye does not do so well in trying to use the third condition, which constrains the overall shape of the distribution. Given a smooth curve (residual flux versus wavelength), the eye cannot easily judge whether such a curve can be made by a suitable sum of blackbodies and recombination spectra, and to attempt to find such a combination by trial and error is a tedious process which is not guaranteed to give a correct answer. For this reason, a flux-ratio diagram was used first, as an objective means to reject those combinations of spectral type and flux fraction that result in residual continuum distributions which violate the third condition. The flux-ratio technique was introduced by Rabin (1980).

A flux-ratio diagram is one in which the ratios of monochromatic fluxes are plotted on a linear scale, rather than a logarithmic scale as in a two-color diagram. Figure 1 shows such a diagram, with the ratio $f_\nu(\lambda 8000)/f_\nu(\lambda 5500)$ plotted against $f_\nu(\lambda 4200)/f_\nu(\lambda 5500)$. The loci of blackbodies,

power laws, recombination spectra, and late-type dwarf stars are shown. The flux ratios for recombination spectra are based on pure hydrogen bound-free and free-free radiation in a Maxwellian gas. The spectra were calculated from the formulas of Seaton (1960), using a computer program written by J. B. Oke. The contribution from the two-photon continuum has been omitted, since it is thought that the electron density in accretion disks exceeds $10^8 cm^{-3}$. The main-sequence line is based on MCSP observations of the stars in Table 1. Blackbodies, stellar atmospheres, and recombination spectra all behave similarly in the diagram, in the sense that in all three cases cooler spectra lie upwards and toward the left.

The Appendix shows that, in a diagram such as Figure 1, a composite object will have flux ratios which lie on a straight line connecting the flux-ratio points of the component objects. For example, the flux ratios of anobject which is part K5 dwarf and part power-law spectrum (say with spectral index $\alpha = 0$) will lie on the line joining the dK5 and the $\alpha = 0$ points in the diagram.

By a simple generalization, it is evident that an object which is, for example, an arbitrary mixture of blackbody spectra hotter than 6000 K and hydrogen recombination spectra from gas at temperatures exceeding 6000 K must correspond to a point which lies within the roughly triangular region connecting points A, B, and C in Figure 2. (In terms of the

Euclidean metric space represented by the diagram, this region is the "convex closure" of the set of points corresponding to blackbodies and recombination spectra.) It can be noted that reasonable power-law flux distributions lie within this region. Model stellar atmospheres at log g = 4.0 and T_{eff} > 8000 K (Kurucz, Peytremann, and Avrett 1974) lie along or very close to the line B - C in the figure.

If it is assumed that the residual flux from a cataclysmic variable star must be composed of such simple elements as hot stellar atmospheres (or blackbodies) and recombination spectra at temperatures greater than 6000 K, then it follows that the flux ratios of the residual energy distributions must lie within the region described above. In particular, for any assumed late-type star, the locus of flux ratios for the residual spectrum falls along the straight line containing the flux ratios of the star and the observed flux ratios of the composite object; naturally, the point representing the observed flux ratios must lie between the points denoting the cool star and the residual flux. Of these residual points only those which lie inside the region ABC represent physically plausible flux distributions.

In Figure 2, this is illustrated for four cases. The observed (composite) flux ratios of SS Aur are $x = f_\nu(\lambda 4200)/f_\nu(\lambda 5500) = 0.65$ and $y = f_\nu(\lambda 8000)/f_\nu(\lambda 5500) = 1.91$. Subtracting various amounts of a K2V star will leave residual

fluxes whose flux ratios lie along the line segment labelled "1" in the figure; the broken portion of the line (to the right of point D) represents "unphysical" residual energy distributions, in the sense that no combination of the hot atmospheres, blackbodies, or recombination spectra can produce flux ratios which lie on the broken portion of the line. Line 2 shows the location of residual spectra when varying amounts of an M1.5 star's spectrum are subtracted from the observed spectrum of SS Aur. The observed flux ratios of U Gem during eclipse, $x = 0.79$ and $y = 4.06$, are also shown. Line 3 (subtraction of an M4.5 star) shows that unphysical residual energy distributions may be encountered "on both sides" of the allowed region, depending upon what fraction of the light is assumed to be due to the secondary star. Finally, line 4 (U Gem with a K2 secondary star assumed) shows that in certain cases some postulated secondary stars cannot produce any satisfactory residual spectra.

A further property of the flux-ratio diagram is illustrated by the SS Aur - K2 star line in Figure 2. The linear distances a and b (between K2 and SS Aur, and SS Aur and point D, respectively) can be used to set a lower limit on the fractional contribution of the residual flux to the total composite light at $\lambda 5500$. The fraction of light at $\lambda 5500$ which is due to the K2 star is $b/(a + b)$ and the fraction due to the accretion disk is $a/(a + b)$ (see the Appendix). For any other physically plausible residual spectrum (that is,

for other points lying along the solid portion of line 1), the accretion disk is relatively brighter at λ5500. Thus if the absolute magnitude of the postulated K2 secondary star is known, a lower limit on the visual luminosity of the accretion disk is available from inspection of the diagram. In cases such as that of U Gem (line 3), both lower and upper limits on the visual luminosity of the disk may be obtained (using an assumed absolute magnitude for the secondary star).

In Figure 2, the region bounded by the lines A - B - C - A is postulated to be the region in which the flux ratios of the residual energy distributions (i.e., observed minus secondary star) must lie. This region includes all spectra which can be formed by any arbitrary combination of blackbodies hotter than 6000 K and hydrogen recombination radiation from gas hotter than 6000 K. (It has already been mentioned that early-type model stellar atmospheres fall in this region; power-law spectra of reasonable spectral index are also included, although this is probably not important for cataclysmic variable stars.) The justification for taking 6000 K as the lower limit to the temperature of the emitting gas in an accretion disk follows from recent work by Williams (1980).

Williams considered a steady-state viscous accreting disk. In such a disk, the effective temperature of the (optically thick) disk surface varies with radius according

to

$$T_{eff}(x) = T_* \, x^{-3/4} \, (1-x^{-1/2})^{1/4}, \quad 1 < x \leq x_{max} \qquad (2)$$

where $x = r/r_{inner}$ and $x_{max} = r_{outer}/r_{inner}$. T_* varies slowly with the mass of the accreting object, the inner radius of the disk, and the mass accretion rate; for values thought to be typical of quiescent dwarf novae, $T_* \approx$ 60,000 K (Herter et al. 1979; Williams 1980). For $T_{eff}(x) \gtrsim 10^4$ K, the accretion disk is optically thick, but for T_{eff} below about 10^4 K, the opacity of the gas drops rapidly with decreasing temperature. This gas is thus optically thin (Bath et al. 1974). Williams showed that since the optically thin gas cannot radiate efficiently (Kirchhoff's law), it maintains itself at a kinetic temperature near 7000 K, hotter than the temperature predicted from equation (2), which applies to optically thick disks.

Williams' conceptual model of an accretion disk thus has an optically thick inner disk for $T_{eff} > 10^4$ K, and an optically thin outer disk which has a nearly constant kinetic temperature, $T_{outer} \simeq 7000$ K. The relative sizes of the two regions and the details of the transition from one to the other are model-dependent and vary inter alia with the mass accretion rate and the viscosity of the disk material. (The viscosity determines the particle density in the disk by fixing the rate of mass transport through the disk.)

In this paper, to avoid errors caused by too rigid adherence to a particular disk model, the temperature of both optically thick and thin parts of the disk will be allowed to be as low as 6000 K, and any combination of radiation from gas hotter than 6000 K will be assumed to be a legitimate disk model.

Madej and Paczynski (1977) have proposed for U Gem a model in which the material transferred from the secondary star is not accreted between eruptions. Rather, it accumulates in a ring (or "toroidal star") which maintains an effective temperature near 6500 K uniformly over its surface. Such a disk would have a spectrum similar to that of a late F or early G star; the corresponding point in Figure 1 lies near the blackbody point for T = 8000 K. Thus the region A - B - C includes this alternative to steady-state viscous accreting disk models.

Figure 3 shows the same flux-ratio diagram with the cataclysmic variable stars from the MCSP survey plotted. No reddening corrections have been made; only for the old nova BT Mon is the correction likely to be important. Open circles represent quiescent dwarf novae (WZ Sge is included in this group, although it appears to be a hybrid object). Filled circles are dwarf novae in outburst, UX UMa-type stars, or old novae. The half-filled circle is AM CVn. As expected, the quiescent dwarf novae are on the average redder than the other objects, and they lie closer to the main-sequence line,

indicating that the secondary stars contribute a larger fraction of the light at λ5500. Table 2 lists the values of the flux ratios for each star.

TABLE 2

FLUX RATIO DATA FOR CATACLYSMIC VARIABLE STARS[1]

N	Object	"V"	x	y	z	Remarks
Old Novae						
1	V603 Aql	11.6	1.11	0.82	1.06	smoothed spectrum
2	BT Mon	15.4	0.74	1.16	0.52	note 2
UX UMa-type Objects						
3	TT Ari	11.4	1.15	0.78	1.25	smoothed spectrum
4	RW Tri	14.2	0.79	1.50	0.70	smoothed; note 3
	UX UMa	12.7	1.11	0.95	1.01	phase = 0.45
5	UX UMa	12.7	1.10	0.90	0.84	phase = 0.77
	UX UMa	12.8	1.15	0.90	1.04	phase = 1.06
Dwarf Novae in Outburst						
6	Z Cam	12.3?	0.96	1.06	0.72	standstill
7	SY Cnc	12.3	1.01	0.97	0.84	decreasing to minimum
8	YZ Cnc	11.5	1.34	0.66	1.20	super-outburst
9	EM Cyg	12.2	0.90	1.03	0.72	
	SS Cyg	8.5	1.19	0.80	1.08	note 4
10	SS Cyg	8.7	1.18	0.82	1.05	note 4
	SS Cyg	8.8	1.18	0.82	1.02	note 4
11	AB Dra	13.9	1.00	0.95	1.02	
Quiescent Dwarf Novae						
12	RX And	14.4	0.86	2.00	1.69	smoothed spectrum
13	AE Aqr	11.3	0.33	1.91	0.20	(note 5)
14	SS Aur	14.6	0.65	1.91	1.13	
15	Z Cam	13.6	0.47	2.00	0.47	
16	YZ Cnc	14.9	0.82	1.50	1.42	
17	WW Cet	14.2	0.82	1.64	1.39	
18	EM Cyg	13.6	0.44	1.64	0.39	
19	SS Cyg	11.7	0.48	1.87	0.71	
	U Gem	14.1	0.93	2.49	1.00	phase = 0.81
20	U Gem	15.1	0.79	4.06	1.22	phase = 0.00 (eclipse)
	U Gem	14.8	0.79	3.22	1.13	phase = 0.44
	U Gem	14.5	0.82	3.44	0.98	phase = 0.67
21	AH Her	13.9	0.63	1.57	0.75	
22	EX Hya	13.7	0.85	1.25	0.99	phase = 0.5
23	T Leo	15.8	0.94	1.18	1.66	
24	X Leo	15.9	0.70	1.77	0.88	
25	CN Ori	....	0.65	2.03	0.86	
26	RU Peg	12.6	0.46	1.56	0.45	
27	BX Pup	16.6	0.65	1.96	0.94	
28	WZ Sge	15.4	1.11	0.72	0.90	
29	SU UMa	14.8	0.88	1.25	1.63	smoothed spectrum (note 5)
Other						
30	AM CVn	14.1	1.41	0.58	1.47	= HZ 29

NOTES TO TABLE 2

[1]"V" is AB(λ5500), x is $f_\nu(\lambda 4200)/f_\nu(\lambda 5500)$, y is $f_\nu(\lambda 8000)/f_\nu(\lambda 5500)$, and z is $f_\nu(\lambda 3560)/f_\nu(\lambda 5500)$.

[2]BT Mon is probably reddened by 0.2 - 0.3 mag. Applying a reddening correction of E(B-V) = 0.3 mag changes the flux ratios to x′ = 1.05, y′ = 0.79, and z′ = 0.92.

[3]References for the orbital phases of the eclipsing variables may be found in Chapter 3. For RW Tri, the phase is 0.69.

[4]The three observations of SS Cyg were obtained on successive nights during a 7-day outburst.

[5]Smoothing of the spectra of RX And and SU UMa may cause x to be overestimated by about 10%.

IV. THE BALMER JUMP

Figure 4 is a flux-ratio diagram made from fluxes at λλ3560, 5500, and 8000. The main sequence (for stars later than K0), blackbodies (hotter than 6000 K), and hydrogen recombination spectra are shown. The points A (T = ∞) and B (T = 6000 K blackbody radiation) retain their meaning from Figure 2; point C (6000 K recombination radiation) is off the figure to the right, and the lines B - C_1 and A - C_2 intersect at point C. The abscissa is $z = f_\nu(\lambda 3560)/f_\nu(\lambda 5500)$, which is a measure of the strength of the Balmer jump. The symbols for the observed stars are the same as in Figure 3.

In Figure 4, blackbodies and stellar atmospheres move up and to the left with cooler temperatures, as they do in Figures 1 - 3. Recombination spectra, on the other hand, behave differently, since the emission Balmer jump becomes stronger at lower temperatures. This provides a powerful tool for the analysis of composite spectra, as shown by the open circles (representing quiescent dwarf novae) in the figure. Many of these points lie above the line B - C_1, that is, they lie outside the allowed range of flux ratios for accretion disk spectra. This means that the secondary stars contribute a non-negligible fraction of the light at λ5500. Furthermore, in most cases the secondary stars cannot be early K stars, since the lines along which the residual flux

ratios must lie would then not intersect the accretion disk region A - B - C.

A straightforward interpretation of this fact is possible. The quiescent dwarf novae generally have red Paschen continua; that is, $y = f_\nu(\lambda 8000)/f_\nu(\lambda 5500) > 1$. This can be due either to a significant contribution from a late-type star, or to a significant contribution from a sufficiently cool recombination spectrum. In the latter case, however, there should also be a large Balmer jump in emission; that is, $z = f_\nu(\lambda 3560)/f_\nu(\lambda 5500) >> 1$. The observations show that this is not the case, and the diagram provides a reliable way to specify a lower limit to the "redness" of the secondary star's continuum. For example, Figure 4 shows that the secondary star in SS Cyg must have a Paschen slope redder than $y = 1.73$, or the flux ratios of the residual energy distribution will not be appropriate to an accretion disk.

(It should be noted that in Figure 4, the locus of early-type model stellar atmospheres [Kurucz, Peytremann, and Avrett 1974] falls below and to the left of the line A - B. This is because early-type stars have Balmer jumps in absorption, while blackbody spectra do not. The "allowed" range for accretion disk spectra in Figure 4 should be extended to include these models. The lines A - C_2 and B - C_1 are not affected by this extension, however, and in Table 3, described below, only limits which are derived from these lines are included.)

V. RESULTS

After the flux-ratio diagrams were used to establish preliminary upper and lower limits on the magnitudes of the accretion disks, some of the spectra were examined in more detail to refine these limits. All of these stars were quiescent dwarf novae. An interactive computer program written by B. A. Zimmerman was used to display the residual energy distributions, after various amounts of secondary spectrum had been subtracted from the observed spectrum. The MCSP spectra of main sequence stars 1 - 4 and 6 in Table 1 were used, and the resolution of these spectra was degraded to match the cataclysmic variable star data. The residual energy distributions were examined for smoothness, freedom from features due to red stars, etc. Figures 5 - 8 show representative displays from the interactive program. The results of this refining process have been incorporated into Table 3. Usually, the consequence of the refinement is to make the lower limits on the visual magnitudes of the disk brighter by a few tenths of a magnitude.

Table 3 presents upper and lower limits to the visual luminosities of the disk component of the light for the cataclysmic variables studied, as a function of the spectral type assumed for the secondary star. This spectral type is parametrized by y_2, the ratio of the star's fluxes at $\lambda 8000$ and $\lambda 5500$. The corresponding upper and lower limits to the

TABLE 3

UPPER AND LOWER LIMITS TO DISK VISUAL LUMINOSITIES:

ABSOLUTE VISUAL MAGNITUDES AND FRACTIONAL CONTRIBUTIONS

N	Object	y_2:	1.40	1.60	1.80	2.00	2.20	2.40	2.60	2.80	3.00	3.20	3.60	4.40	6.00	7.60	11.00
0	Sample entry apparent V mag		Bright limits on absolute magnitude of disk at λ5500, if any. Fraction of total light at λ5500 which is due to disk, at bright limit. Faint limits on absolute magnitude of disk at λ5500. Fraction of total light at λ5500 which is due to disk, at faint limit.														
1	V603 Aql		no upper limits														
	11.6		no upper limits														
			4.99	4.83	4.82	4.84	4.89	4.93	4.98	5.04	5.10	5.16	5.29	5.53	5.94	6.91	8.60
			0.70	0.79	0.84	0.87	0.89	0.91	0.92	0.93	0.94	0.95	0.95	0.97	0.98	0.98	0.99
3	TT Ari		no upper limits														
	11.4		no upper limits														
			4.69	4.54	4.55	4.59	4.65	4.70	4.76	4.82	4.88	4.94	5.07	5.32	5.73	6.71	8.41
			0.76	0.83	0.87	0.90	0.91	0.93	0.94	0.94	0.95	0.95	0.96	0.97	0.98	0.99	0.99
4	RW Tri		N.A.	5.01	4.72	4.62	4.60	4.62	4.66	4.71	4.77	4.83	4.95	5.19	5.61	6.58	8.27
	14.2			0.77	0.85	0.89	0.92	0.93	0.94	0.95	0.95	0.96	0.97	0.97	0.98	0.99	0.99
			N.A.	6.50	6.93	7.39	7.57	7.46	7.41	7.38	7.37	7.38	7.42	7.55	7.87	8.79	10.42
				0.45	0.43	0.39	0.41	0.50	0.56	0.61	0.66	0.69	0.75	0.81	0.88	0.91	0.94
5	UX UMa		no upper limits														
	12.7		no upper limits														
			5.69	5.93	5.84	5.83	5.86	5.86	5.92	5.97	6.03	6.08	6.20	6.43	6.83	7.79	9.48
			0.55	0.58	0.67	0.73	0.77	0.81	0.83	0.85	0.87	0.88	0.90	0.92	0.95	0.96	0.98
6	Z Cam		N.A.	N.A.	N.A.	N.A.	N.A.	N.A.	5.04	5.09	5.16	5.21	5.32	5.54	N.A.	N.A.	N.A.
	11.7								0.92	0.93	0.94	0.94	0.95	0.97			
			N.A.	N.A.	N.A.	N.A.	N.A.	N.A.	6.11	6.14	6.18	6.22	6.32	6.53	N.A.	N.A.	N.A.
									0.81	0.83	0.85	0.87	0.89	0.92			
7	SY Cnc		no upper limits														
	12.3		no upper limits														
			6.07	5.81	5.72	5.69	5.70	5.72	5.76	5.80	5.85	5.90	6.00	6.22	6.62	7.58	9.25
			0.46	0.61	0.70	0.76	0.80	0.83	0.85	0.87	0.89	0.90	0.92	0.94	0.96	0.97	0.98
8	YZ Cnc		no upper limits														
	11.5		no upper limits														
			3.94	3.82	3.90	3.98	4.11	4.10	4.21	4.28	4.36	4.43	4.58	4.84	5.26	6.25	7.96
			0.86	0.91	0.93	0.94	0.94	0.96	0.96	0.96	0.97	0.97	0.98	0.98	0.99	0.99	0.99
9	EM Cyg		N.A.	N.A.	4.78	4.69	N.A.	N.A.	N.A.	N.A.	N.A.	N.A.	N.A.	N.A.	N.A.	N.A.	N.A.
	12.2				0.85	0.89											
			N.A.	N.A.	5.77	5.70	N.A.	N.A.	N.A.	N.A.	N.A.	N.A.	N.A.	N.A.	N.A.	N.A.	N.A.
					0.69	0.76											

TABLE 3 - CONTINUED

N	Object	y_2: 1.40	1.60	1.80	2.00	2.20	2.40	2.60	2.80	3.00	3.20	3.60	4.40	6.00	7.60	11.00
10	SS Cyg	N.A.	N.A.	N.A.	N.A.	3.41	3.45	3.49	3.55	3.58	3.67	3.80	4.03	N.A.	N.A.	N.A.
	8.7					0.97	0.98	0.98	0.98	0.98	0.99	0.99	0.99			
		N.A.	N.A.	N.A.	N.A.	5.20	5.24	5.29	5.36	5.42	5.48	5.61	5.85	N.A.	N.A.	N.A.
						0.86	0.88	0.90	0.91	0.92	0.93	0.94	0.95			
11	AB Dra	no upper limits														
	13.9	no upper limits														
		5.87	5.62	5.54	5.52	5.53	5.55	5.58	5.63	5.67	5.72	5.83	6.05	6.45	7.41	9.08
		0.51	0.65	0.73	0.79	0.82	0.85	0.87	0.89	0.90	0.91	0.93	0.95	0.96	0.97	0.98
12	RX And	N.A.	N.A.	N.A.	N.A.	N.A.	6.33	6.33	6.35	6.38	6.43	6.52	6.73	7.12	8.08	9.75
	14.4						0.74	0.77	0.80	0.83	0.84	0.87	0.90	0.94	0.95	0.97
		N.A.	N.A.	N.A.	N.A.	N.A.	6.38	6.79	7.24	7.77	8.18	8.31	8.54	8.79	9.68	11.28
							0.73	0.69	0.64	0.57	0.52	0.56	0.64	0.76	0.82	0.88
13	AE Aqr	N.A.	N.A.	N.A.	8.70	N.A.	N.A.	N.A.	N.A.	N.A.	N.A.	N.A.	N.A.	N.A.	N.A.	N.A.
	11.3				0.16											
		N.A.	N.A.	N.A.	9.82	N.A.	N.A.	N.A.	N.A.	N.A.	N.A.	N.A.	N.A.	N.A.	N.A.	N.A.
					0.07											
14	SS Aur	N.A.	N.A.	N.A.	N.A.	N.A.	6.63	6.61	6.61	6.64	6.68	6.76	6.96	7.35	8.30	9.97
	14.6						0.68	0.73	0.76	0.79	0.81	0.84	0.88	0.92	0.94	0.96
		N.A.	N.A.	N.A.	N.A.	N.A.	7.00	7.23	7.11	7.30	7.48	7.82	7.96	8.39	9.27	10.86
							0.60	0.60	0.67	0.67	0.67	0.67	0.75	0.82	0.87	0.92
15	Z Cam	N.A.	N.A.	N.A.	N.A.	N.A.	N.A.	7.55	7.49	7.47	7.48	7.52	7.67	N.A.	N.A.	N.A.
	13.6							0.53	0.59	0.63	0.67	0.73	0.80			
		N.A.	N.A.	N.A.	N.A.	N.A.	N.A.	7.58	7.62	7.81	7.91	7.77	7.69	N.A.	N.A.	N.A.
								0.52	0.56	0.56	0.58	0.68	0.79			
16	YZ Cnc	no upper limits														
	14.9	no upper limits														
		5.66	6.04	6.37	6.49	6.76	7.00	7.23	7.42	7.42	7.42	7.47	7.61	7.93	8.85	10.48
		0.56	0.56	0.56	0.60	0.60	0.60	0.60	0.60	0.65	0.68	0.74	0.81	0.87	0.91	0.94
17	WW Cet	no upper limits														
	14.2	no upper limits														
		5.61	5.86	6.19	6.49	6.43	6.67	6.90	7.11	7.30	7.48	7.02	7.58	8.21	9.12	10.74
		0.57	0.60	0.60	0.60	0.67	0.67	0.67	0.67	0.67	0.67	0.81	0.81	0.84	0.88	0.93
18	EM Cyg	N.A.	N.A.	6.89	6.52	N.A.	N.A.	N.A.	N.A.	N.A.	N.A.	N.A.	N.A.	N.A.	N.A.	N.A.
	13.6			0.44	0.59											
		N.A.	N.A.	7.50	7.47	N.A.	N.A.	N.A.	N.A.	N.A.	N.A.	N.A.	N.A.	N.A.	N.A.	N.A.
				0.31	0.38											

TABLE 3 - CONTINUED

N	Object	y_2: 1.40	1.60	1.80	2.00	2.20	2.40	2.60	2.80	3.00	3.20	3.60	4.40	6.00	7.60	11.00
19	SS Cyg	N.A.	N.A.	N.A.	N.A.	7.06	6.94	6.89	6.89	6.90	6.93	7.01	7.20	N.A.	N.A.	N.A.
	11.7					0.53	0.61	0.67	0.71	0.75	0.77	0.81	0.86			
		N.A.	N.A.	N.A.	N.A.	7.06	7.30	7.33	7.37	7.40	7.40	7.35	7.31	N.A.	N.A.	N.A.
						0.53	0.53	0.58	0.62	0.65	0.69	0.76	0.85			
21	AH Her	N.A.	5.85	5.43	5.29	5.25	5.25	5.29	5.33	5.38	5.44	5.55	5.79	6.20	7.17	8.85
	13.9		0.60	0.75	0.82	0.86	0.88	0.90	0.91	0.92	0.93	0.94	0.96	0.97	0.98	0.99
		N.A.	6.21	6.54	6.49	6.76	7.00	7.23	7.24	7.19	7.17	7.17	7.25	7.53	8.43	10.04
			0.52	0.52	0.60	0.60	0.60	0.60	0.64	0.69	0.73	0.79	0.85	0.91	0.93	0.96
22	EX Hya	no upper limits														
	13.7	no upper limits														
		6.32	6.76	6.95	6.79	6.72	6.68	6.67	6.68	6.69	6.72	6.79	6.97	7.32	8.26	9.91
		0.41	0.40	0.43	0.53	0.61	0.67	0.72	0.75	0.78	0.80	0.84	0.88	0.92	0.94	0.96
23	T Leo	no upper limits														
	15.8	no upper limits														
		5.00	5.38	5.71	6.01	6.17	6.41	6.59	6.61	6.64	6.67	6.76	6.96	7.33	8.27	9.93
		0.70	0.70	0.70	0.70	0.72	0.72	0.73	0.76	0.79	0.81	0.84	0.88	0.92	0.94	0.96
24	X Leo	N.A.	N.A.	N.A.	N.A.	N.A.	N.A.	6.30	6.32	6.35	6.40	6.50	6.71	7.10	8.05	9.73
	15.9							0.78	0.81	0.83	0.85	0.87	0.90	0.94	0.95	0.97
		N.A.	N.A.	N.A.	N.A.	N.A.	N.A.	7.00	7.21	7.40	7.58	7.90	7.98	8.24	9.13	10.74
								0.65	0.65	0.65	0.65	0.65	0.75	0.84	0.88	0.93
25	CN Ori	N.A.	N.A.	N.A.	N.A.	N.A.	7.39	7.30	7.27	7.26	7.27	7.33	7.50	7.85	8.79	10.45
	----						0.51	0.58	0.64	0.68	0.71	0.76	0.82	0.88	0.91	0.94
		N.A.	N.A.	N.A.	N.A.	N.A.	7.78	8.34	8.61	8.49	8.42	8.36	8.37	8.59	9.45	11.04
							0.42	0.35	0.34	0.40	0.46	0.55	0.67	0.79	0.85	0.90
26	RU Peg	N.A.	6.79	6.11	N.A.	N.A.	N.A.	N.A.	N.A.	N.A.	N.A.	N.A.	N.A.	N.A.	N.A.	N.A.
	12.6		0.39	0.62												
		N.A.	8.66	7.84	N.A.	N.A.	N.A.	N.A.	N.A.	N.A.	N.A.	N.A.	N.A.	N.A.	N.A.	N.A.
			0.10	0.25												
27	BX Pup	N.A.	N.A.	N.A.	N.A.	7.18	7.04	6.99	6.98	6.99	7.01	7.09	7.27	7.64	8.58	10.25
	16.6					0.50	0.59	0.65	0.70	0.73	0.76	0.80	0.85	0.90	0.93	0.95
		N.A.	N.A.	N.A.	N.A.	7.48	7.99	8.44	8.43	8.33	8.27	8.22	8.25	8.47	9.35	10.93
						0.43	0.38	0.33	0.38	0.44	0.50	0.58	0.70	0.81	0.86	0.91
29	SU UMa	no upper limits														
	14.8	no upper limits														
		5.48	5.86	6.19	6.49	6.76	6.74	6.73	6.74	6.76	6.79	6.87	7.05	7.41	8.34	9.99
		0.60	0.60	0.60	0.60	0.60	0.66	0.70	0.74	0.77	0.79	0.83	0.87	0.92	0.94	0.96

NOTE TO TABLE 3

See "Sample entry" for explanation of the entries in the main body of the table. The parameter y_2 is the value of the flux ratio $f_\nu(\lambda 8000)/f_\nu(\lambda 5500)$ for the secondary star, and is allowed to vary between 1.40 and 11.00. "N.A." (not allowed) indicates that the observed spectrum is not consistent with a secondary star having the tabulated value of y_2. The magnitudes in the table are derived assuming that the secondary stars follow the main sequence color – absolute magnitude relation, equation (1).

fraction of light at λ5500 which is due to the disk are also tabulated. (Here as before, "disk component" means all the light from the system which is not from the secondary star. This includes contributions from the white dwarf primary star and from the bright spot at the outer edge of the disk.) From these quantities, limits on the total light from the cataclysmic variable systems can be derived. The sources for the entries in Table 3 include the analysis of flux-ratio diagrams (Figures 3 and 4) and inspection of residual fluxes generated by Zimmerman's interactive program.

For each object in the table, there are four rows of numbers; for some of the objects, the first two rows are replaced by the notation "no upper limits." If the first row of numbers is present, each entry in the row is the absolute magnitude at λ5500 for the brightest disk which is consistent with the observed spectrum, using a secondary star of the given spectral type (y_2 is noted at the top of each column of the table). The second row gives the fraction of observed light at λ5500 which is contributed by this brightest disk. The third and fourth numbers are the absolute magnitude and fraction of light contributed (at λ5500) for the faintest disk which is consistent with the data. For many of the erupting dwarf novae and the UX UMa-type objects and for some of the quiescent dwarf novae, it was not possible to set upper limits on the luminosity of the disk, and this is indicated by the entry, "no upper limits", in the first two

rows. The notation "N.A." indicates that it is not possible to fit the observations using a secondary star which has the tabulated value of y_2.

For the outburst observations of SS Cyg, Z Cam, and EM Cyg, upper limits have been set from the observations of the same objects in quiescence. This was possible because the magnitude difference between the observations is known, and upper limits are available for the observations at quiescence. (For Z Cam at standstill, the AAVSO magnitude of 11.7 was used instead of the observed MCSP magnitude of 12.3 .)

The stars BT Mon, U Gem, WZ Sge, and AM CVn have been omitted from Table 3. The magnitude limits for BT Mon are sensitive to the adopted value of the interstellar reddening. U Gem has been discussed in Chapter 2. The secondary star in WZ Sge is expected to be dark or at least very faint (Robinson, Nather, and Patterson 1978; Fabian et al. 1978). Both stars in AM CVn are thought to be degenerate (Robinson and Faulkner 1975).

Several sources of error affect the entries in Table 3. First are photometric errors in the MCSP observations. Random errors in the flux ratios are small and can be estimated from the quality index of Chapter 4. Errors in the absolute calibration of the flux densities are also expected to be no more than a few percent. The smoothing operation which was carried out on five of the spectra is not expected to produce errors in these continuum flux ratios, except for the ratio

between fluxes at 4200 Å and 5500 Å, where strong lines on either side of the 4200 Å passband may have raised the apparent flux density there by about 10 %. Where this is likely to have occurred, it has been noted in Table 2. Second are errors associated with the placement of the main sequence line in the flux-ratio diagrams. At a fixed value of the ratio y, the main sequence has an intrinsic width of about 0.06 in x and 0.03 in z (Bell and Gustafsson 1978; D. Rabin 1980, private comminication) due to different amounts of line blanketing in stars of differing metal abundance. A third possible source of error is in the calculation of the recombination spectrum, which omitted the contribution of helium. This effect is in fact unimportant, because only the recombination point at 6000 K affects the location of the region (A - B - C in the flux-ratio diagram) which contains the physically plausible disk models, and helium will be almost entirely neutral (no recombination) at 6000 K.

For most of the observations plotted in Figures 3 and 4, these sources of error are unimportant. They become significant for the few objects whose plotted points lie on or near the main-sequence line (AE Aqr, RU Peg, and EM Cyg), or near the boundary of the region A - B - C (e.g., WZ Sge, AM CVn, and YZ Cnc in outburst). For the former set of stars, small changes in the observed flux ratios produce large changes in the absolute magnitudes and light fractions listed in Table 3, but this is simply a reflection of the difficulty of mea-

suring accurately the small contribution which the disk makes to the total light from the system. WZ Sge and AM CVn are not included in Table 3 in any case; for other stars like YZ Cnc in outburst, a small change in the observed flux ratios also produces a substantial change in the tabulated values, and for these stars the values in Table 3 should be regarded as indicative only.

The entries in Table 3 refer, of course, to the absolute magnitudes of the disks at the time the MCSP observations were obtained. For systems like UX UMa, RW Tri, or V603 Aql which are more or less constant in magnitude, the results of Table 3 are representative and may be compared directly with other work. For the more variable systems, distances or distance moduli, derived from Table 3 and the apparent MCSP magnitudes, will be more useful quantities for comparison. Fluctuations of a few tenths of a magnitude are common for a dwarf nova in quiescence, and successive outbursts of the same dwarf novae often differ by more than one magnitude in the visual passband.

VI. THE SECONDARY STARS IN CATACLYSMIC VARIABLE SYSTEMS

It must be emphasized that all entries in Table 3 are based on the assumption that the secondary stars follow the main-sequence color - absolute magnitude relation given by equation (1). There is in fact reason to believe that the secondary stars in at least some systems deviate from this

main-sequence relation, by amounts which vary from one star to another (see, e.g., Chapter 2 and Patterson 1979b). In other words, the effective temperature of a secondary star in a cataclysmic variable system is not necessarily the same as the effective temperature of a main-sequence star having the same radius. Chapter 2 showed in the case of U Gem how if additional information, such as the orbital period and the masses, is available, then it is possible to make an empirical correction to the absolute magnitude of the secondary star, and hence to the entries in Table 3. The correction is based on determining the ratio of the radius of the secondary star to the radius of a main-sequence star of the same spectral type. This correction process has not been done in Table 3, because the necessary information is not available in many cases. In the remarks on individual stars which follow, however, an indication of the size of the correction is made whenever possible.

It is of interest to understand why the secondary stars do not obey the main-sequence color - magnitude relation. The secondary star fills its Roche lobe and transfers mass to the primary star. The mass transfer results in a change of the gravitational potential energy, Ω, of the secondary star; the change in Ω is the energy required to bring matter up from the interior of the star to replace matter lost from the surface. If the nuclear luminosity of the star is normal, then the radiated luminosity will be diminished by an amount

$$| \Delta L | = \left| \frac{d\Omega}{dm} \dot{M} \right| = \frac{3}{7} \frac{Gm}{r} \dot{M}$$

where $\Omega = -(3/7)\ Gm^2/r$ is the gravitational potential energy for a polytrope of index n = 3/2, and assuming that d(log r)/d(log m) = +1. Using values of m = 0.5 $M_\odot$, r = 0.5 $R_\odot$, and $\dot{M} = 10^{17}$ gm $s^{-1} = 1.6 \times 10^{-9}$ $M_\odot$ yr^{-1}, we find

$$\Delta L = 8.2 \times 10^{31} \text{ erg } s^{-1} = 0.021\ L_\odot$$

This manifests itself as a change in the effective temperature of the star:

$$\Delta T_{eff} \simeq \frac{1}{4} T_{eff} \frac{\Delta L}{L} = 470 \text{ K},$$

for an 0.5 $M_\odot$ star with L = 0.041 $L_\odot$ and T_{eff} = 3700 K (Veeder 1974). Mass loss rates in quiescent dwarf novae are probably somewhat less than 10^{17} gm s^{-1}. In UX UMa-type systems and old novae, where the disks are bright and the bolometric corrections are large (Paczynski and Schwarzenberg-Czerny 1980), 10^{17} gm s^{-1} is probably a reasonable estimate for the mass transfer rate. The temperature deficit is even more severe for less massive stars, since L diminishes with decreasing mass. Thus a substantial change in effective temperature, and therefore in the observed spectral type, can be brought about by the phenomenon of mass transfer.

It is not clear, of course, whether the Roche-lobe filling star in a cataclysmic variable system should have a normal main-sequence nuclear luminosity, in view of its ab-

normal environment. For example, synchronous rotation of the secondary star will lessen the hydrostatic pressure at the core of the star, with a consequent reduction in nuclear luminosity (Papaloizou and Whelan 1973). Additionally, the peculiar surface boundary conditions of a fully convective low mass secondary star will strongly influence the star's deep interior structure. Further discussion of this point is beyond the scope of this study.

A final consideration is that the secondary stars in cataclysmic variable systems may be evolved, in which case there would be no unique relation between radius and effective temperature, such as there is for the main-sequence. Patterson (1979b) has proposed such a scenario for the secondary star in AE Aqr. Since the primary stars are compact, evolved objects, the possibility that the secondary stars have also evolved significantly should be borne in mind.

What must be recognized from this discussion of the physical state of the secondary stars is that <u>neither the mass nor the observed spectral type of the secondary star alone can properly be used to predict its luminosity</u>, since several relevant physical effects are capable of altering the usual mass - luminosity, mass - radius, and spectral type - luminosity relations which have been established for normal main-sequence stars. Empirical corrections can be made, however, if sufficient information is available.

VII. DISCUSSION OF INDIVIDUAL STARS

V603 Aql. Payne-Gaposchkin (1957) finds the absolute magnitude for the post-nova to be +3.55 (photographic). This is consistent with the limits shown in Table 3. Recent observations by satellite and from the ground (Boggess et al. 1980; Slovak 1980) indicate that V603 undergoes eclipses. This implies that the inclination of the system is fairly high. Since the mass function (Kraft 1964) is

$$\frac{m_2^3 \sin^3 i}{(m_1+m_2)^2} = 7.6 \times 10^{-4} M_\odot$$

the secondary star must be quite small. Nearly all the light must therefore arise from the disk.

RW Tri. Smak (1979) finds $m_1 \cong m_2 \cong 0.4 M_\odot$ from a study of the emission line velocities and the eclipses of this nova-like system. This suggests that $y_2 > 4.0$ in Table 3, in which case the absolute magnitude for the disk is fainter than about 5.0 mag.

Z Cam. Kraft, Krzeminski, and Mumford (1969) found a spectral type of dG1 for the secondary star. This is not consistent with the MCSP spectrum at minimum light, which requires a spectral type of approximately K5 or later. The most probable spectral type is near K7.

EM Cyg. Robinson (1974) found the secondary star to be of type G - K. From Table 3, it appears that the spectral type is in the range K2 to K5. EM Cyg is a double-lined

eclipsing binary, so the masses can be measured directly. Robinson finds $m_1 = 0.9\ M_\odot$ and $m_2 = 0.7\ M_\odot$. There is no discrepancy in this case between the observed spectrum and the spectrum predicted from the mass of the secondary star, and Robinson points out that the secondary star lies on the ZAMS mass - radius line. Therefore no correction to the magnitudes of Table 3 is needed.

SS Cyg. Joy (1956) gave dG5 as the spectral type of the secondary star. Recent studies by Stover et al. (1980) and by Cowley, Crampton, and Hutchings (1980) classify the secondary as a K5 - K7 star, consistent with Table 3. The interactive computer program indicates that K5 provides a slightly better fit than either K2 or K7. There is sharp disagreement about the masses of the components in SS Cyg.

AB Dra. This object should be reobserved when it is closer to minimum light, in order to get better limits on the spectral type of the secondary star.

RX And. Kraft (1962) found an apparent orbital eccentricity of 0.4 from the emission line radial velocities. Since it is expected that the orbits of close binary systems are circular, the apparent eccentricity must be caused by gas streaming motions. Thus the orbital motion of the white dwarf should probably be regarded as unknown.

AE Aqr. Crawford and Kraft (1956) found a spectral type of K5 IV-V for the secondary star. Patterson (1979b) finds dK1 from UBV photometry, after correcting for the disk

component of the light. The MCSP data indicate that the spectral type is intermediate between K2 and K5. The long orbital period implies that the mass density of the secondary star is 1.06 gm cm^{-3}, and Patterson estimates that the secondary star should be 0.6 mag brighter than a normal dwarf. Applying this correction to the limits in Table 3 gives $8.1 < M_V < 9.2$ at the time of the single MCSP observation. As Patterson points out, the disk luminosity varies by several magnitudes.

SS Aur. Vasilevskis et al. (1975) report a relative trigonometric parallax of 8 ± 4 arc milliseconds; the absolute parallax is about 10 arc ms, which gives a distance modulus of 5 mag. The lower limits on the absolute magnitude of the disk are inconsistent with the MCSP absolute magnitude of $M_V(tot) = 14.6 - 5 = 9.6$ derived from the parallax result, unless the secondary star has a very red spectrum ($y_2 \gtrsim 7.6$).

Eggen (1967) gives $M_V = 6.3$ on the assumption that SS Aur is a member of the Hyades moving group. The MCSP upper limits are consistent with this value for the total light, if $y_2 \lesssim 2.8$; alternatively, an enlarged secondary star would raise the upper limits and allow a secondary star of later spectral type.

RU Peg. Kraft (1962) gives G8IVn for the spectral type of the secondary star. Kraft found the secondary star to be more massive than the primary, but a new emission line radial velocity study by Kiplinger (1979) finds that the primary

star is more massive, as in other cataclysmic variable systems. The MCSP data indicate that the secondary star has a continuum slope like that of a K2 or K3 dwarf. Eggen (1967) finds $M_V = +7.0$ for the blue component, by using a common proper motion companion to establish the distance to RU Peg. The magnitude limits of Table 3 are consistent with his result.

BX Pup. This star lies in the field of the galactic cluster NCG 2482. Moffat and Vogt (1975) find $V - M_V = 9.50$ for the cluster, which has an earliest spectral type near A2. The MCSP limits in Table 3 are consistent with cluster membership. Moffat and Vogt point out, however, that one of every two stars in the direction of the cluster is a field star. Definite claims that BX Pup is a cluster member must await a radial velocity study. Membership in a cluster of known age would be of value in studying the evolution of cataclysmic variable stars.

SU UMa. This star is likely to have an orbital period shorter than 2 hours (Patterson 1979a). This suggests that the secondary star should be of late spectral type, $y_2 \gtrsim 6.0$. The observed colors mimic rather closely those of pure recombination at about 40 000 K.

VIII. CONCLUSION

The emphasis in this chapter has been on using the MCSP observations to deduce the properties of individual cata-

clysmic variable stars. Some conclusions can also be drawn about the class of objects as a whole, based on this work.

A. The secondary stars

In those cases where the MCSP observations can be used to define the spectral type of the secondary star precisely enough, the new spectral types are generally later (cooler) than older spectral types based on the MK or similar classification criteria. Examples include SS Cyg (old type G5, new type about K5) and Z Cam (old type G1, new type probably near K7). One can attribute this discrepancy to the difficulty of using classification criteria which depend on the appearance of spectral lines in the photographic region of the spectrum, on objects where veiling of the lines by excess blue light is strong. Many of the important lines for classification, such as the Balmer series and the K line, appear in emission in cataclysmic variable stars. Additionally, the expected rapid rotation of the secondary stars tends to wash out the weak metal lines which strengthen with decreasing temperature; this leads to an estimate of the spectral type which is too early.

In other cases, the MCSP spectrum of a cataclysmic variable star is not sufficient to allow the spectral type of the secondary star to be specified. This is the case for many of the quiescent dwarf novae as well as for the UX UMa variables and the classical post-novae. In some cases,

higher resolution spectroscopy in the optical region may in the future provide the necessary additional information to narrow the permissible range of type for the secondary star. In other cases, photometry in the infrared part of the spectrum, where the energy distribution of a K star peaks, may be helpful in setting limits on the spectral types; preliminary experimentation with infrared flux-ratio diagrams indicates, however, that rather high precision observations are needed to make effective use of the infrared wavelengths. Observations of the ellipsoidal variations of the secondary stars in the infrared can in favorable cases be used to measure directly the fractional contribution of the secondary star to the total light from the system (G. Berriman 1980, private communication).

The MCSP survey of quiescent dwarf novae has revealed a few systems which should be investigated in more detail. CN Ori, for example, is quite red, almost certainly indicating the presence of an M-type star. A high resolution spectrum in the red and near infrared would probably reveal molecular band absorption. AH Her appears very similar to SS Cyg and probably contains a late K-type star. These and other systems should be studied spectroscopically to determine orbital periods and mass functions, so that corrections to the absolute magnitudes in Table 3 can be determined. Interestingly, no new cataclysmic variable system with colors as red as U Gem was observed in the survey. This may be

because of the small sample size, the relatively high inclination of the U Gem orbit to the line of sight, or some peculiarity in the U Gem system (IUE spectra show no ultraviolet emission lines for U Gem at quiescence, although they are plentiful in other systems; see Fabbiano et al. 1980).

B. The accretion disks

The spectra of cataclysmic variable systems which are dominated by the disks (post-novae, dwarf novae in outburst) make it clear that there is no such thing as a "standard" disk with the canonical power law spectrum, $f_\nu \propto \nu^{1/3}$. YZ Cnc in superoutburst, for example, has a spectrum which approximates $f_\nu \propto \nu^{1.1}$ over the optical wavelength region. Many other disks are flatter than $f_\nu \propto \nu^{1/3}$ (see Figure 3). It is no longer adequate to approximate the spectrum of a steady-state viscous disk by such a power law, which is only to be expected if the disk radiates as a series of blackbodies over a wide range of temperatures (Lynden-Bell 1969). Fortunately, recent efforts by several groups have shown that reasonable disk spectra can be made if realistic radiation processes are incorporated into the model (see, e.g., Herter et al. 1979; Mayo, Whelan, and Wickramasinghe 1979).

Kraft and Luyten (1965) find a mean absolute visual magnitude of +7.5 for quiescent dwarf novae, based on statistical parallaxes. The absolute visual magnitude for classical post-novae is about +4, and UX UMa-type stars are thought to have similar luminosities (Warner 1976). The

results of this chapter pertain to individual stars and are often only lower limits to the visual luminosity; moreover, the lower limits are a function of the spectral type of the secondary star. Thus a comparison with the mean properties for the post-novae and dwarf novae is difficult to make until the present data can be refined. Inspection of Table 3 does indicate that there is no obvious disagreement between the results of the present study and the mean values quoted above. The tabulated values for quiescent dwarf novae indicate that there is a large dispersion in their absolute visual magnitudes (compare U Gem with M_V(disk) $\sim$ 10.5 [Chapter 2] and SS Cyg with M_V(disk) $<$ 7.4 . Some of this dispersion may be due to inclination effects, since accretion disks are not spherically symmetric radiators. In so far as the present data bear on the point, they also tend to support arguments that the absolute magnitudes of UX UMa variables are in the same range as those of dwarf novae in outburst.

C. Future Work

This chapter has shown that flux-ratio diagrams are powerful tools in the analysis of composite spectra, but they need to be supplemented with other tools, such as high resolution spectroscopy and infrared and ultraviolet photometry, to give a more useful picture of the structure of cataclysmic variable systems. For example, flux-ratio diagrams alone cannot specify the spectral types of the secondary stars well enough except in special cases. Im-

provements in the flux-ratio analysis technique itself are possible; these include more restrictions on the set of physically plausible disk models (but this requires much confidence in the theory of accretion disk spectra) and flux ratios chosen to correspond to absorption features in late-type stars (but rotational broadening of the lines confuses the interpretation of these ratios).

Spectroscopy of both emission and absorption lines around the orbital cycles of cataclysmic variables is needed to establish periods and masses for the component stars. These data can be used to determine the magnitude corrections which are required because the secondary stars are abnormal.

Bolometric corrections are needed so that luminosities and mass transfer rates can be calculated for each system. This requires observations in the ultraviolet and sometimes in the x-ray and infrared regions of the spectrum. The extreme ultraviolet ($\lambda < 912$ Å) would be especially useful, but for most objects it is unfortunately unobservable because of interstellar absorption.

The MCSP data provide a crucial link between the ultraviolet and the infrared observations. For this reason alone, spectrophotometry between 0.3 μ and 1 μ should be acquired for as many cataclysmic variable systems as possible. Figures 3 and 4 show how especially important it is to have photometry in the near-infrared. Ideally, each star should be observed many times, to insure that the variations in its

spectral energy distribution are known properly.

The MCSP data are also useful for measuring the integrated fluxes in the emission lines. These fluxes serve as a direct probe of physical conditions in the circumstellar region. New spectrophotometric instruments, which have somewhat higher resolution than the MCSP and which sample the entire spectrum at once rather than by scanning, will be ideal for acquiring this kind of data.

APPENDIX

THE FLUX – RATIO DIAGRAM

Let monochromatic fluxes at wavelengths $\lambda 1$, $\lambda 2$, and $\lambda 3$ be denoted by $f(\lambda 1)$, etc. Let x denote the ratio $f(\lambda 2)/f(\lambda 1)$, and y denote the ratio $f(\lambda 3)/f(\lambda 1)$. It is important that the same wavelength appear in the denominator of both x and y.

Suppose that a composite spectrum is made up from two component spectra, 1 and 2, whose flux ratios are (x_1, y_1) and (x_2, y_2). In particular, let the flux at $\lambda 1$ be given by

$$f_{tot}(\lambda 1) = (1 + \alpha)\ f_1(\lambda 1)$$

where α, defined by the equation $f_2(\lambda 1) = \alpha\ f_1(\lambda 1)$, is the flux at $\lambda 1$ due to component number 2, normalized to the flux at $\lambda 1$ due to component number 1. Then

$$f_{tot}(\lambda 2) = f_1(\lambda 2) + f_2(\lambda 1)\ \frac{f_2(\lambda 2)}{f_2(\lambda 1)}$$

$$= f_1(\lambda 1) + \alpha\ f_1(\lambda 1)\ x_2$$

Thus

$$x_{tot} = \frac{f_{tot}(\lambda 2)}{f_{tot}(\lambda 1)} = \frac{x_1 + \alpha\ x_2}{1 + \alpha} = \beta\ x_1 + (1-\beta)\ x_2$$

where $\beta = 1/(1 + \alpha)$.

By replacing $\lambda 2$ in the above expressions by $\lambda 3$, it can also be shown that

$$y_{tot} = \beta\ y_1 + (1-\beta)\ y_2\ .$$

If the ordered pairs (x_1,y_1), (x_2,y_2), and (x_{tot},y_{tot}) are thought of as vectors, then the equations above reduce to

$$\vec{x}_{tot} = \beta\ \vec{x}_1 + (1-\beta)\ \vec{x}_2,\ 0<\beta\leq 1.$$

This means that $\vec{x}_{tot}$ lies on the straight line connecting $\vec{x}_1$ and $\vec{x}_2$. Moreover, the coefficient β is the distance from $\vec{x}_2$ to $\vec{x}_{tot}$, normalized to the total distance from $\vec{x}_2$ to $\vec{x}_1$ (see Figure A1). If for example $\beta = 1/2$, then $\alpha = 1$, meaning that half the flux at $\lambda 1$ is from component 1, and half the flux is from component 2. β varies between 1 and 0 as α varies between 0 and infinity.

This result, that the flux ratios of a composite spectrum lie on a straight line connecting the flux ratios of the component spectra, is what makes the diagram so useful. Note that this straight line property <u>does not hold</u> for the usual logarithmic two-color diagram, where the plotted quantities are magnitude differences rather than flux ratios.

If the composite spectrum has three components, then the composite flux ratios must lie within the triangle whose vertices are the flux ratios of the components. By induction, it can be shown that for any set of component spectra, the flux ratios of a composite spectrum must lie in the region known as the "convex closure" of the set of component flux ratios. (The convex closure of a set of points is the largest region bounded by lines drawn among the points.) Equally important, if a spectrum has flux ratios which lie

outside the convex closure, that spectrum cannot be constructed from the given set of component spectra.

REFERENCES

Abt, H. A. 1970, Ap. J. Suppl., 19, 387.

Bath, G. T., Evans, W. D., Papaloizou, J., and Pringle, J. E. 1974, M.N.R.A.S., 169, 447.

Bell, R. A., and Gustafsson, B. 1978, Astr. Ap. Suppl., 34, 229.

Boeshaar, P. 1976, Ph.D. thesis, Ohio State University.

Boggess, A., Drechsel, H., Holm, A., and Rahe, J. 1980, IAU Circ. 3485.

Cowley, A. P., Crampton, D., and Hutchings, J. 1980, preprint.

Crawford, J. A., and Kraft, R. P. 1956, Ap. J., 123, 44.

Eggen, O. J. 1967, Mem. R. A. S., 70, 111.

Fabbiano, G., Hartmann, L., Raymond, J., Steiner, J., and Branduardi-Raymont, G. 1980, preprint.

Fabian, A. C., Lin, D. N. C., Papaloizou, J., Pringle, J. E., and Whelan, J. A. J. 1978, M.N.R.A.S., 184, 835.

Gliese, W. 1969, Catalogue of Nearby Stars (Karlsruhe: G. Braun).

Herter, T., LaCasse, M. G., Wesemael, F., and Winget, D. E. 1979, Ap. J. Suppl., 39, 513.

Joy, A. H. 1956, Ap. J., 124, 317.

Joy, A. H., and Mitchell, S. A. 1948, Ap. J., 108, 234.

Kiplinger, A. L. 1979, A. J., 84, 655.

Kraft, R. P. 1962, Ap. J., 135, 408.

Kraft, R. P. 1964, Ap. J., 139, 457.

Kraft, R. P., and Luyten, W. J. 1965, Ap. J., 142, 1041.

Kraft, R. P., Krzeminski, W., and Mumford, G. S. 1969, Ap. J., 158, 589.

Kurucz, R. L., Peytremann, E., and Avrett, E. H. 1974, Blanketed Model Atmospheres for Early-Type Stars (Washington: Smithsonian Institution).

Lynden-Bell, D. 1969, Nature, 223, 690.

Madej, J., and Paczynski, B. 1977, The Interaction of Variable Stars with Their Environment (IAU Coll. 42), R. Kippenhahn et al., eds. (Bamberg: Astr. Inst. der Univ. Erlangen-Nurnberg), 313.

Mayo, S. K., Wickramasinghe, D. T., and Whelan, J. A. J. 1979, Changing Trends in Variable Star Research (IAU Coll. 46), F. M. Bateson et al., eds. (Hamilton, N. Z.: University of Waikato), 52.

Moffat, A. F. J., and Vogt, N. 1975, Astr. Ap. Suppl., 20, 85.

Paczynski, B., and Schwarzenberg-Czerny, A. 1980, Acta Astr., 30, 127.

Papaloizou, J. C. B., and Whelan, J. A. J. 1973, M.N.R.A.S., 164, 1.

Patterson, J. 1979a, A. J., 84, 804.

————. 1979b, Ap. J., 234, 978.

Payne-Gaposchkin, C. 1957, The Galactic Novae (Amsterdam: North-Holland).

Rabin, D. M. 1980, Ph.D. thesis, California Institute of Technology.

Robinson, E. L. 1974, Ap. J., 193, 191.

Robinson, E. L., and Faulkner, J. 1975, Ap. J. (Lett.), 200, L23.

Robinson, E. L., Nather, R. E., and Patterson, J. 1978, Ap. J., 219, 168.

Seaton, M. J. 1960, Rep. Progress Phys., 23, 313.

Slovak, M. H. 1980, IAU Circ. 3493.

Smak, J. 1979, Acta Astr., 29, 469.

Stover, R. J., Robinson, E. L., Nather, R. E., and Montemayor, T. J. 1980, preprint.

Upgren, A. R. 1973, A. J., 78, 79.

van Bueren, H. G. 1952, B.A.N., 11, 385.

Vasilevskis, S., Harlan, E. A., Klemola, A. R., and Wirtanen, C. A. 1975, Lick Obs. Pub., 22, Part V.

Veeder, G. J. 1974, A. J., 79, 1056.

Warner, B. 1976, Structure and Evolution of Close Binary Systems, P. Eggleton et al., eds. (Dordrecht: Reidel), 85.

Williams, R. E. 1980, Ap. J., 235, 939.

FIGURE CAPTIONS

Figure 1. The flux-ratio diagram for monochromatic fluxes measured at λλ4200, 5500, and 8000. The loci of late-type main sequence stars, blackbodies, power law spectra, and hydrogen recombination spectra are plotted. Temperatures in units of 1000 K are indicated for the blackbody and recombination radiation curves. The power law curve extends from $\alpha = -1$ to $\alpha = +2$.

Figure 2. The flux-ratio diagram of Figure 1 is repeated. Points corresponding to the observed ratios of SS Aur and U Gem during eclipse are shown. Arrows point to the location (off the top of the diagram) of the points for M1.5 and M4 dwarfs. Point A represents very high temperature blackbodies, or power laws with spectral index $\alpha = 2$. Point B corresponds to 6000 K blackbody radiation. Point C corresponds to 6000 K recombination radiation. It is suggested that physically reasonable accretion disk spectra must have colors which lie within the region bounded roughly by points A, B, and C (heavy outline). The lines labelled with numbers are described in the text.

Figure 3. The flux-ratio diagram of Figure 1, with the observed flux ratios of cataclysmic variable stars. Open circles are quiescent dwarf novae. Filled circles are old novae, UX UMa-type systems, or dwarf novae in outburst. The half-filled circle is the peculiar object

AM CVn (HZ 29). Three independent observations of UX UMa are shown; four observations of U Gem, one during eclipse, are shown. Identifications of individual objects in the figure may be made from Table 2.

Figure 4. A flux-ratio diagram for the ratios $z = f_\nu(\lambda 3560)/f_\nu(\lambda 5500)$ and $y = f_\nu(\lambda 8000)/f_\nu(\lambda 5500)$. The ratio z is sensitive to the Balmer jump. The blackbody and recombination lines are labelled by temperature in units of 1000 K. The region C_2 - A - B - C_1 (extending off the diagram to the right) is the region corresponding to region A - B - C in Figure 1. The open circles are quiescent dwarf novae, and the closed circles are erupting dwarf novae, UX UMa-type objects, and old novae. AM CVn is denoted by a half-filled circle.

Figure 5. A representative display from the interactive computer program which was used to examine the residual energy distributions. The upper solid curve in the MCSP spectrum of SS Aur, from which has been subtracted the spectrum of a dK0 star. The quantity Δ_2 is the magnitude difference at $\lambda 5500$ between SS Aur and the K star. The residual energy distribution is plotted as a series of error bars ($\pm 1\sigma$). The inset box highlights the "wild" up-and-down behavior which is characteristic of one type of unphysical residual energy distribution.

Figure 6. The residual energy distribution of SS Aur when the spectrum of a dK0 star is subtracted. Figure 6 differs from Figure 5 in that Δ_2 is bigger, meaning that less of the total flux is attributed to the K dwarf. The residual spectrum still has unphysical fluctuations (inset box), but their size is reduced. For sufficiently large values of Δ_2, these fluctuations will become acceptably small, but other considerations based on Figure 4 rule out such a model for SS Aur.

Figure 7. The residual energy distribution of SS Cyg, after subtraction of a dM1.5 spectrum. The inset box shows an abrupt falloff of flux at the redward end. This is characteristic of one type of unphysical energy distribution, corresponding to points below the line A - B in Figure 3.

Figure 8. The residual energy distribution of SS Cyg, after subtraction of a dK5 spectrum. The residual fluxes are acceptably smooth. Note the Paschen jump in emission, and its redward extension due to the confluence of the Paschen series. There may be Fe II emission near 5300 Å.

Figure A1. Relation between the flux ratios of a composite spectrum and the flux ratios of its component spectra.

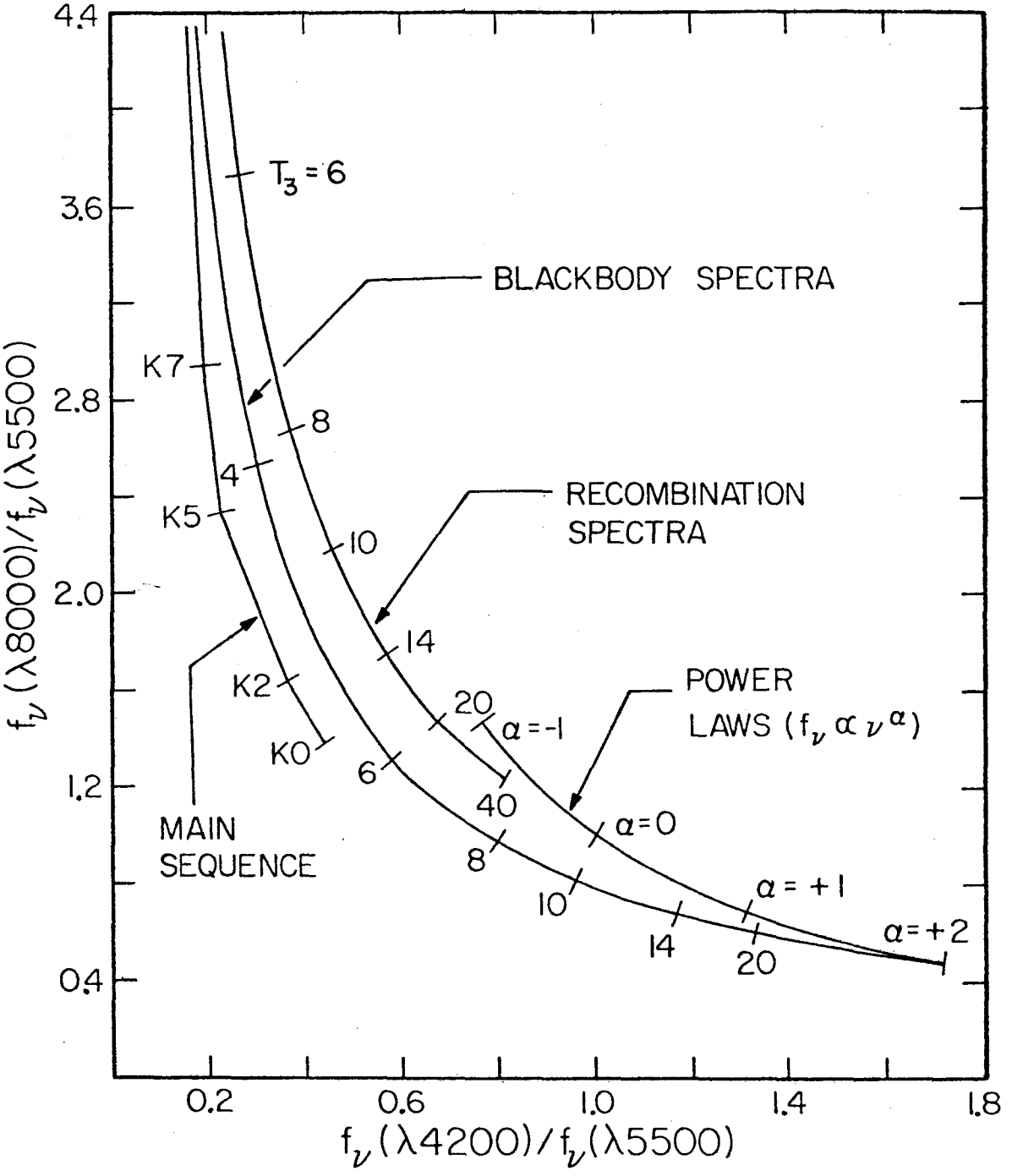
4.4
3.6
2.8
2.0
1.2
0.4
0.2
0.6
1.0
1.4
1.8
$f_\nu(\lambda 8000)/f_\nu(\lambda 5500)$
$f_\nu(\lambda 4200)/f_\nu(\lambda 5500)$
$T_3 = 6$
BLACKBODY SPECTRA
RECOMBINATION SPECTRA
POWER LAWS ($f_\nu \propto \nu^\alpha$)
MAIN SEQUENCE
K7
K5
K2
K0
8
4
10
14
20
6
40
8
10
14
20
$\alpha = -1$
$\alpha = 0$
$\alpha = +1$
$\alpha = +2$

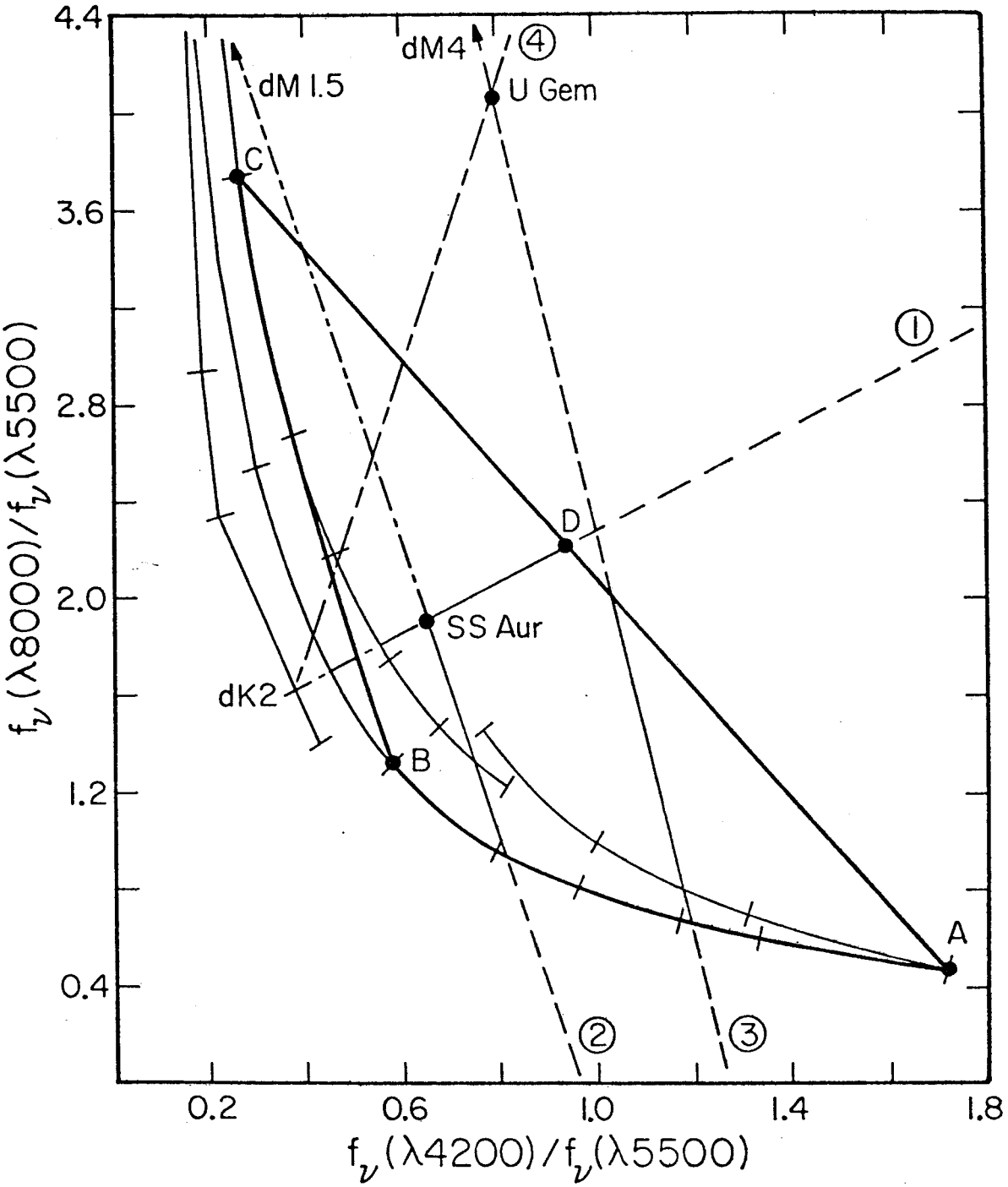
4.4
3.6
2.8
2.0
1.2
0.4
0.2
0.6
1.0
1.4
1.8
$f_\nu(\lambda 8000)/f_\nu(\lambda 5500)$
$f_\nu(\lambda 4200)/f_\nu(\lambda 5500)$
dM 1.5
dM4
④
U Gem
C
①
D
SS Aur
dK2
B
A
②
③

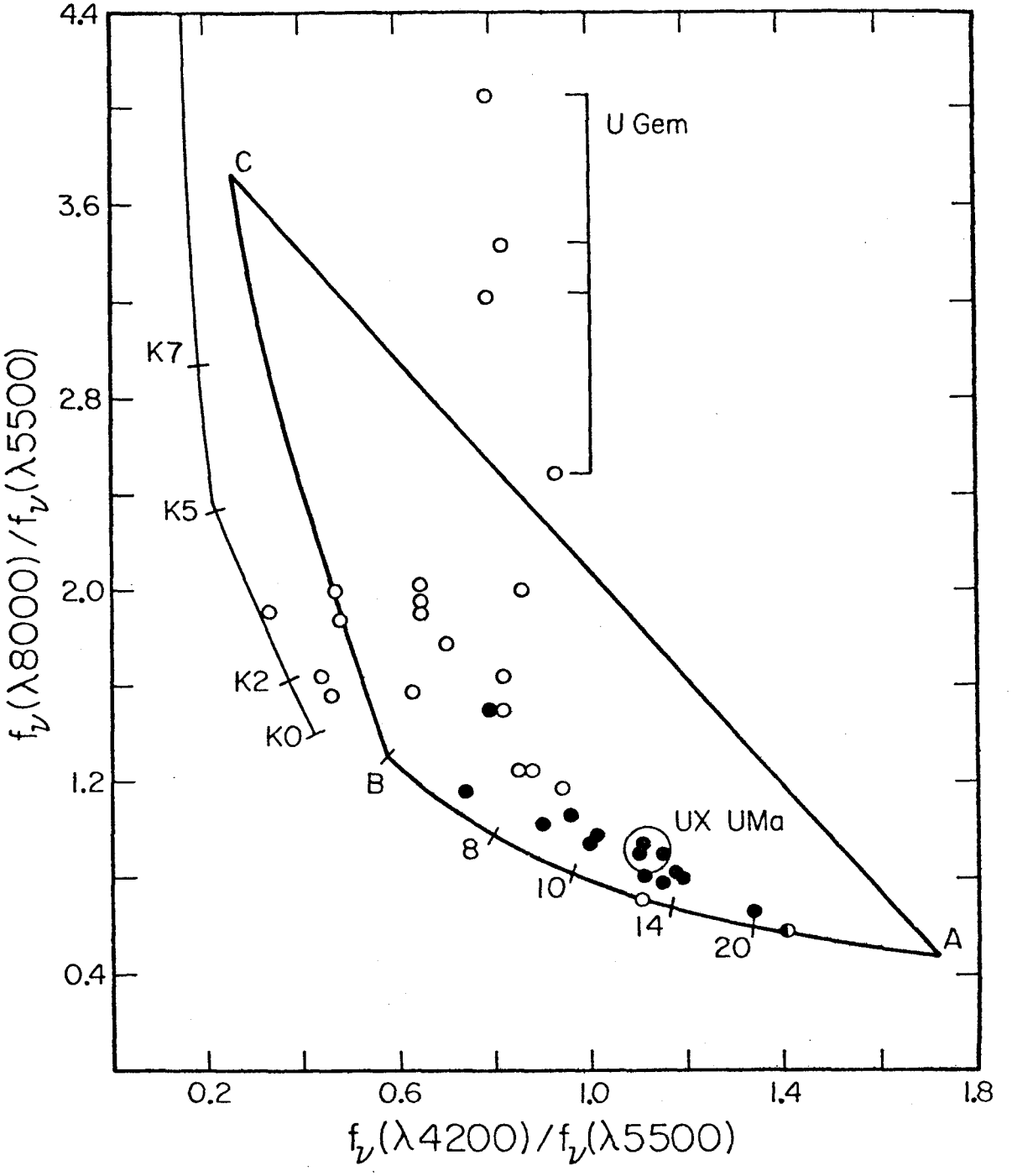
4.4
3.6
2.8
2.0
1.2
0.4
0.2
0.6
1.0
1.4
1.8
$f_\nu(\lambda 8000)/f_\nu(\lambda 5500)$
$f_\nu(\lambda 4200)/f_\nu(\lambda 5500)$
U Gem
C
K7
K5
K2
K0
B
A
8
10
14
20
UX UMa

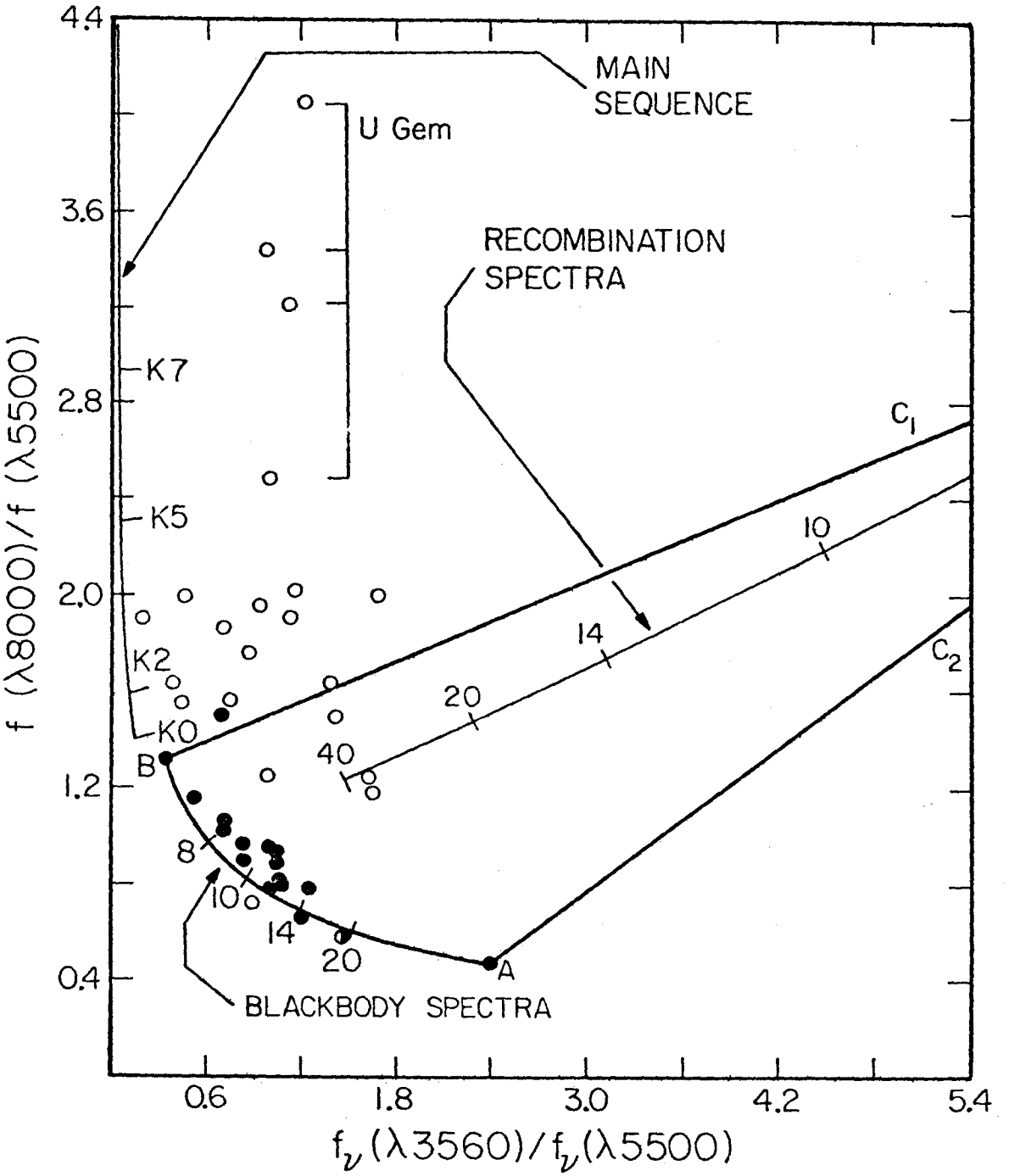
MAIN SEQUENCE
U Gem
RECOMBINATION SPECTRA
K7
K5
K2
K0
B
A
C1
C2
10
14
20
40
8
10
14
20
BLACKBODY SPECTRA
4.4
3.6
2.8
2.0
1.2
0.4
0.6
1.8
3.0
4.2
5.4
f (λ8000)/f (λ5500)
fν(λ3560)/fν(λ5500)

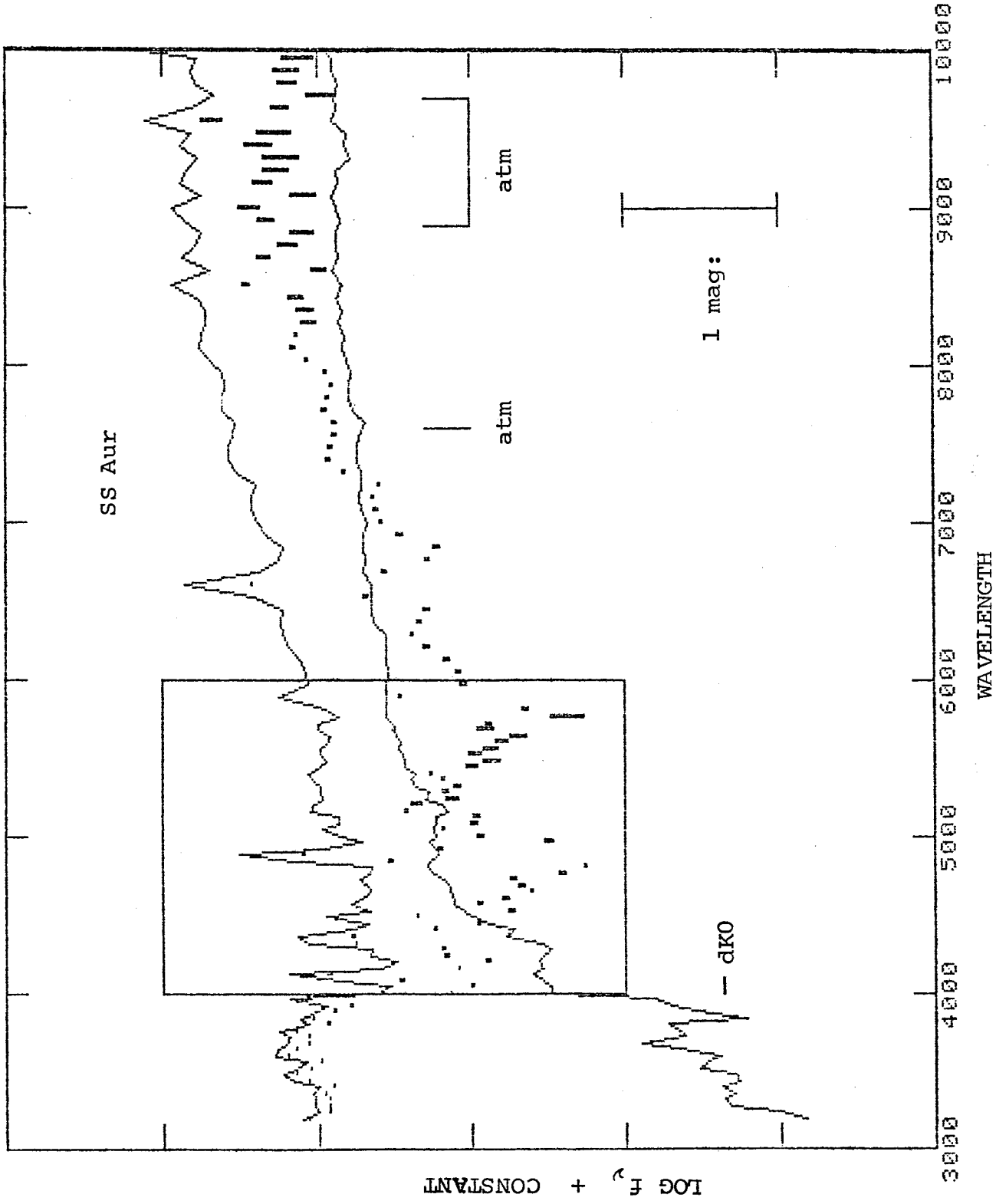
SS Aur
atm
atm
1 mag:
— dK0
3000
4000
5000
6000
7000
8000
9000
10000
WAVELENGTH
LOG f_λ + CONSTANT

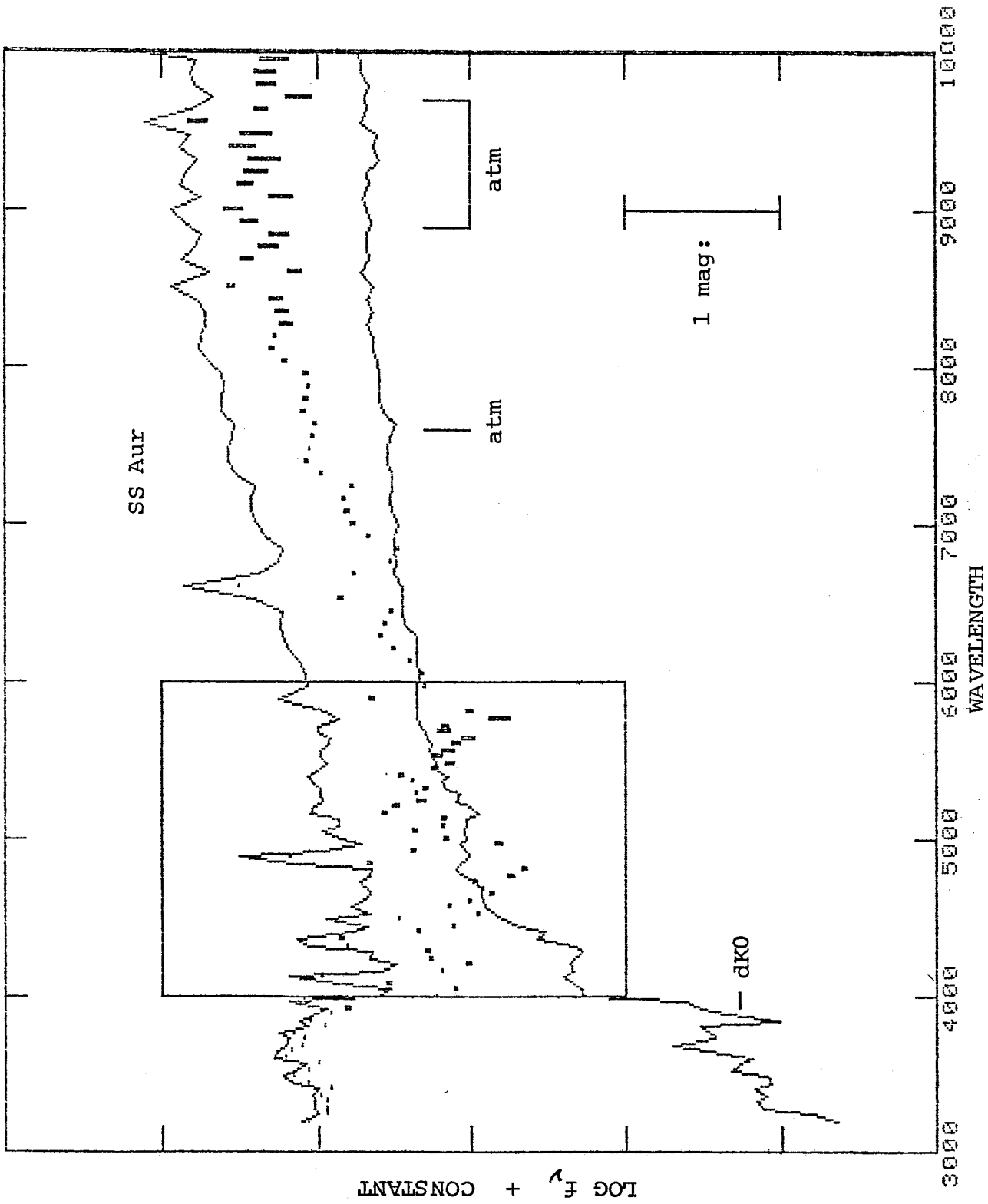
SS Aur
atm
atm
1 mag:
dK0
3000
4000
5000
6000
7000
8000
9000
10000
WAVELENGTH
LOG f_ν + CONSTANT

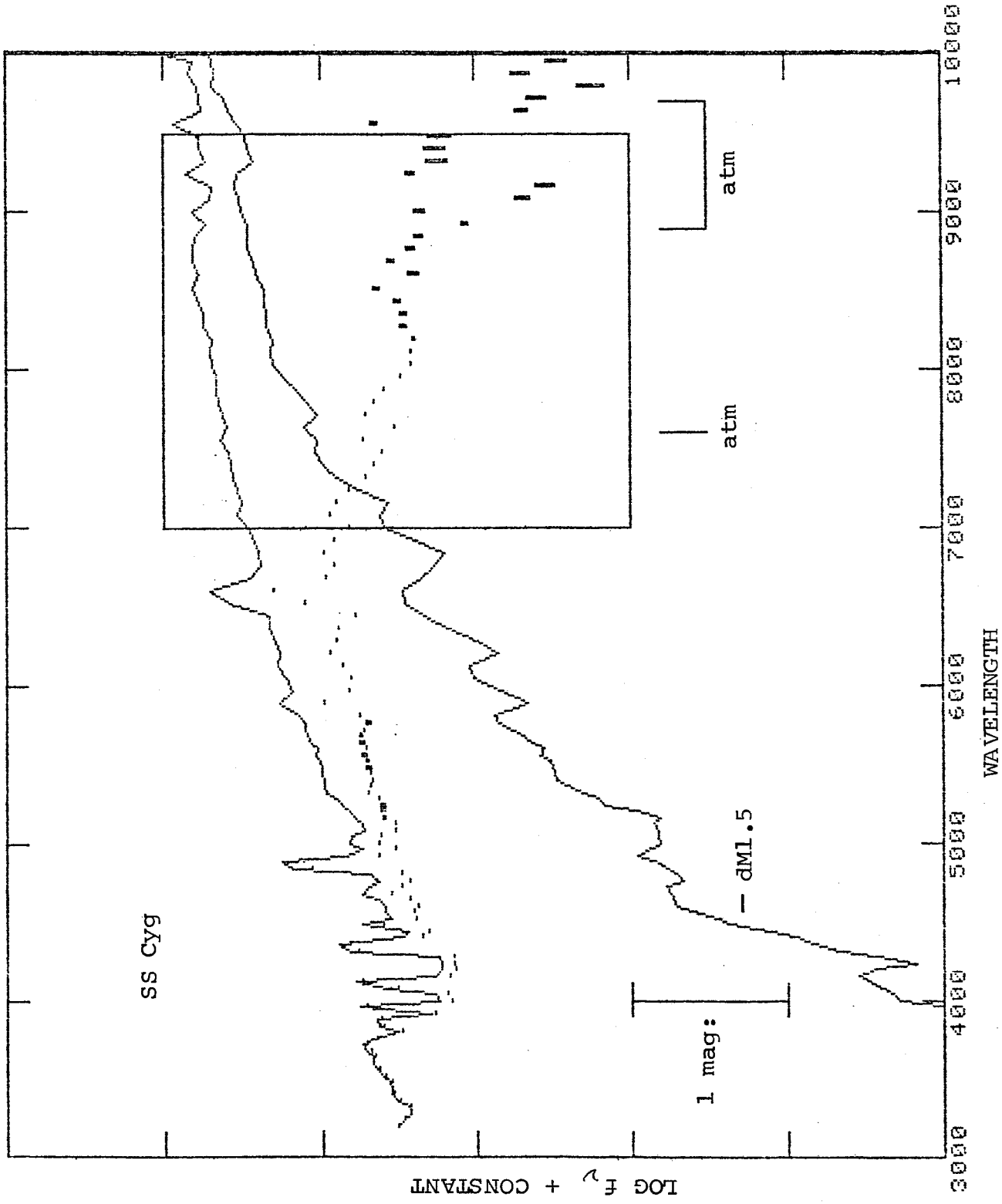
ss Cyg
1 mag:
dM1.5
atm
atm
LOG f_ν + CONSTANT
WAVELENGTH
3000
4000
5000
6000
7000
8000
9000
10000

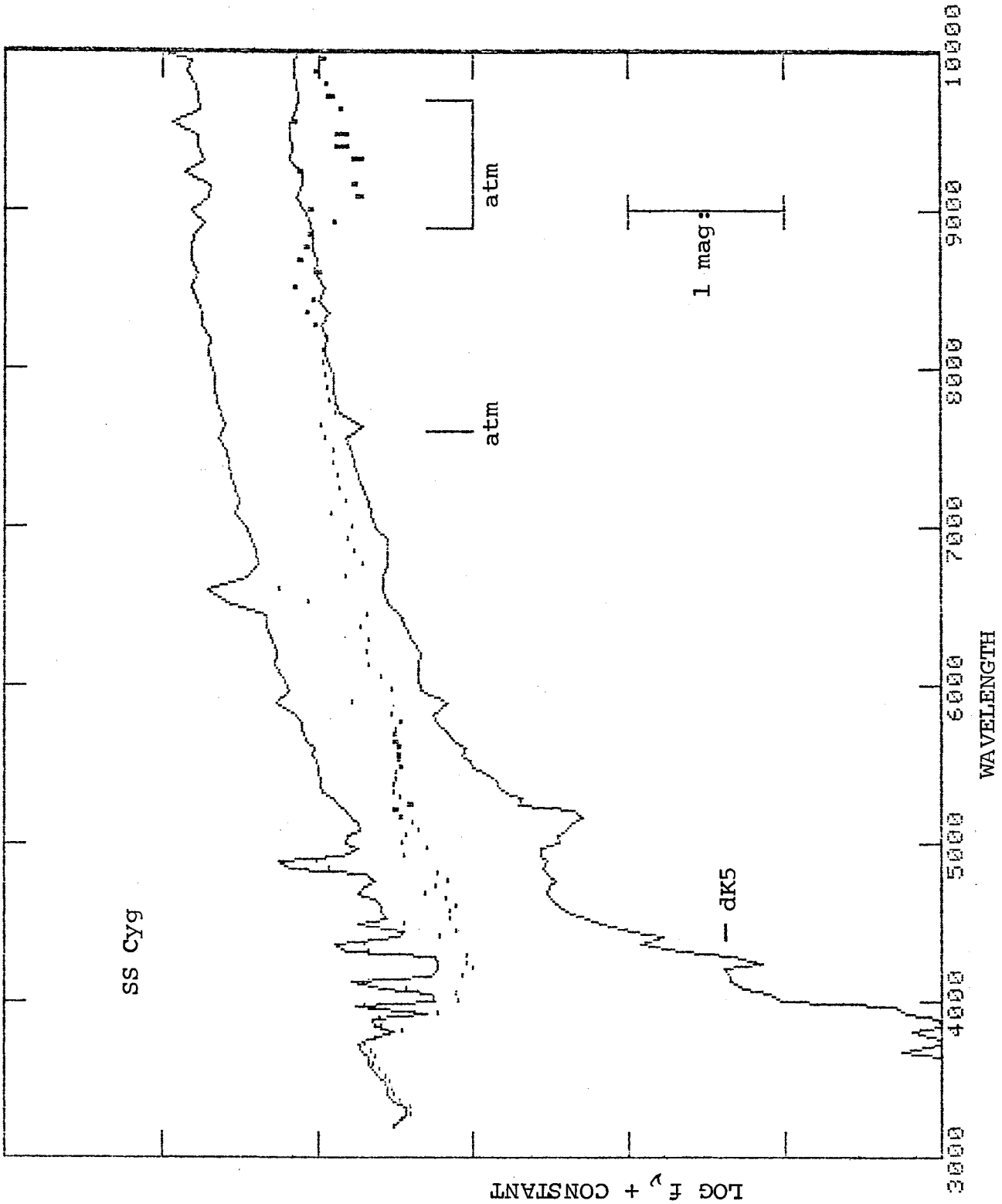
SS Cyg
atm
atm
1 mag
dK5
3000
4000
5000
6000
7000
8000
9000
10000
WAVELENGTH
LOG f_ν + CONSTANT

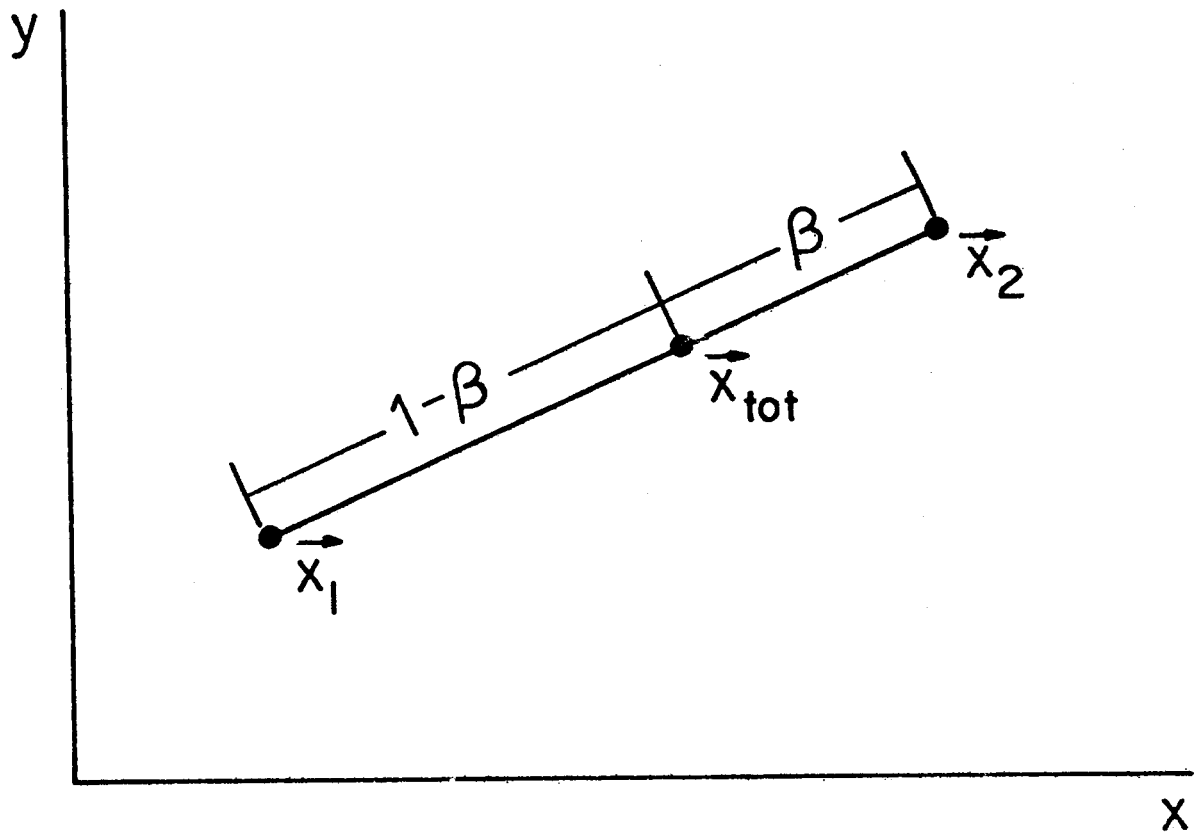
y
x
$\vec{x}_1$
$\vec{x}_{tot}$
$\vec{x}_2$
1-β
β